Atomic Energy Control Board
P.O. Box 1046
Ottawa, Canada
K1P 5S9

Commission de contrôle de l'énergie atomique
C.P. 1046
Ottawa, Canada
K1P 5S9

INFO-0254-1

CRACK PROPAGATION IN TOUGH DUCTILE MATERIALS (Phase I)

by

R.D. Venter, A.N. Sinclair and D. McCammond
University of Toronto

A report prepared for the

Atomic Energy Control Board
Ottawa, Canada

Project 85.1.8

November 1987

Canada

Research report

CRACK PROPAGATION IN TOUGH DUCTILE MATERIALS (Phase I)

A report prepared by R.D. Venter, A.N. Sinclair and D. McCammond, Structural Integrity, Fracture and Fatigue Research Laboratory (SIFFRL), Department of Mechanical Engineering, University of Toronto, under contract to the Atomic Energy Control Board.

SUMMARY

The report describes and presents the J-resistance curves obtained as a function of crack extension for two representative tough ductile materials namely ASTM516 grade 70 plate steel and SA106 grade B pipe steel.

The results were obtained using the ASTM standard method for determining J-R curves, E24.08, 12th Draft, 25th July, 1985. Both compact tension and three point bend tests were employed for the plate steel tests; only compact tension specimens were used to evaluate the pipe steel. All tests were carried out under load control conditions using specimens of different thickness and cut from known orientations within the parent material.

An assessment of the results, while inconclusive in numerous aspects because of the small number of specimens tested at each condition, is nevertheless possible. These conclusions are briefly summarised below.

i) Given the importance to replicate test results it would appear that the test procedure and experimental set-up for compact tension specimen leads to more consistent results as compared to the three point bend tests undertaken. Alignment difficulties, since three point bend tests do require a compressive load application, are the most crucial in the identification of this preference.

ii) For the compact tension pipe steel tests the importance of orientation of the test specimen as cut from the parent pipe is significant. For each of the different thickness specimens tested, the J-resistance curves for crack extension in the circumferential direction was consistently superior to that offered by the crack extension in the axial direction.

iii) The effect of specimen thickness for specimens in the range tested i.e. 0.5 to 1.25 inches would indicate that representative results can be obtained from 1.0 inch thick specimens. This specimen size is convenient to use in laboratory experimentation and certainly allows for a reasonable crack extension of some 1-1.5 mm even under load control conditions.

Within this report the results are discussed and would indicate that the critical direction of crack propagation coincides with a crack growing along the axial direction of the pipe.

RÉSUMÉ

Le rapport indique et décrit les courbes de résistance en J obtenues comme une fonction du prolongement des fissures pour deux matériaux ductiles résistants qui sont représentatifs, à savoir de l'acier en feuille de nuance 70, ASTM516, et de l'acier pour tubulure de grade B, SA106.

Les résultats ont été obtenus au moyen de la méthode standard ASTM utilisée pour déterminer les courbes de résistance en J, E24.08, 12e ébauche, 25 juillet 1985. Les essais d'éprouvettes compact en tension et en flexion trois points ont été utilisés pour les essais sur l'acier en feuille; seuls les spécimens d'éprouvettes compact en tension ont été utilisés pour évaluer l'acier pour tubulure. Tous les tests ont été menés dans des conditions de contrôle de la charge au moyen de spécimens de différentes épaisseurs qui ont été coupés, selon une orientation déterminée, dans des parties du matériau d'origine.

Il est toutefois possible de faire une évaluation des résultats, bien qu'elle ne soit pas concluante à divers aspects en raison du faible nombre de spécimens testés pour chaque condition. Ces conclusions sont résumées succinctement ci-dessous.

i) Vu l'importance de reproduire exactement les résultats des essais, il semble que le montage expérimental et la procédure de l'essai des spécimens d'éprouvettes compact en tension ont entraîné des résultats plus uniformes que ceux des essais d'éprouvettes en flexion trois points. Les problèmes d'alignement sont les plus importants pour l'identification de cette préférence, parce que les essais d'éprouvettes en flexion trois points exigent l'application d'une charge compressive.

ii) En ce qui touche les essais d'éprouvettes compact en tension par rapport à l'acier pour tubulure, il est très important de tenir compte de l'orientation des spécimens qui sont coupés dans le matériau d'origine. Pour chacun des différents spécimens d'épaisseur testés, la courbe de résistance en J pour les prolongements dans la direction de la circonférence était constamment supérieure à celle que présentait le prolongement de la fissure dans la direction de l'axe.

iii) L'effet de l'épaisseur des spécimens dans le cas des spécimens de la plage testée, c'est-à-dire de 0,5 à 1,25 pouce indiquerait que des résultats représentatifs peuvent être obtenus pour les spécimens de 1 pouce d'épaisseur. La taille de ce spécimen est pratique pour les expériences de laboratoire et elle permet d'avoir un prolongement raisonnable de la fissure d'environ 1 à 1,5 mm, même dans des conditions de contrôle de la charge.

Dans ce rapport, les résultats sont discutés et indiqueraient que la direction critique de la propagation de la fissure coincide avec une fissure qui grandit le long de l'axe de la tubulure.

DISCLAIMER

The Atomic Energy Control Board is not responsible for the accuracy of the statements made or opinions expressed in this publication and neither the Board nor the authors assume liability with respect to any damage or loss incurred as a result of the use made of the information contained in this publication.

ACKNOWLEDGEMENT

The authors wish to acknowledge the considerable contributions made by Dr. G.I. Ogundele and Messers. K. Gilbert and G. Kokodyniak of the Structural Integrity, Fracture and Fatigue Research Laboratory in the Department of Mechanical Engineering. Their involvement in the preparation, compilation and assessment of the material presented in this report was invaluable.

Special thanks are also due to Babcock and Wilcox Canada for providing a short length of the SA106 grade B pipe steel from which the test specimens used in this study were fabricated.

TABLE OF CONTENTS

A. INTRODUCTION 1

B. TEST SPECIMENS AND TESTING METHODS 3
1. General 3
2. Tests on ASTM516 Grade 70 Plate Steel 3
3. Tests on SA106 Grade B Pipe Steel 4

C. J-RESISTANCE CURVES 14
1. General 14
2. Analysis of Test Data 14
2.1 Plate Steel Results 14
2.2 Pipe Steel Results 14

D. COMPARISON OF J-RESISTANCE CURVES 35
1. General 35
2. Plate Steel Results 35
3. Pipe Steel Results 35

E. ASSESSMENT OF RESULTS 45

F. CONCLUSIONS 51

G. RECOMMENDATIONS 52

REFERENCES 53

APPENDICES
Test Method for Determining J-R Curves ..... APPENDIX A
Experimental Test Data ..... APPENDIX B

A. INTRODUCTION

Pressure retaining components are generally fabricated from materials which remain tough and ductile under all service conditions. For the design thicknesses encountered in CANDU applications, this means that fracture would tend to occur within the elastic-plastic and fully plastic regimes. However, defect assessment techniques, prescribed by the regulatory codes and standards, only provide plastic collapse and linear elastic fracture mechanics criteria for application to fracture appraisal. Hence the controls in place may result in the requirement of overly conservative integrity reserve in defective components or in acceptance standards for condition monitoring.

In October 1985, a comprehensive study into the understanding of crack and fracture behaviour in tough ductile materials was completed. This study entitled "Crack and Fracture Behaviour in Tough Ductile Materials" and documented as AECB INFO-0169 described the fundamental fracture mechanics concepts, their extension to include elasto-plastic considerations and the preferred options available for the development of appropriate design methodologies. The specific recommendations of this study are summarized below:

i) the experimental development of J-resistance curves

ii) utilization of the J-T approach

iii) development of the twin J/CTOA criteria

iv) investigation into near full scale tests to validate analysis techniques and confirm laboratory data obtained from specimens

v) analysis of different crack configurations, i.e. circumferential, longitudinal, angled cracks, through thickness, etc. to assess mixed mode configurations.

Following the general thrust of these recommendations, the objectives of the present undertaking was to assess the viability of a combination of both energy and crack opening displacement/angle based fracture toughness criteria as a means towards the establishment of a representative model for understanding the crack growth behaviour under elasto-plastic conditions. The planned approach was to experimentally determine J-resistance curves using both compact tension and three point bend specimens using an ASTM 516 grade 70 plate steel, and to assess the results in terms of a lower bound criteria based on these specimen geometries and the influence of the constraint imposed by the variation in specimen thickness. Two other promising aspects which were initially proposed were i) to conduct an exploratory experimental investigation into the determination of CTOD/CTOA as a function of the increased crack length and ii) to extend the J-resistance measurements to include specimens cut from a SA106 grade B pipe steel.

It is appropriate to indicate that during this planned program, a significant shift of emphasis in the work undertaken was made. While consistent with the recommendations of the AECB INFO-0169 report, an increasing component of the work was directed to obtain J-resistance data for the SA106 grade B pipe steel. The reasons for this choice are:

i) the obvious advantages to obtain J-resistance curves from the more representative pipe steel as opposed to plate steel, and

ii) from the initial experimentation undertaken on the plate steel, it was concluded that very little data could be derived from a preliminary CTOD/CTOA experimental investigation. In brief, any meaningful direct local measurements of these parameters would have been exceedingly difficult to accomplish within the resources available.

It should also be noted that prior to this decision not to experimentally investigate these parameters, consideration was given to the theoretical evaluation of the CTOD/CTOA parameters as a function of crack extension. The suitability of various finite element software packages were assessed, and a revised version of the comprehensive ADINA package was acquired. Investigation into the usage of this package, following a number of trial runs, clearly revealed that significant modifications to the ADINA package were required to accommodate a realistic crack growth/initiation capability within this program. It was anticipated that such theoretical data, derived from the ADINA package, could have provided useful support for any experimental investigation. This was not possible to accomplish.

This report outlines the experimental procedures and results of J-resistance curves obtained for both ASTM 516 grade 70 plate steel and SA106 grade B pipe steel. It is clearly evident from this data that the J-resistance curve itself is a difficult parameter to develop in a consistent and reproducible manner in spite of refined experimental procedures. Nevertheless, trends do emerge which contribute to the understanding and need to develop practical methods of analysis in support of regulatory codes applicable to the elasto-plastic considerations in tough ductile materials.

The precise difficulties and questions which should be borne in mind when reading this report are:

i) Can J-resistance curves obtained from small specimens be used to reliably generate large crack growth J-resistance curves? The answer to this question appears to be negative.

ii) The suitability of using the J-integral concept for elastic-plastic fracture and the test methods for determining J-resistance curves i.e. load control vs. displacement control and how these test conditions relate to the various practical loading conditions.

iii) The relatively poor correlations, often resulting in a less conservative prediction of J-resistance curves, obtained by researchers using far- and near-field finite element methods of analysis to predict or simulate laboratory test data under controlled conditions of geometry and loading. The extension of these analyses to practical situations is therefore limited.

The results presented in this report serve to provide some insight into the basic fundamental difficulties which require resolution before any correlation of test data of J-resistance curves can be reliably used to support and develop conservative design approaches.

B. TEST SPECIMENS AND TESTING METHODS

1. General

A series of test specimens, of the compact tension and three point bend configuration, were prepared for testing. The specimens were cut from an ASTM516 grade 70 flat plate steel and an SA106 grade B pipe steel. The objective of these tests was to determine the J integral as a function of the crack extension for different specimen thicknesses and orientation within the parent material.

2. Tests on ASTM516 Plate Steel

A selection of the possible orientations of specimens which could be cut from the parent plate is shown in Figure 2-1. All specimens in the present study were cut from the T-L orientation only, from an ASTM516 grade 70 plate steel obtained from a commercial supplier. The proposed number of tests i.e. the test matrix of both the compact tension and three point bend specimen configuration is shown in Table 2-1. Figures 2-2, and 2-3 provide an illustration of the dimensions of the 0.5 inch thick compact tension and three point bend specimens respectively. All external surfaces of each specimen were accurately machined; the notched section of all specimens were electro-discharge machined (EDM) with allowance for the maintenance of a lip as required for the attachment of the displacement clip gauge. A compact tension specimen showing this lip is presented in Figure 2-4.

All tests were carried out in accordance with the proposed ASTM standard [Ref. 1]. The pertinent details and other relevant information are provided in Appendix A. The experimental test set up for both the compact tension and three point bend tests is shown in Figures 2-5 and 2-6.

The experimental data for each test identified in the test matrix, see Table 2-1, is presented in graphical form in Appendix B, Figures B-1 to B-6. Figures B-1 to B-3 illustrate the data points for the three point bend tests in which the determined value for the J integral is plotted as a function of the measured crack extension for each of the 0.5 inch, 1 inch and 1.25 inch thick specimens. The equivalent data for the compact tension specimens is presented in Figures B-4 to B-6. The coding for each test specimen, cut from the T-L direction, is defined below.

For compact tests: XX NN.Z, where

- XX is denoted by CT referring to compact tension
- NN is the specimen thickness, NN is 05, 10 and 125 for 0.5 inch, 1 inch and 1.25 inch specimens respectively
- Z identifies the specimen number.

For three point bend tests: XX NNTL.Z where

- XX is denoted by B referring to three point bend
- NN is again the specimen thickness
- TL is the orientation
- Z identifies the specimen number.

For example B10TL 1-4 would indicate a three point bend test of one inch thickness in the TL direction (see Figure 2-1). The 1-4 indicates that four specimens were tested, the first denoted by B10TL-1 and the last by B10LT-4.

3. Tests on SA106 grade B Pipe Steel

A large number of compact tension specimens were cut and prepared from an SA106 grade B Pipe Steel. The pipe was of a sufficiently large diameter (24 inch diameter, with a 2.5 inch wall thickness) to permit the standard compact tension specimens to be cut in the four orientations shown in Figure 2-7 which, for convenience, have been designated as A, B, C and D. These particular orientations were selected to assess the possible variation of the J resistance curve for each of these planes. Within a cylindrical coordinate definition, the fracture surface plane of specimens cut with orientations A and C correspond to a plane normal to the θ axis, whereas the orientations B and D coincide with the plane perpendicular to the Z (axial) axis. Note that an overpressure situation in the pipe corresponds to a fracture surface as seen with orientations A and C. By contrast, a guillotine-type failure is best studied with B or D specimens.

The test matrix of compact tension specimens prepared from the SA106 pipe steel is presented in Table 2-2; a range of specimens of 0.5 inch, 1 inch and 1.25 inch thickness for each of the orientations A, B, C and D have been used. The coding for each test is described as PIPE NN.YZ, where NN identifies the specimen thickness as for the steel plate tests, Y is the orientation of the fracture surface coinciding with A, B, C or D as shown in Figure 2-7, and Z identifies the specimen number for a given thickness and orientation.

The test data of the J-integral as a function of the crack extension are presented in Appendix B, Figures B-7 to B-10 provide the test data for each of the orientations A, B, C and D respectively for one inch thick specimens.

Figures B-11 and B-12 illustrate the test data obtained for the 1.25 inch thick specimens cut from the orientation denoted by A and B respectively.

Figures B-13 to B-15 illustrate the test data obtained for a series of 0.5 inch thick specimens corresponding to the A orientation. In this particular series of tests, the compact tension specimens were cut from positions corresponding to the outer, center and inner locations of the through thickness of the pipe wall. For these tests, the letter Y in code PIPE NN.YZ becomes a 2-character designation; the first character represents orientation A, B, C, or D as before, and the second character specimen location: O for outer, C for center and I for inner. For example PIPE 05.AI1-5 identifies the pipe steel specimen of 0.5 inch thickness with orientation A cut from the inner third of the pipe wall thickness. To complete the test matrix a series of 0.5 inch thick compact tension specimens cut from the B orientation, and centred in the through thickness of the pipe wall, was undertaken; this test data is presented in Figure B-16.

Table 2-1: Test Matrix for ASTM516 grade 70 Plate Steel

SPECIMEN THICKNESS	CONFIGURATION	
INCHES	COMPACT TENSION SPECIMENS	3-POINT BEND SPECIMENS
0.50	6(5)	4(4)
1.00	8(7)	4(4)
1.25	4(4)	4(3)

Notes: Numbers in parenthesis identify number of specimens tested.
All specimens are of the T-L orientation, see Figure 2-1.

Table 2-2: Test Matrix for SA106 Pipe Steel Compact Tension Specimens

ORIENTATION	THICKNESS OF SPECIMEN		
	1.25 INCHES	1.0 INCHES	0.5 INCHES
A (C-L)	6	6	15*
B (L-C)	6	6	5
C (C-R)	NIL	6	NIL
D (L-R)	NIL	6	NIL

* Five specimens were cut at each of the inner, center and outer locations of the through wall thickness of the pipe steel.

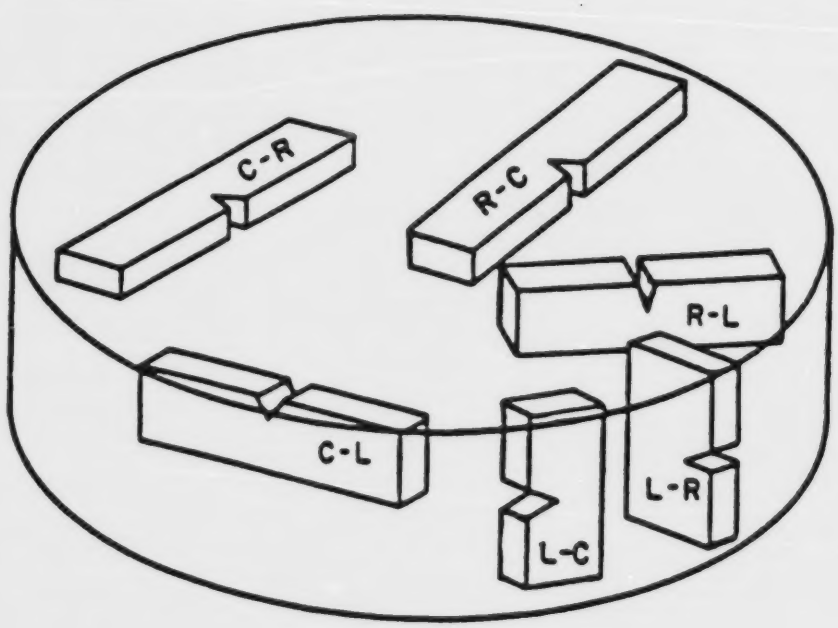

Crack Plane Orientation Identification Code for Drawn Bars

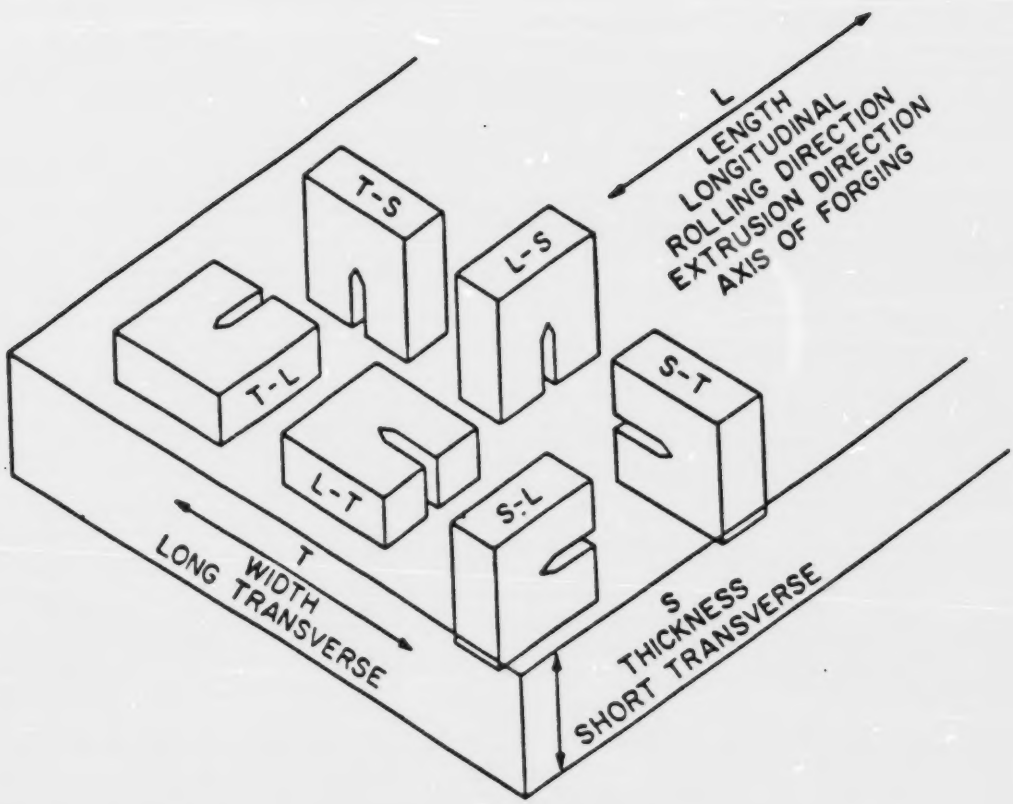

Figure 2-1: Crack Plane Orientation Identification Code for Rolled Plate.

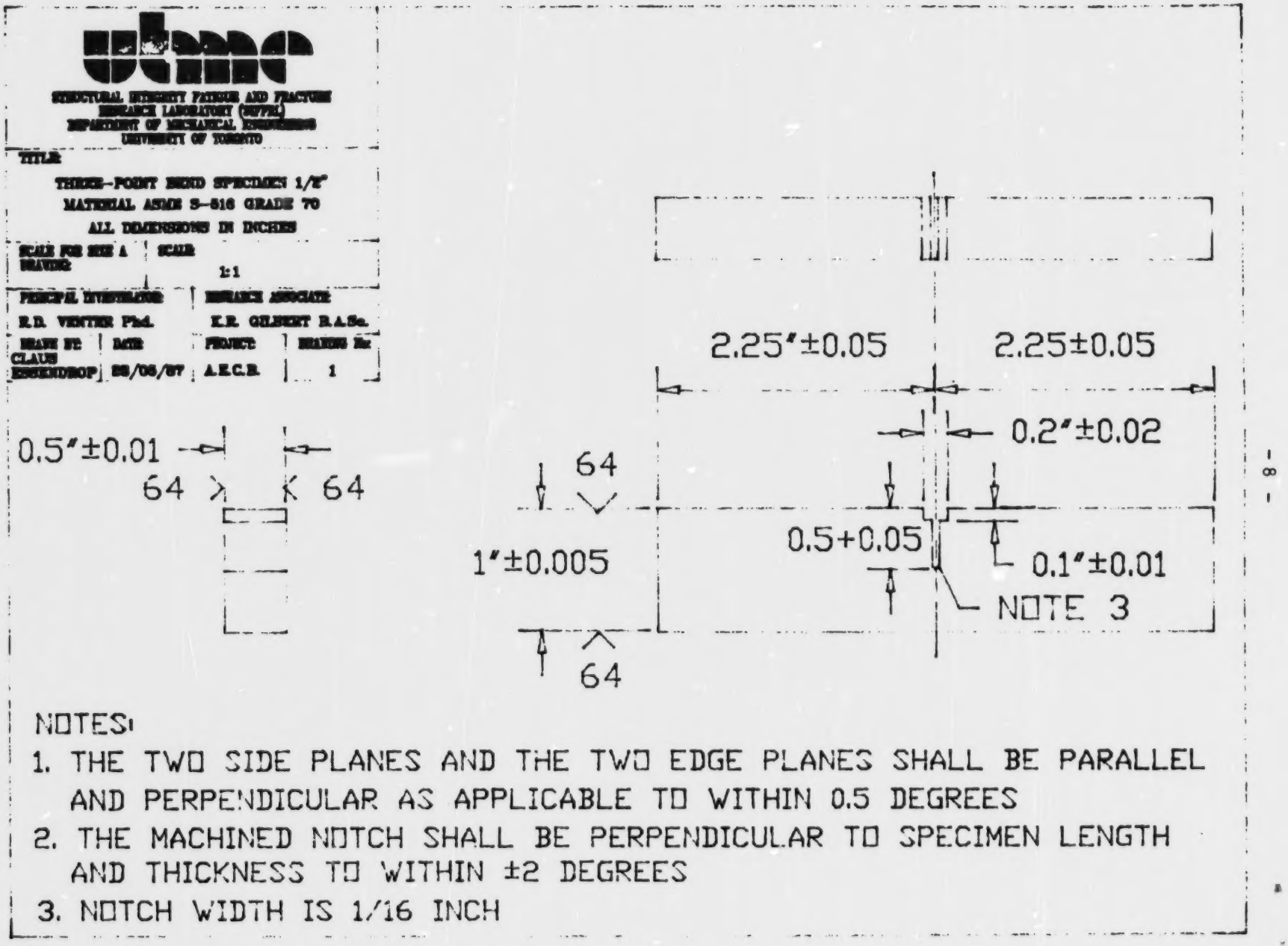

Figure 2-2: Compact Tension Specimen Showing Dimensions for 0.5 inch Thick Specimen.

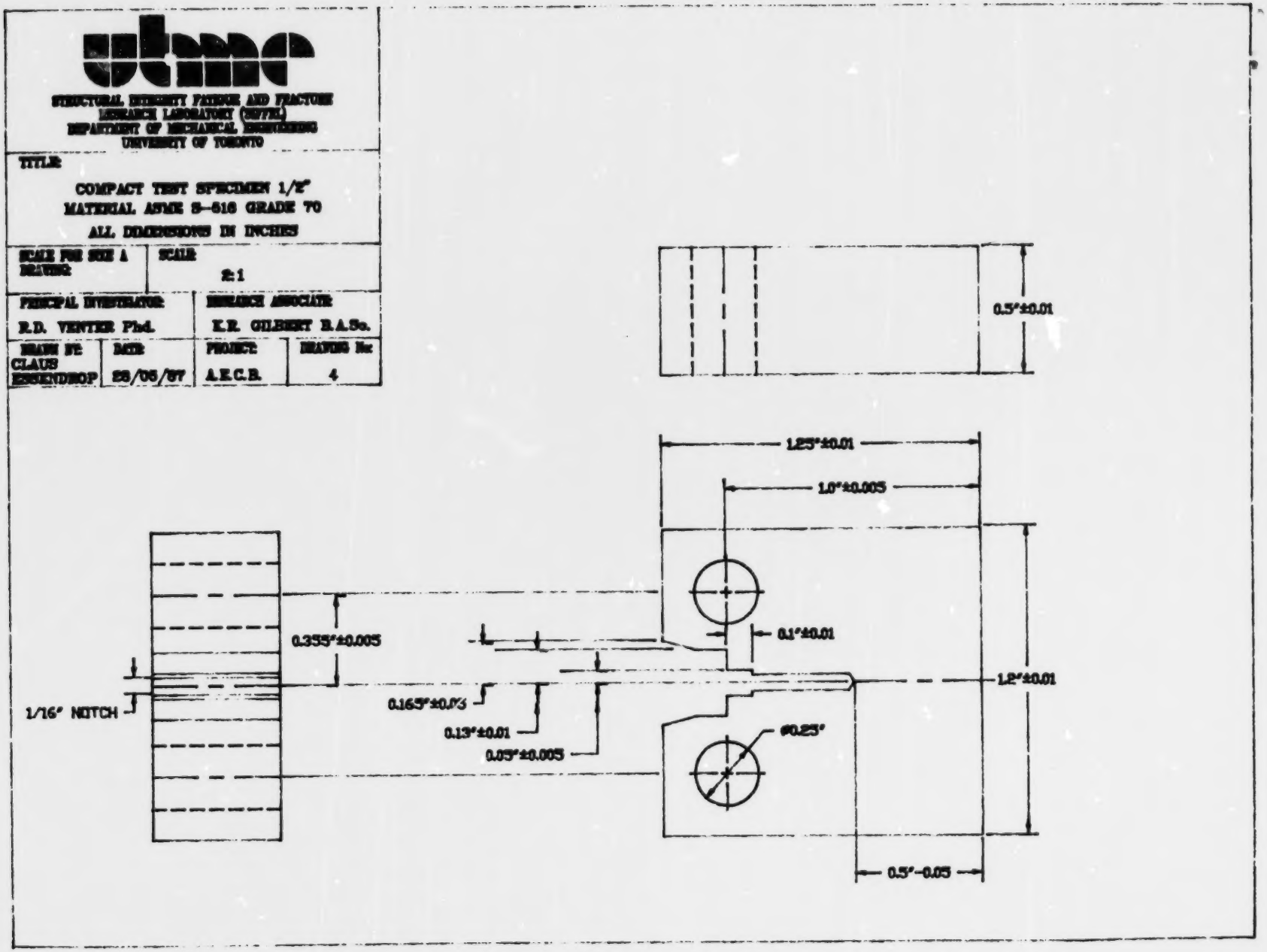

Figure 2-3: Three Point Bend Specimen Showing Dimensions for 0.5 inch Thick Specimen.

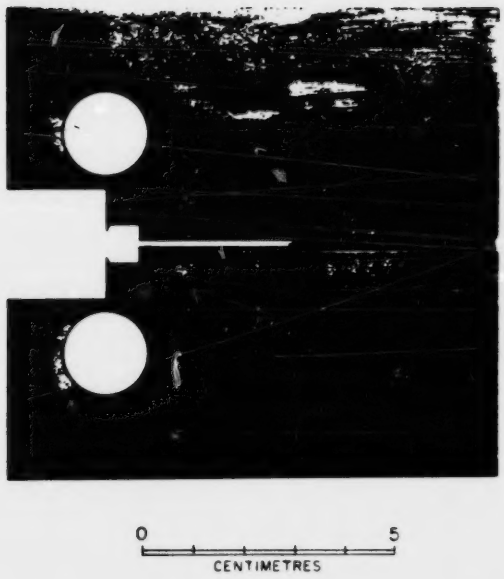

Figure 2-4: Compact Tension Specimen. The Notched Section was Cut Out with EDM Machining Techniques. The Lip for Attaching the Clip Gauge is Clearly Illustrated.

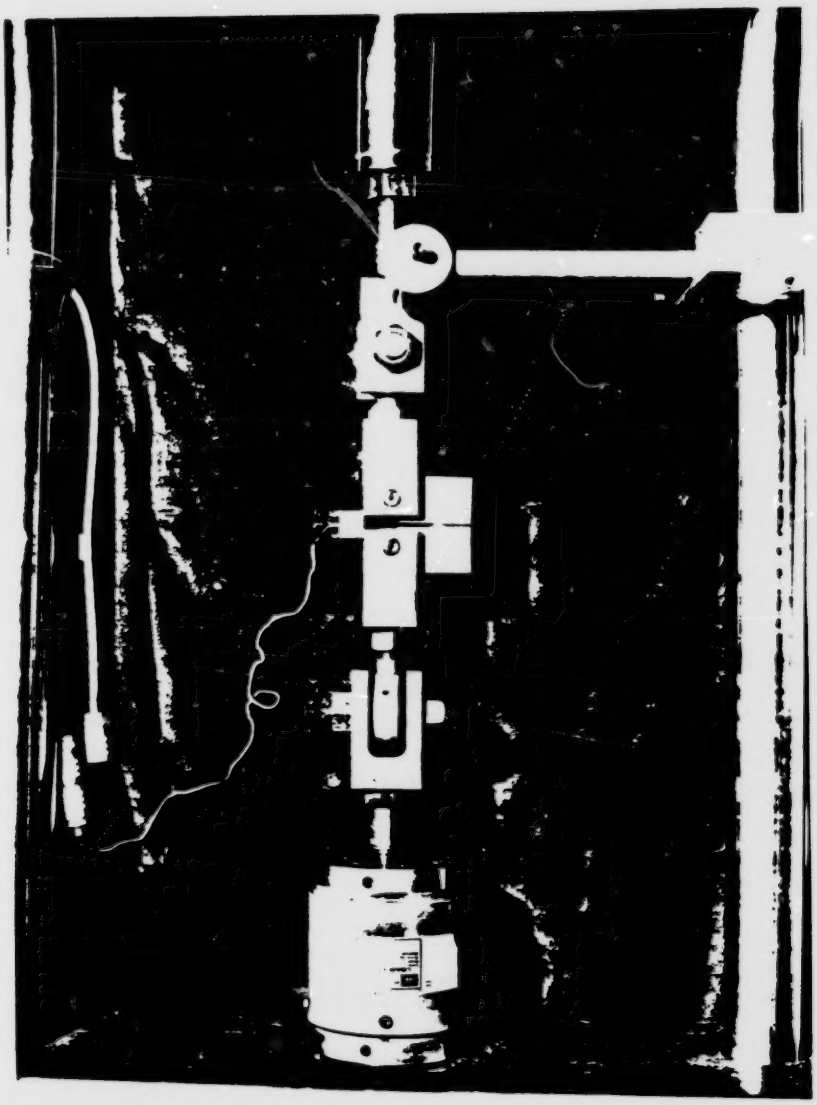

Figure 2-5: Experimental Set-Up for Compact Tension Tests. The Specimen is Attached by Clevis Pins to the Actuator of an MTS System with Clip Gauge in Position.

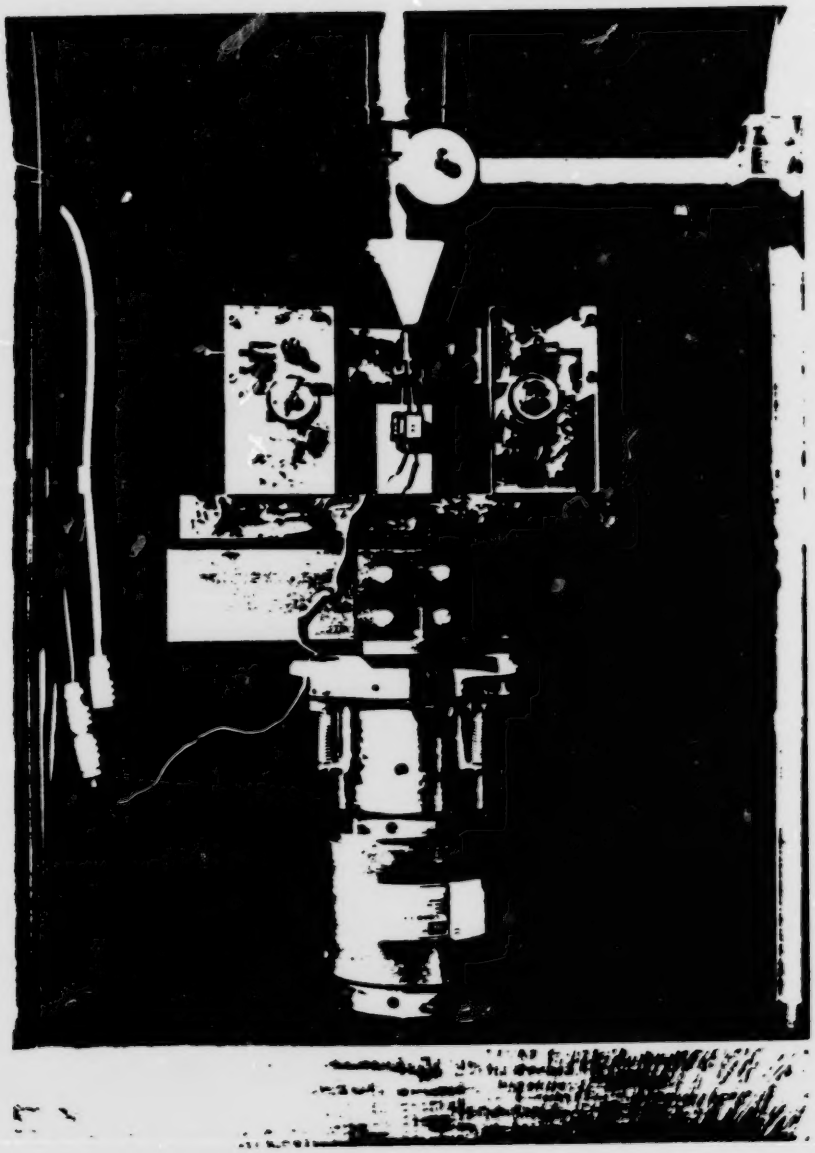

Figure 2-6: Experimental Test Set-Up for Three Point Bend Tests. The Load is Applied Through a Rounded Punch.

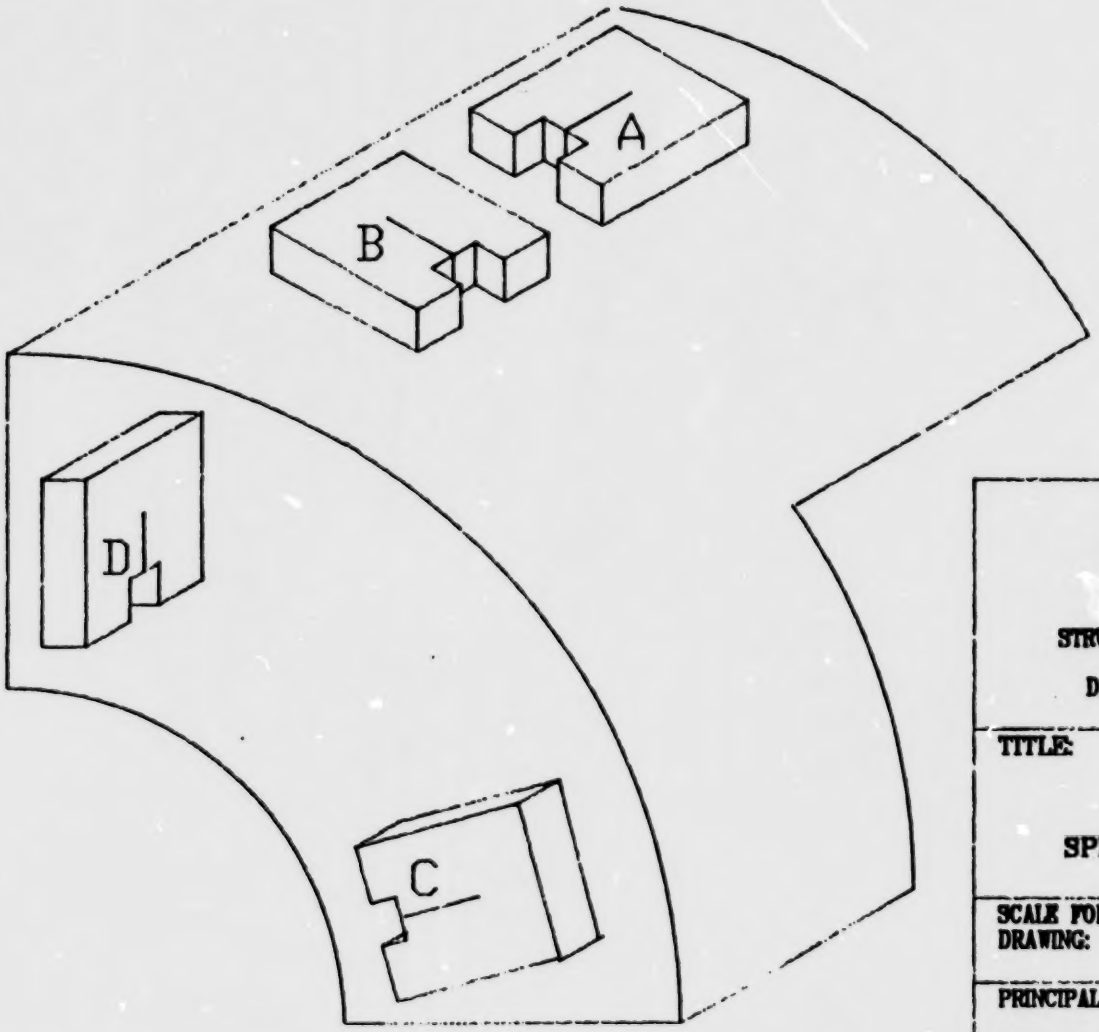

STRUCTURAL INTEGRITY FATIGUE AND FRACTURE
RESEARCH LABORATORY (SIFFRL)
DEPARTMENT OF MECHANICAL ENGINEERING
UNIVERSITY OF TORONTO

TITLE:

SPECIMEN ORIENTATION IN PIPE

SCALE FOR SIZE A DRAWING:	SCALE: Not to Scale		
PRINCIPAL INVESTIGATOR: DR. R. D. Venter		RESEARCH ASSOCIATE: K. R. Gilbert	
DRAWN BY: K.R.G.	DATE: 07/04/87	PROJECT:	DRAWING No: AECB-01

Figure 2-7: Selected Orientations of Compact Tension Specimens Cut from A106 Pipe Steel. Fracture Surfaces for Specimens A and C coincide with the 0 Plane. Fracture Surfaces for Specimens B and D coincide with

C. J-RESISTANCE CURVES

1. General

The experimental data obtained from all tests carried out and identified in the test matrices for both the plate steel and pipe steel (as presented in Tables 2-1 and 2-2) are presented in Appendix B. In Figure B-9, for example, the six duplicate tests, coded PIPE 10.C1 through to PIPE 10.C6 are independently identified. In this section, the results of each such set of tests have been grouped together and a J-resistance curve for this particular data set developed. The data points shown in Figure B-9 are shown as one in Figure 3-9. A power law function given by $J = H(\Delta a)^n$ has been fitted to this data using a least squares approach. It will be noted that all data points in Figure B-9 coincide exactly with those in Figure 3-9. In developing the J-resistance curves, the data points below 100 KJ/m^2 as well as all negative 'Δa' values have been neglected. This is further discussed in Appendix A.

2. Analysis of Test Data

Figures 3-1 through to 3-14 illustrate the J-resistance curves determined for each test case. To avoid confusion, a brief overview of these graphical results is given below for the plate steel and pipe steel specimens.

2.2 Plate Steel Results

Figures 3-1 to 3-3 illustrate the J-resistance curves obtained for the three point bend tests when using 0.5, 1.0 and 1.25 inch thick specimens respectively. The corresponding set of results when using compact tension specimens as opposed to three point bend tests are given in Figures 3-4 to 3-6 for the three specimen thicknesses.

2.3 Pipe Steel Results

Figures 3-7 to 3-16 provide all J-resistance curves derived from experimental data using compact test specimens which are 1 inch (Figures 3-7 to 3-10), 1.25 inches (Figures 3-11 and 3-12) and 0.5 inches (Figures 3-13 to 3-16) thick respectively.

The multiple J-resistance curves so determined for each particular thickness of compact tension specimen tested serve to assess the influence of orientation and location of the specimen in relation to the parent material from which the specimen was cut. The empirical constants for each of the J-resistance curves presented in Figures 3-1 through to 3-16 are recorded in Table 3-1. It will be noted that the magnitude of the constants H and n exhibit considerable variation; no attempt has been made to normalize these constants with respect to either H or n, since there is no reference point on which to base such calculations.

For the J-resistance curves presented in Figures 3-1 through to 3-16, the corresponding blunting line, given by $J = 2\sigma_f \Delta a$ where σ_f is the flow stress, has been superimposed on each illustration. The flow stress is defined as the arithmetic mean of the yield and ultimate tensile stress of the test material. An effective blunting line drawn parallel to the blunting line passing through the origin but offset by a crack extension of 0.15 mm is also shown. The point of intersection between the effective blunting line and the power law function can be determined.

Using only those experimental results for crack extension which exceed this intersection value of Δa, a least squares linear regression analysis was carried out to determine the R-line (defined below) for values of Δa beyond the effective blunting line. The intersection of the R-line and the blunting line defines an estimate of J_{IC}. It will be observed that it was not possible given the small crack extensions to determine the R-line for each of the test data sets presented in Figures 3-1 to 3-16.

The key relationships required to estimate the J_{IC} value are summarized below:

i) solution for point of intersection of the power law function and the effective blunt line is given by

$$H(\Delta a)^n - 2\sigma_f \Delta a + 2\sigma_f(0.15) = 0$$

ii) least squares linear regression for data points which exceed Δa determined in (i), to yield the R-line:

$$J = \alpha + \beta \Delta a$$

iii) solve for the intersection, i.e. Δa value of the R-line and the blunting line

$$\Delta a = \frac{\alpha}{(2\sigma_f - \beta)} = \Delta a_J$$

iv) the value of J at this value of Δa_J is given by

$$J_{IC} = 2\sigma_f \Delta a_J$$

The material properties for the yield and ultimate tensile stress of the plate and pipe steel used in this study are presented in Table 3-2. This information was obtained from experimental tensile tests carried out on the pipe material and on 0.5, 1.0 and 1.25 inch thick plate steel. This data was used to determine the blunting line for the respective specimens. A true stress–strain curve for the SA106 pipe steel is presented in Figure 3-17.

Table 3-1: Constants H and n for J-Resistance Curves

(a) Plate Tests

PLATE TESTS: ASTM516 PLATE STEEL		
SPECIMEN CODE	CONSTANTS H	n
CT05.1-5	286	0.238
CT10.1-8	280	0.464
CT125.1-4	231	0.766
B05TL.1-4	298	0.301
B10TL.1-4	349	0.390
B125TL.1-4	365	0.106

(b) Pipe Tests

PIPE TESTS: SA106 PIPE STEEL		
SPECIMEN CODE	CONSTANTS H	n
PIPE 05.AO1-5	166	0.146
PIPE 05.AC1-5	193	0.209
PIPE 05.AI1-5	159	0.113
PIPE 05.B1-6	325	0.240
PIPE 10.A1-6	202	0.371
PIPE 10.B1-6	396	0.458
PIPE 10.C1-6	253	0.402
PIPE 10.D1-6	437	0.496
PIPE 125.A1-6	195	0.213
PIPE 125.B1-6	384	0.383

Table 3-2: Material Properties

Material	σ_y MPa	σ_{ult} MPa	$2\sigma_f$ MPa
0.5 inch thick ASTM516 plate steel	360	545	905
1.0 inch thick ASTM516 plate steel	304	503	807
1.25 inch thick ASTM plate steel	327	533	860
SA106 pipe steel	288	600	888

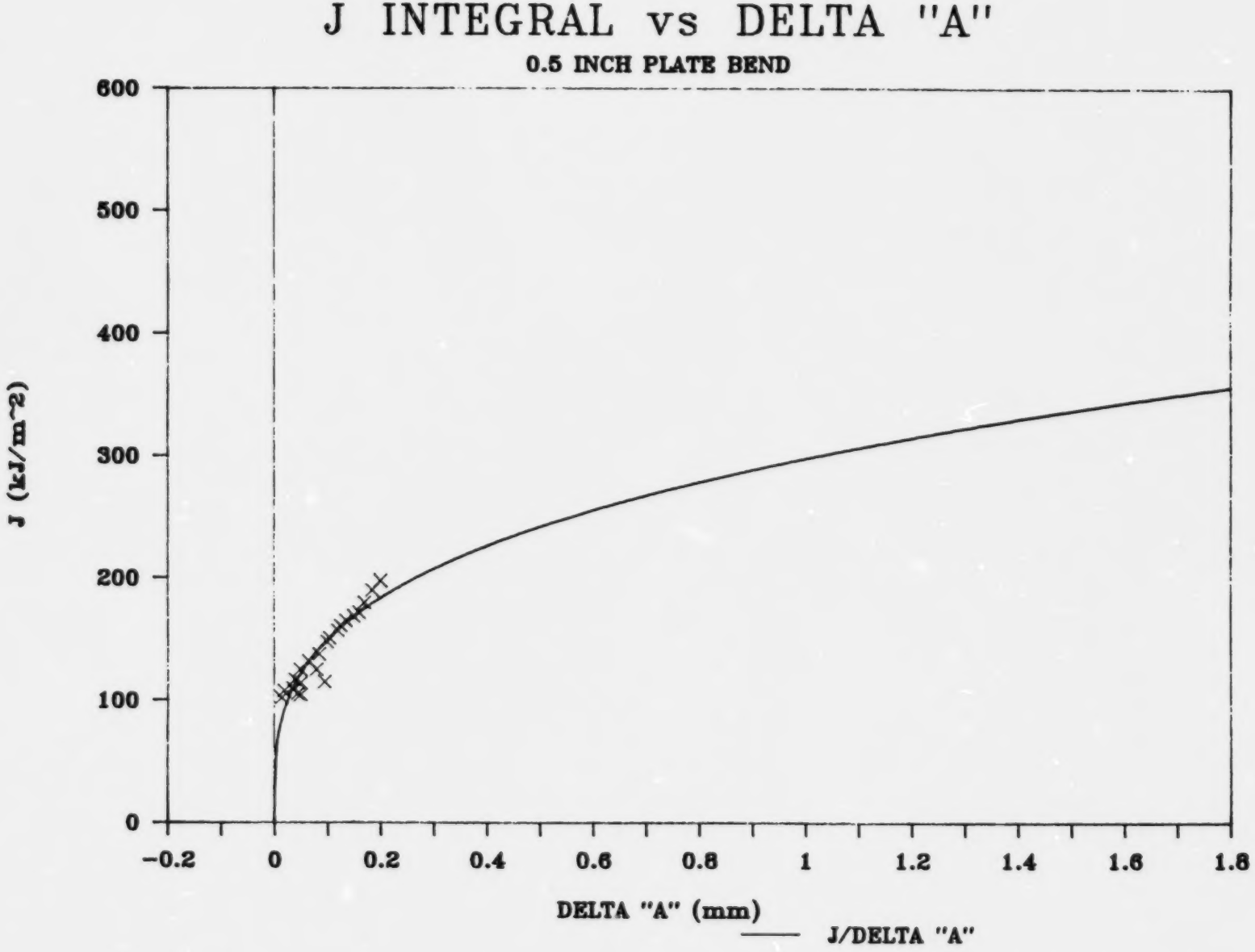

Figure 3-1: J-Resistance Curve Fitted to Data for 0.5 inch Thick Plate Steel Bend Test Specimens.

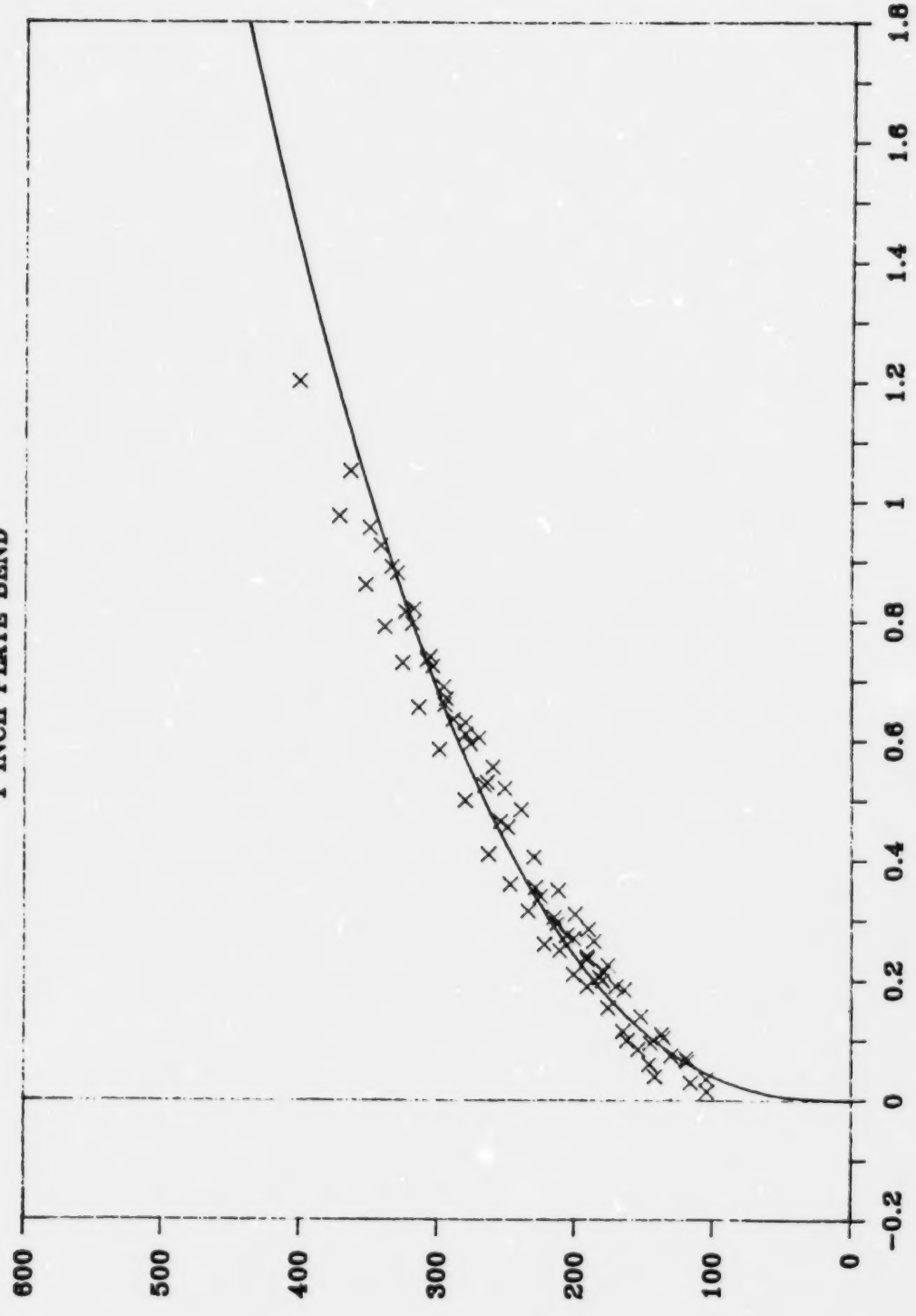

Figure 3-2: J-Resistance Curve Fitted to Data for 1.0 inch Thick Plate Steel Bend Test Specimens.

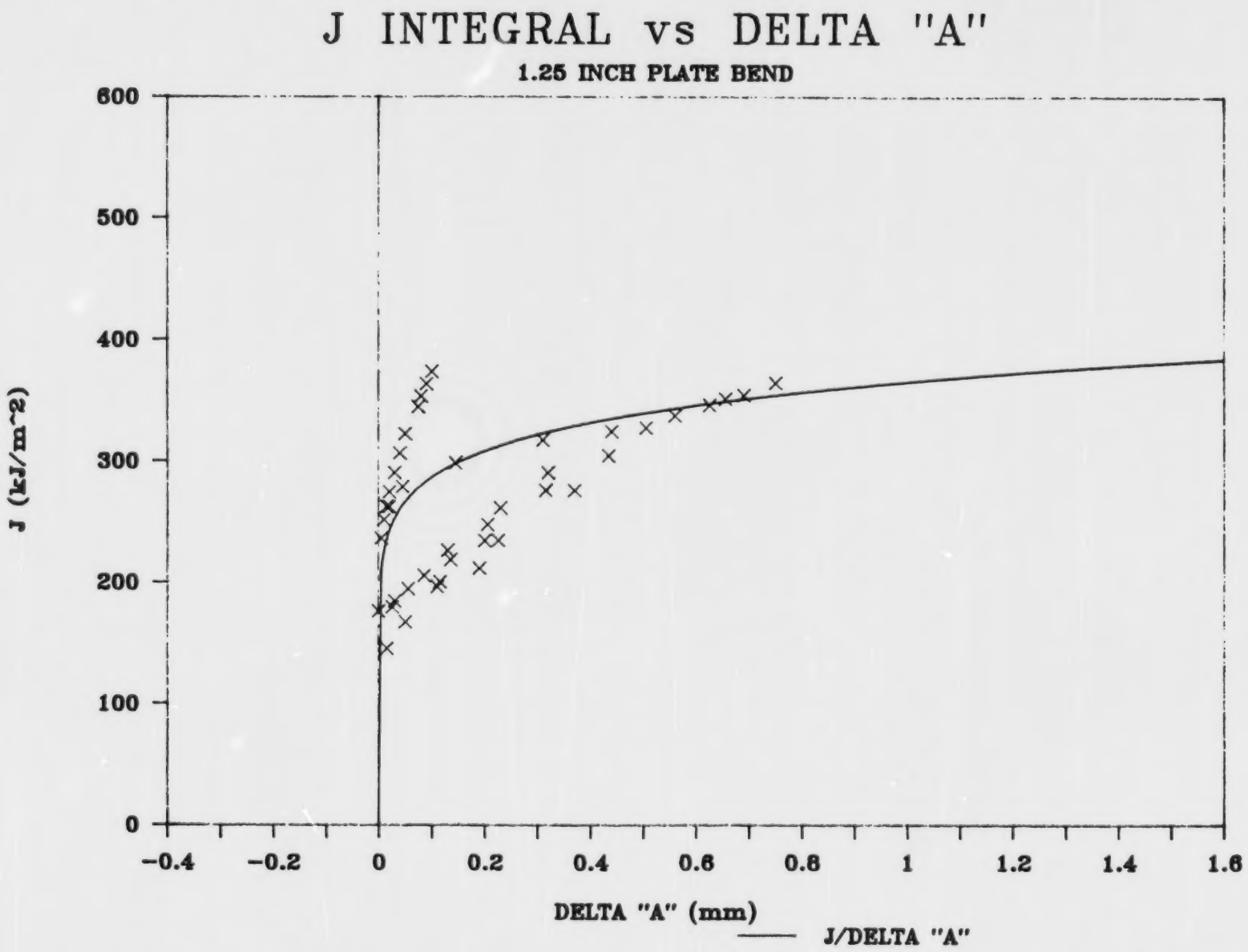

Figure 3-3: J-Resistance Curve Fitted to Data for 1.25 inch Thick Plate Steel Bend Test Specimens.

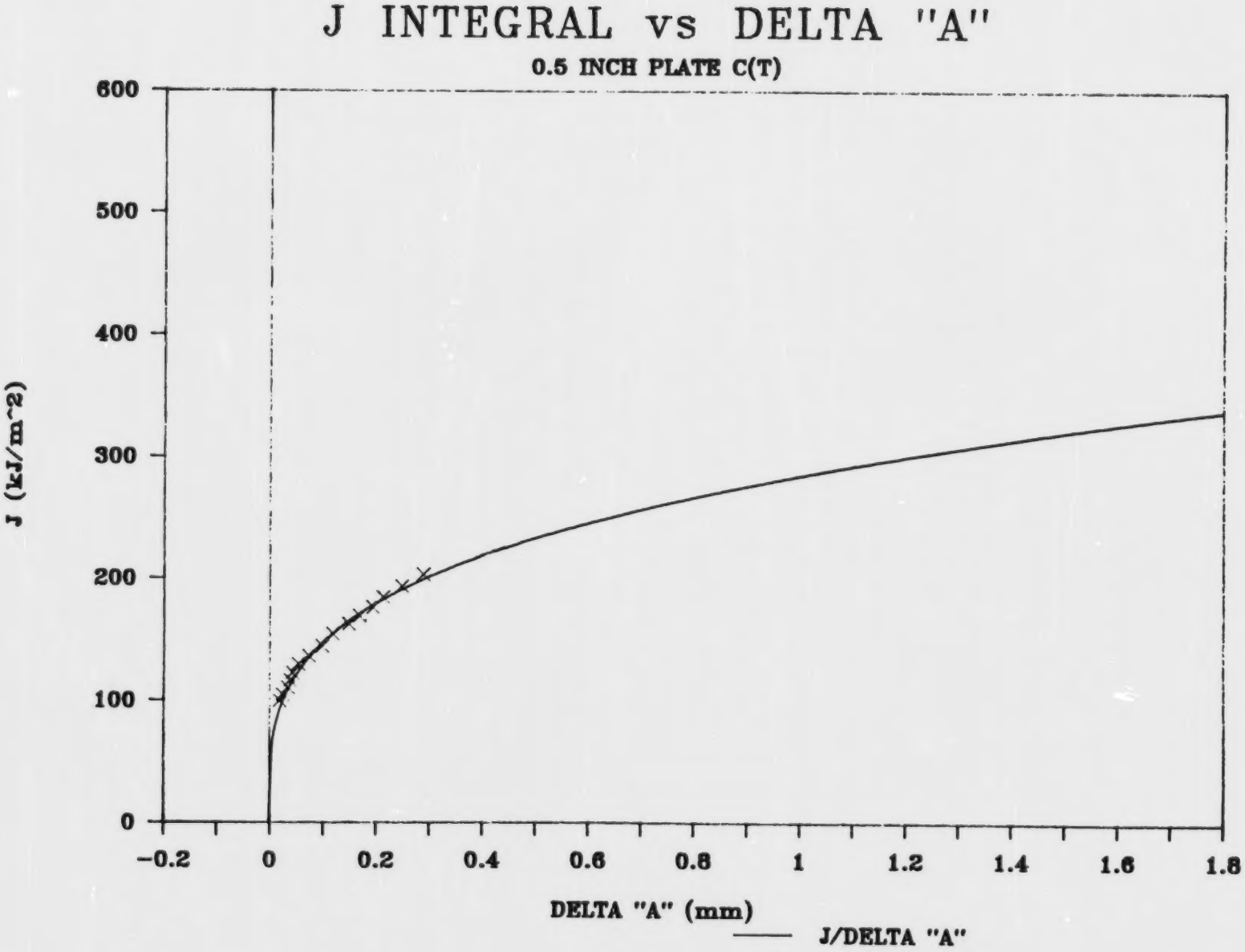

Figure 3-4: J-Resistance Curve Fitted to Data for 0.5 inch Thick Plate Steel Compact Tension Test Specimens.

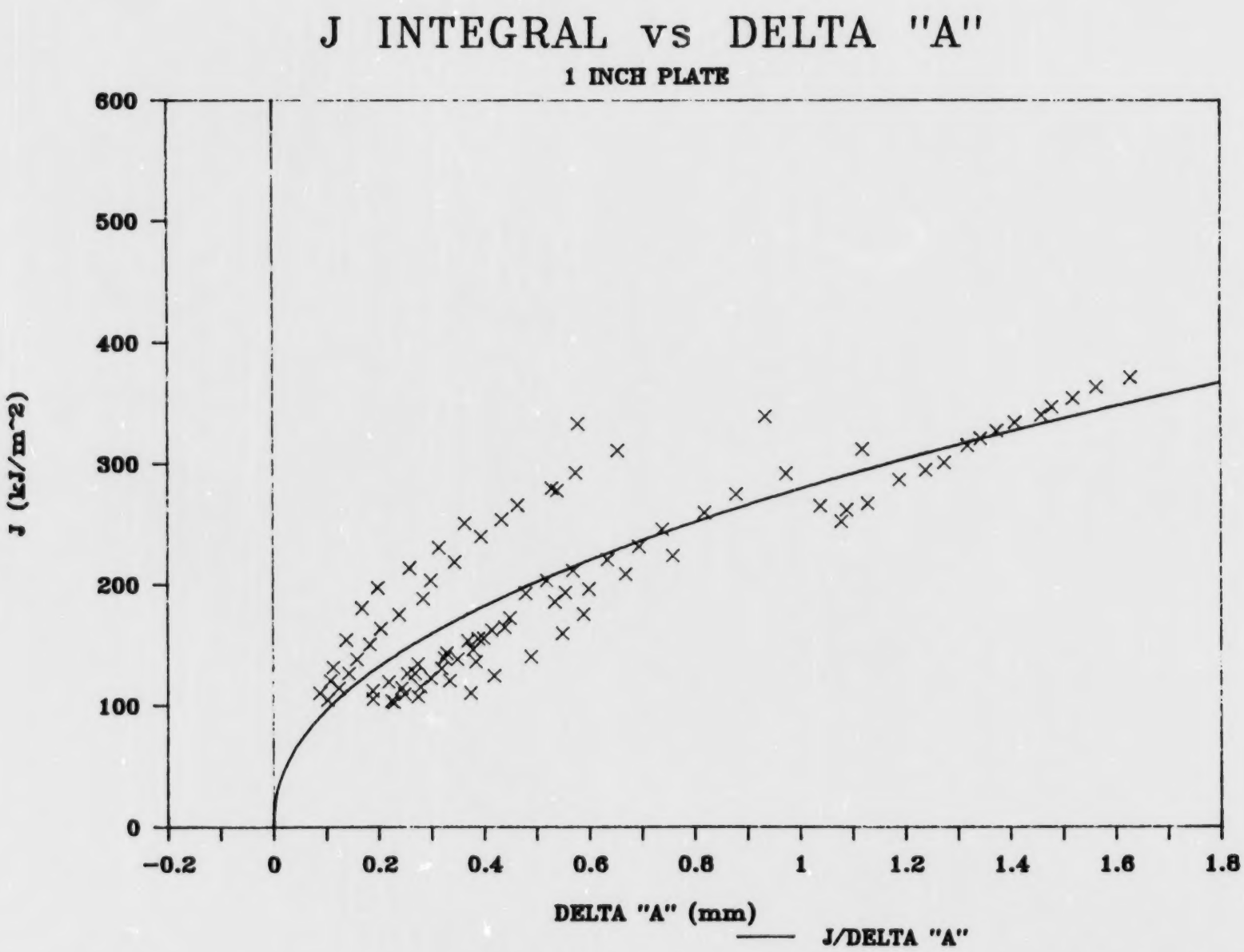

Figure 3-5: J-Resistance Curve Fitted to Data for 1.0 inch Thick Plate Steel Compact Tension Test Specimens.

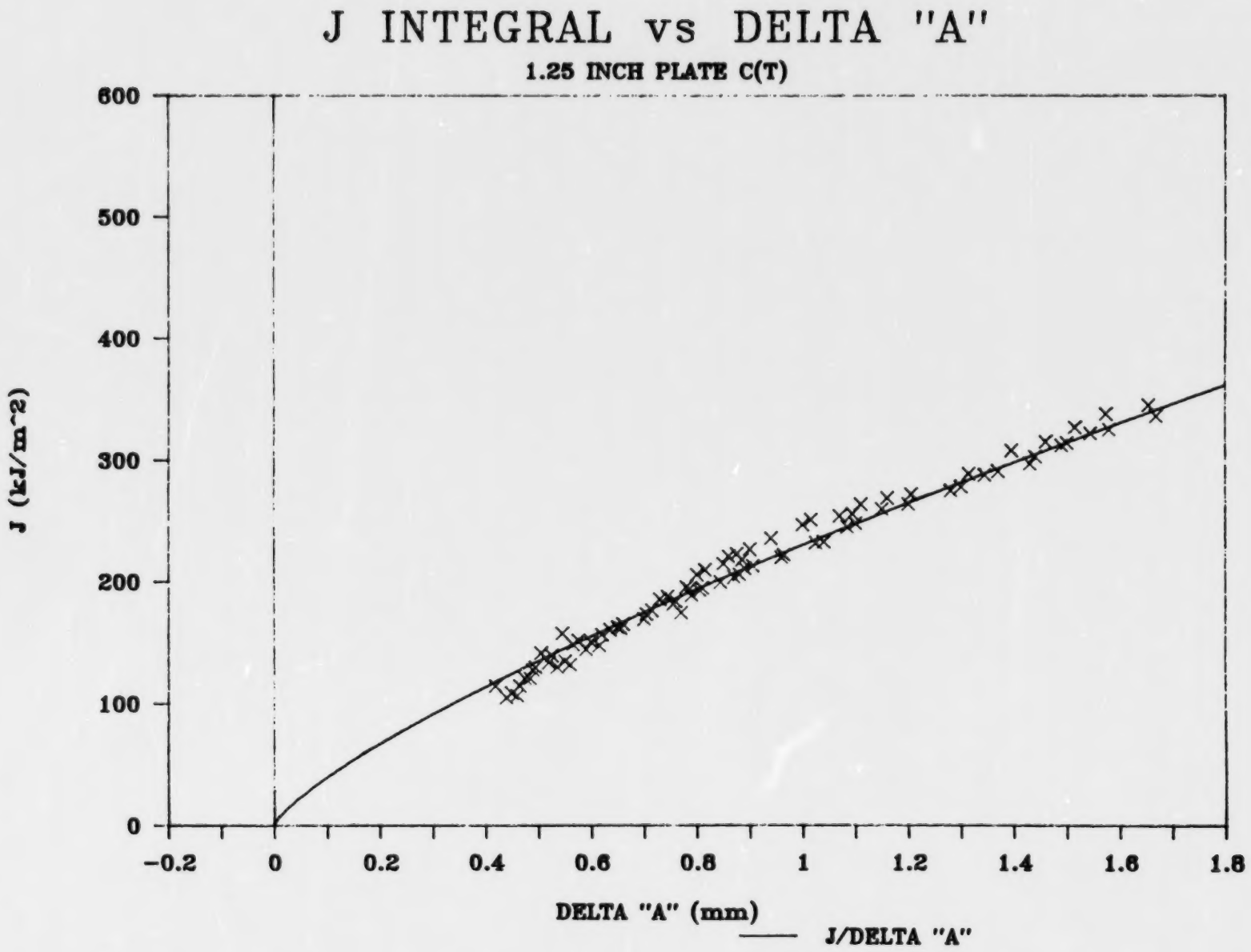

Figure 3-6: J-Resistance Curve Fitted to Data for 1.25 inch Thick Plate Steel Compact Tension Test Specimens.

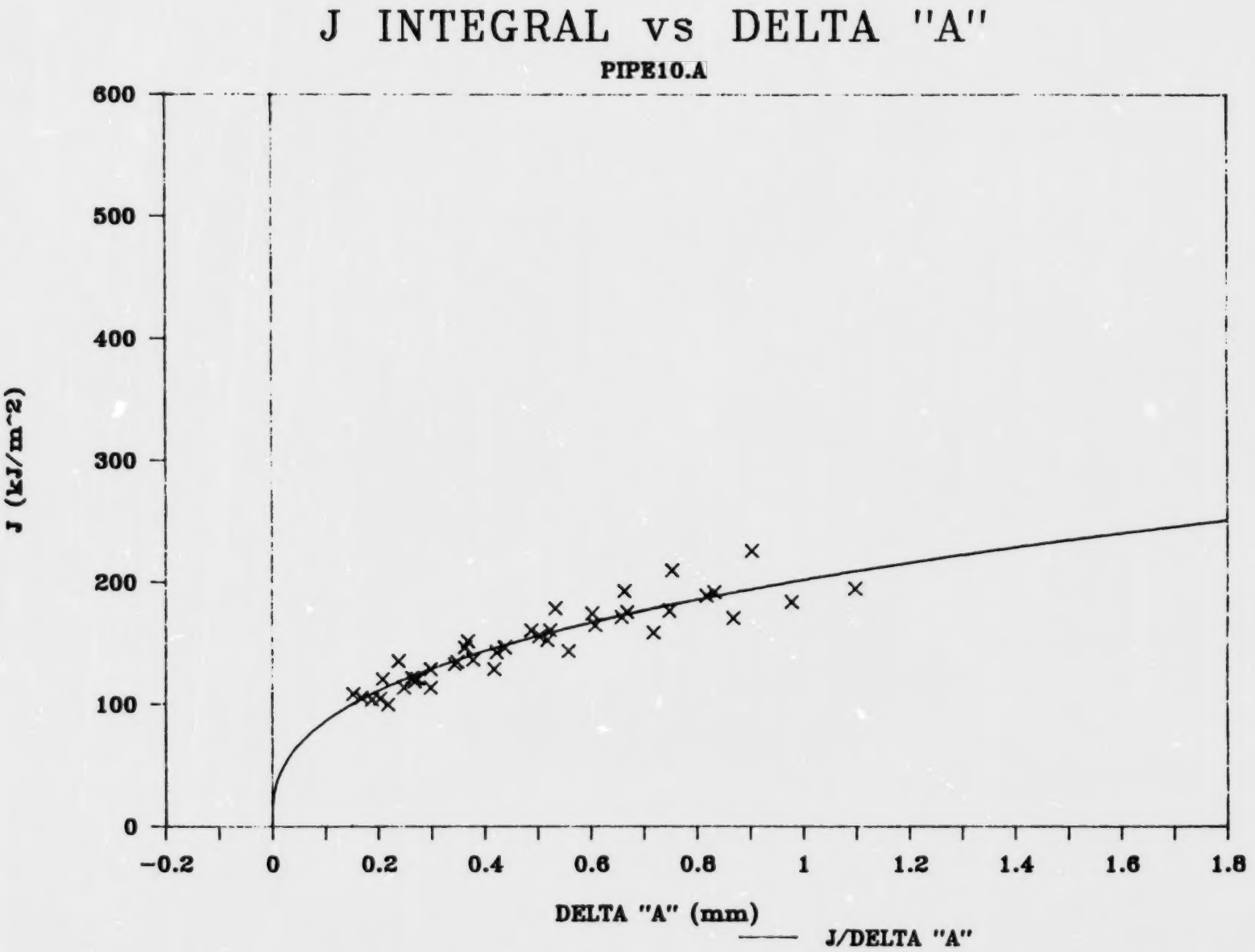

Figure 3-7: J-Resistance Curve Fitted to Data for 1.0 inch Thick Pipe Steel Compact Tension Test Specimens. Specimens Coded as PIPE 10.A1-6, Indicating 'A' Orientation.

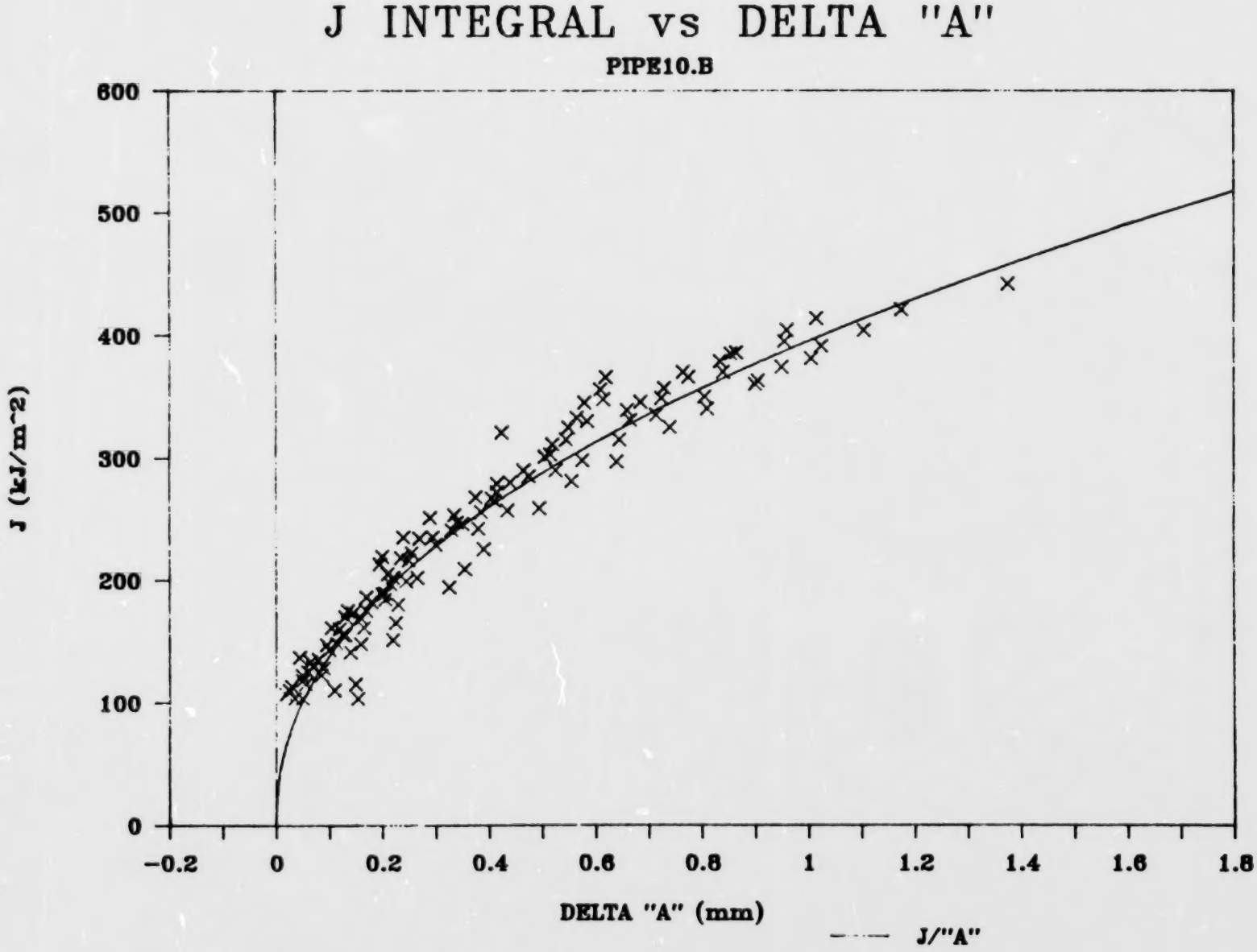

Figure 3-8: J-Resistance Curve Fitted to Data for 1.0 inch Thick Pipe Steel Compact Tension Test Specimens. Specimens Coded as PIPE 10.B1-6, Indicating 'B' Orientation.

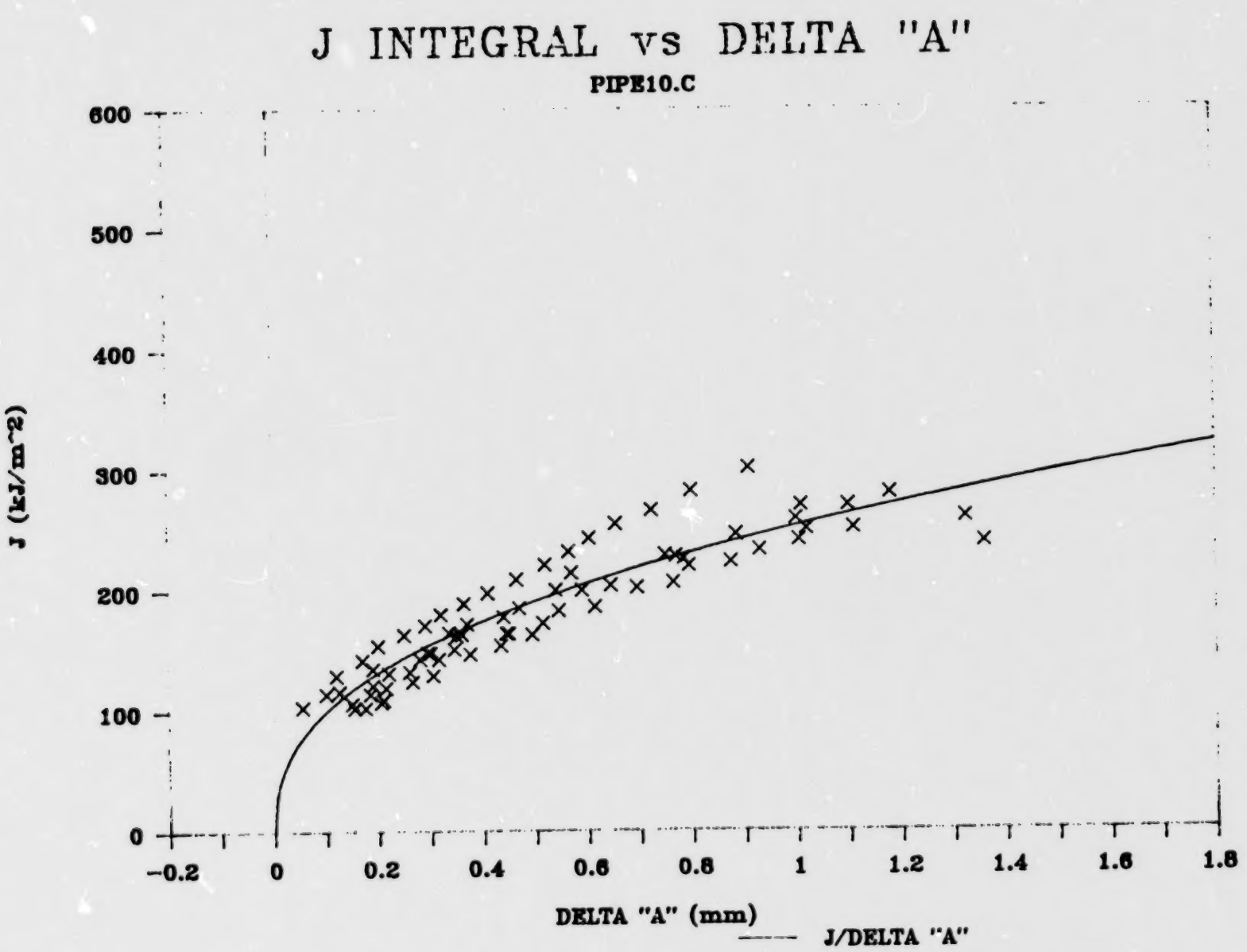

Figure 3-9: J-Resistance Curve Fitted to Data for 1.0 inch Thick Pipe Steel Compact Tension Test Specimens. Specimens Coded as PIPE 10.C1-6, Indicating 'C' Orientation.

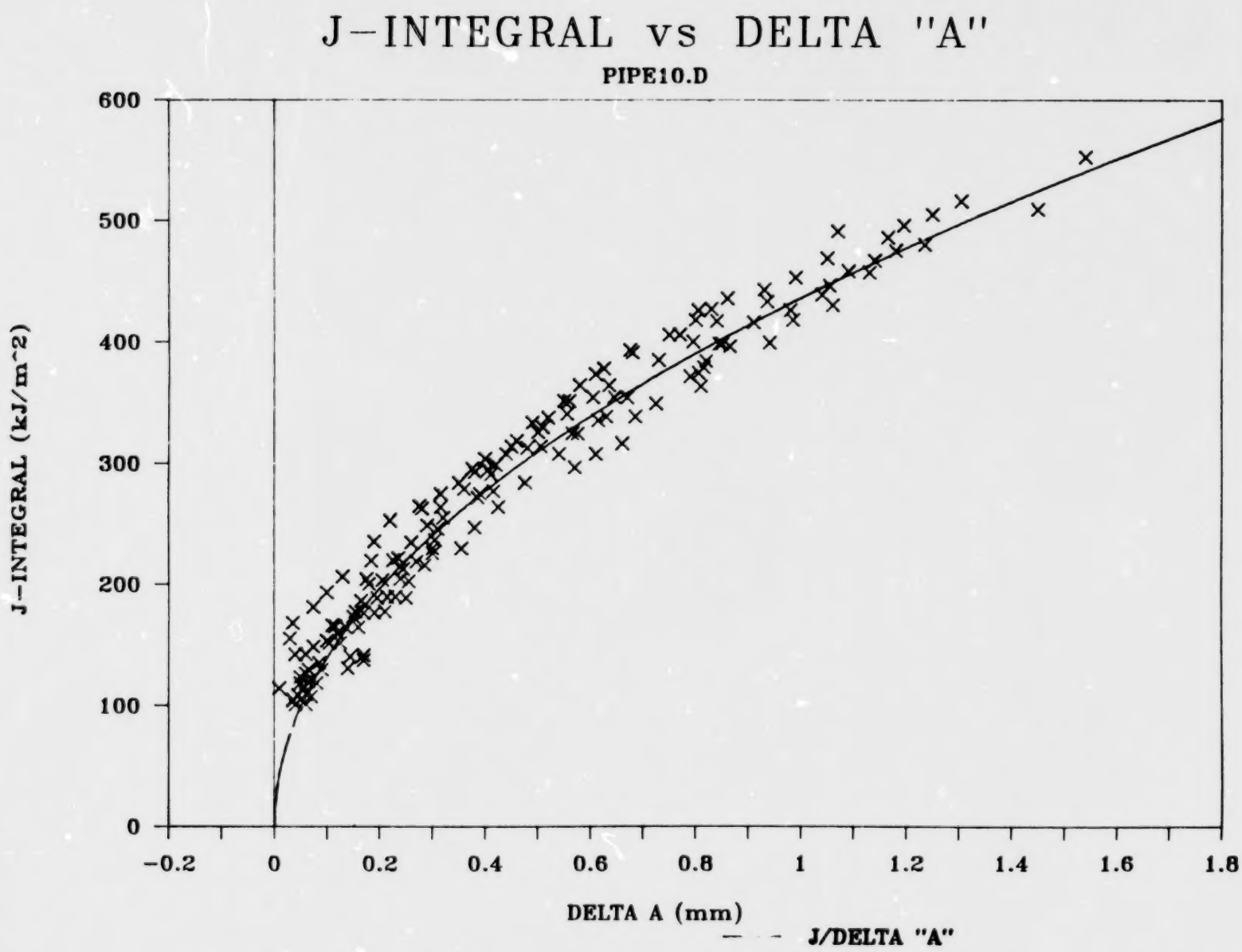

Figure 3-10: J-Resistance Curve Fitted to Data for 1.0 inch Thick Pipe Steel Compact Tension Test Specimens. Specimens Coded as PIPE 10.D1-6, Indicating 'D' Orientation.

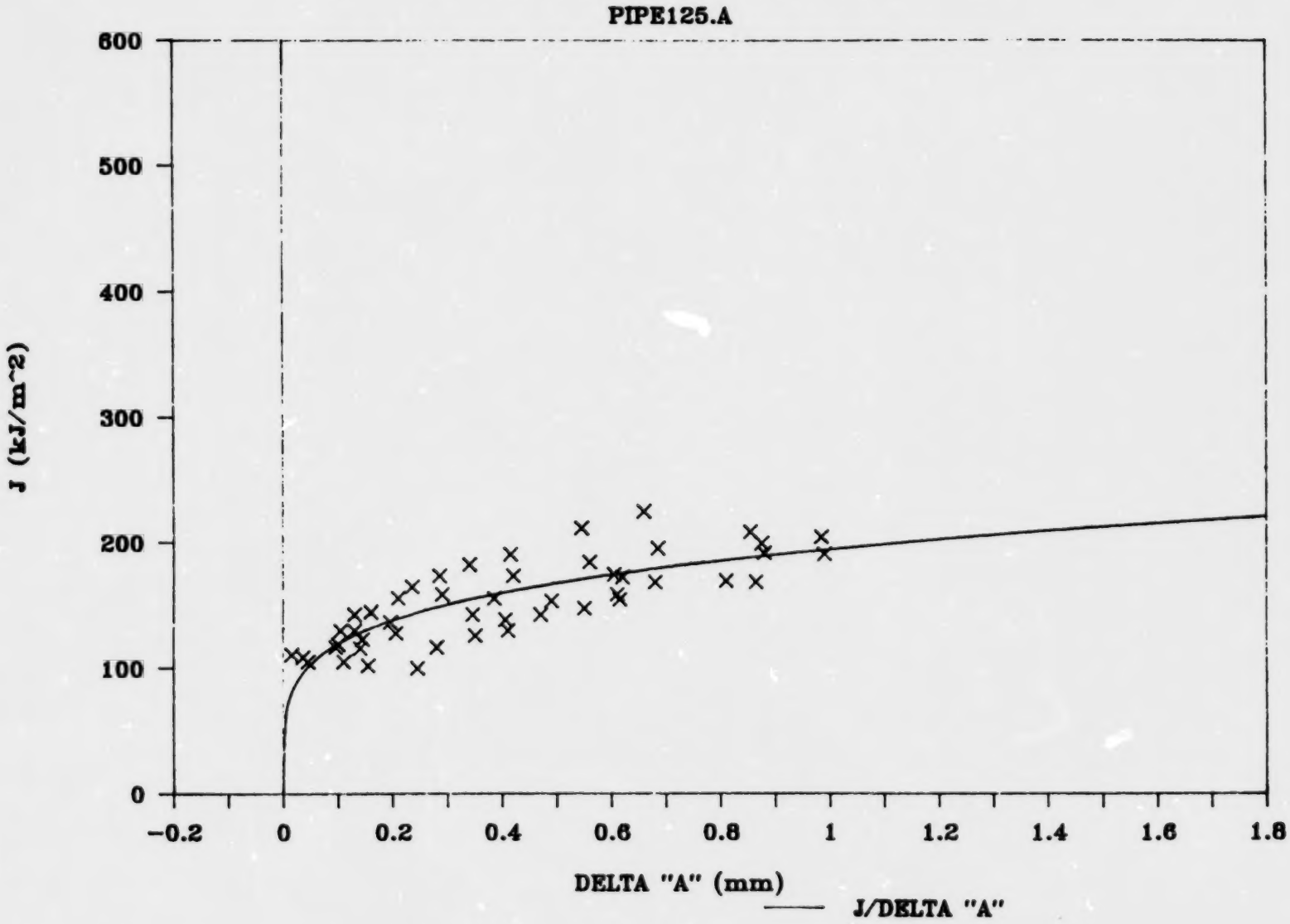

Figure 3-11: J-Resistance Curve Fitted to Data for 1.25 inch Thick Pipe Steel Compact Tension Test Specimens. Specimens Coded as PIPE 125.A1-6, Indicating 'A' Orientation.

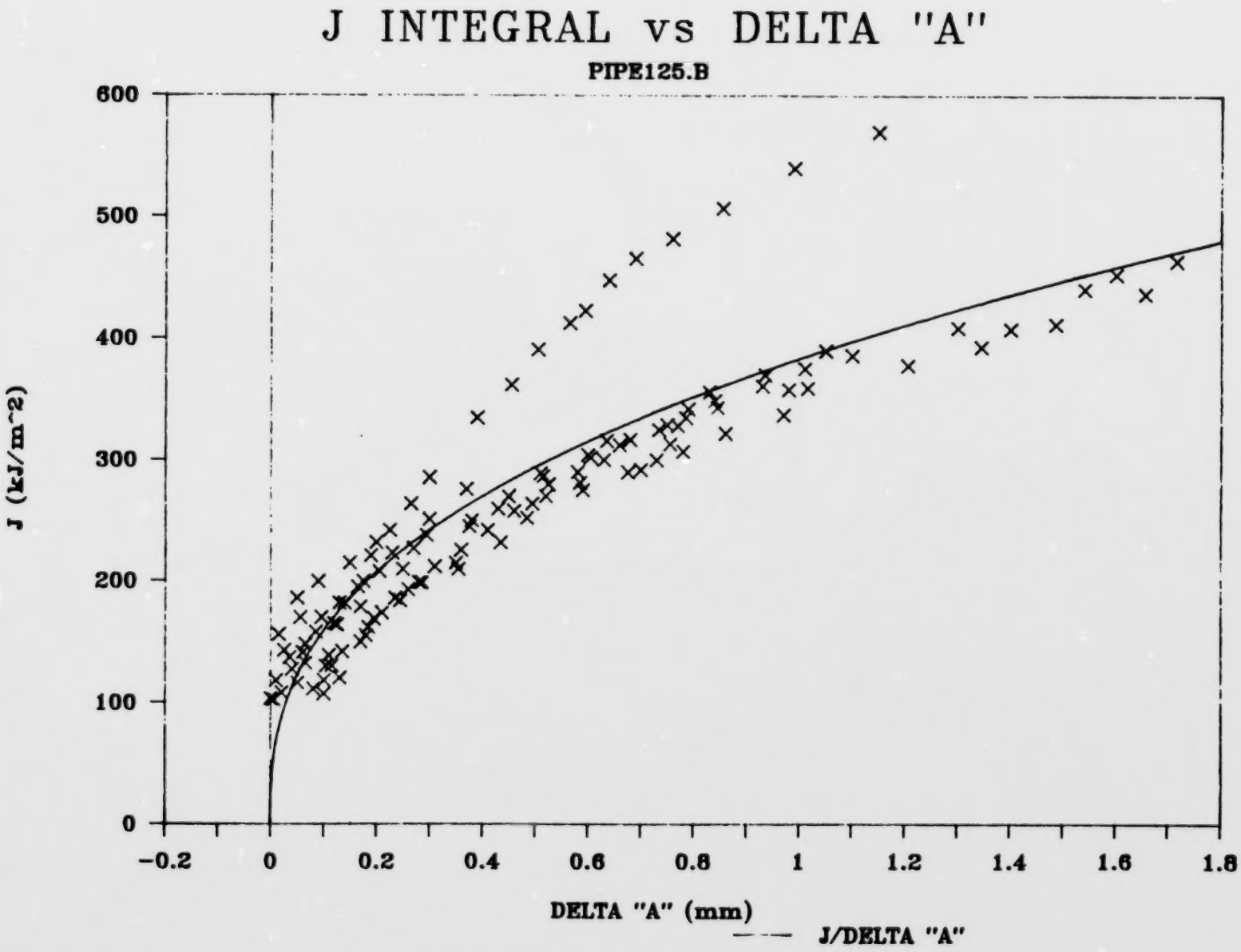

Figure 3-12: J-Resistance Curve Fitted to Data for 1.25 inch Thick Pipe Steel Compact Tension Test Specimens. Specimens Coded as PIPE 125.B1-6, Indicating 'B' Orientation.

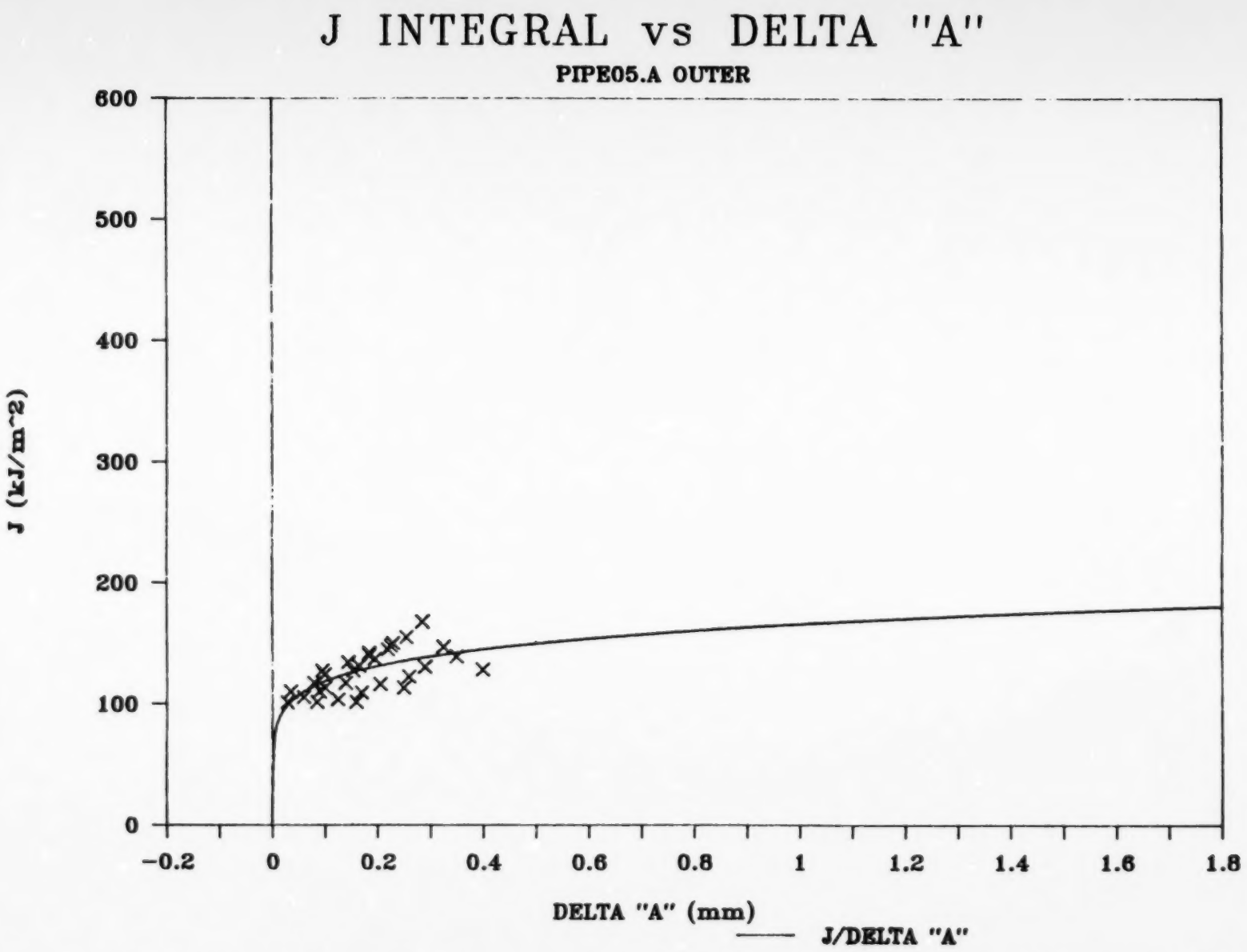

Figure 3-13: J-Resistance Curve Fitted to Data for 0.5 inch Thick Pipe Steel Compact Tension Test Specimens. Specimens Coded as PIPE 05.A01-5, Indicating 'A' Orientation and 'O' Outer Location.

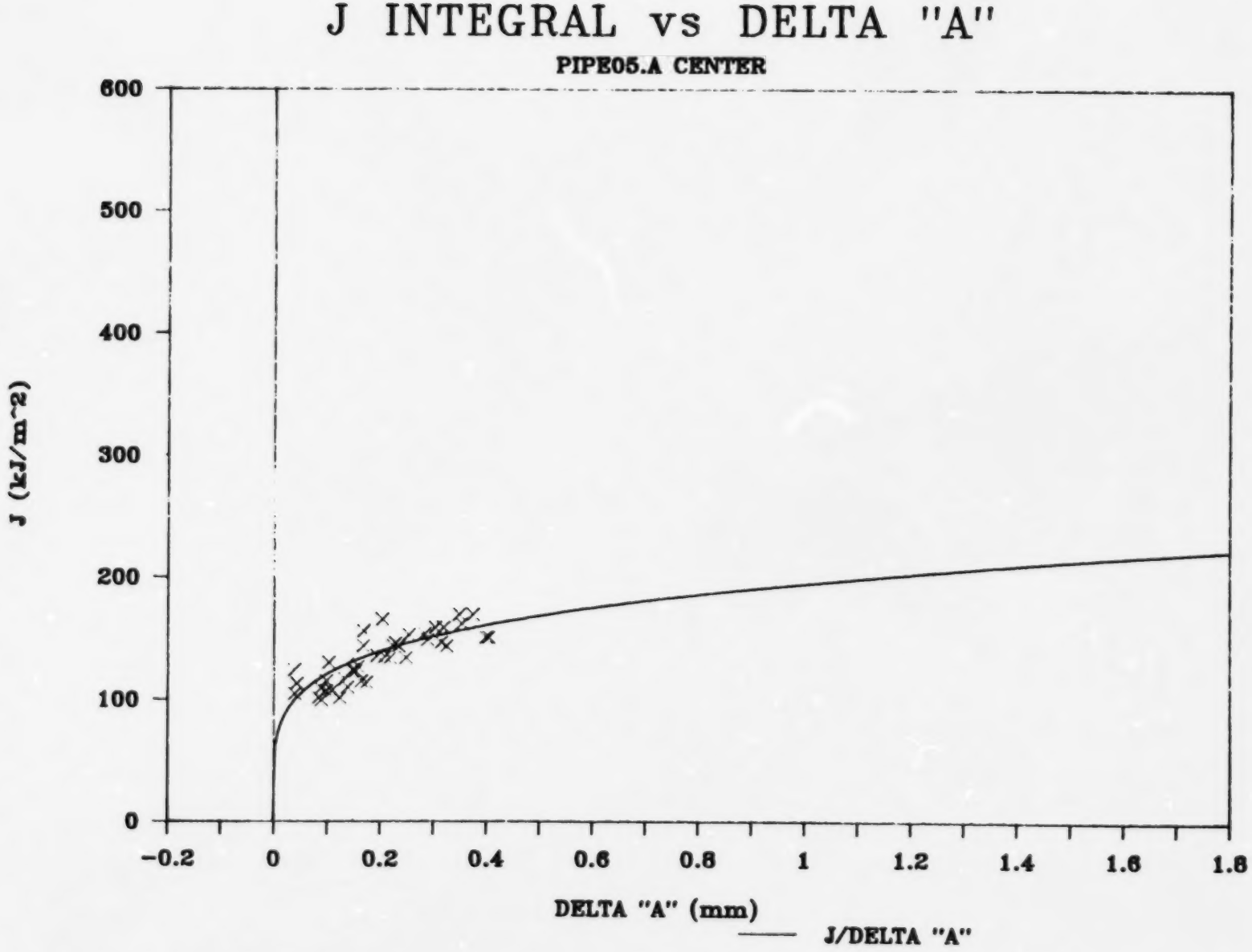

Figure 3-14: J-Resistance Curve Fitted to Data for 0.5 inch Thick Pipe Steel Compact Tension Test Specimens. Specimens Coded as PIPE 05.AC1-5, Indicating 'A' Orientation and 'C' Center Location.

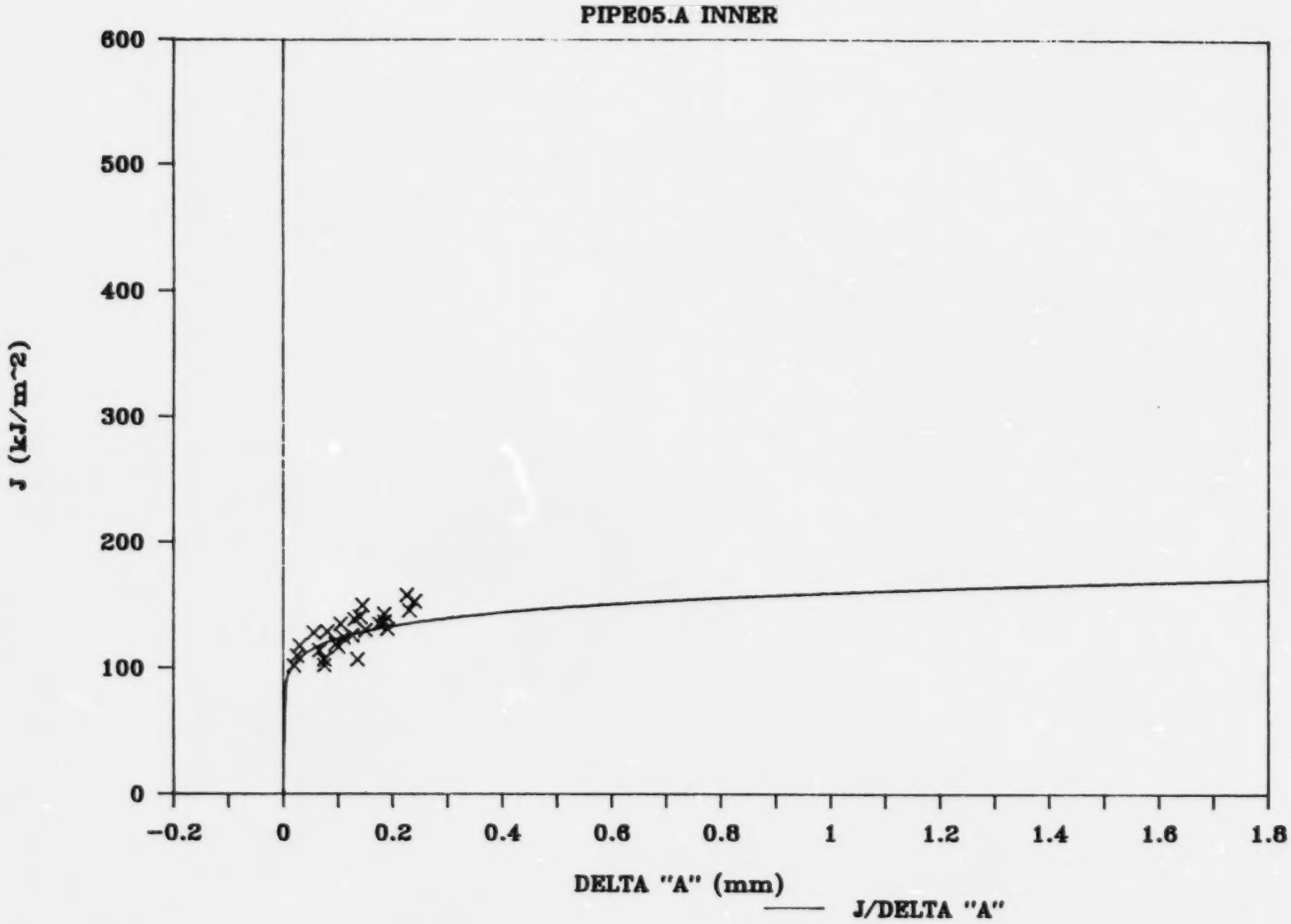

Figure 3-15: J-Resistance Curve Fitted to Data for 0.5 inch Thick Pipe Steel Compact Tension Test Specimens. Specimens Coded as PIPE 05.A11-5, Indicating 'A' Orientation and '1' Inner Location.

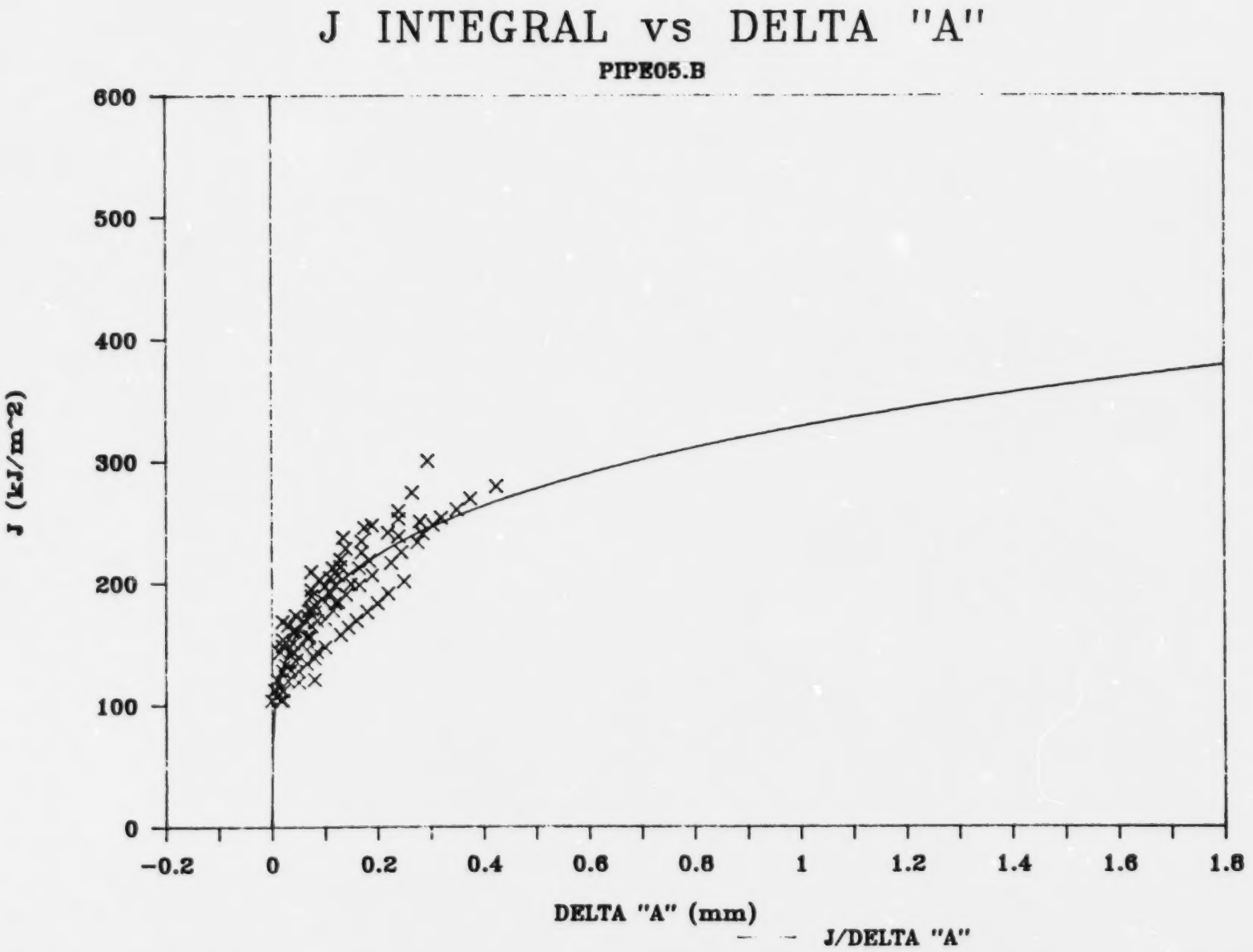

Figure 3-16: J-Resistance Curve Fitted to Data for 0.5 inch Thick Pipe Steel Compact Tension Test Specimens. Specimens Coded as PIPE 05.B1-5, Indicating 'B' Orientation.

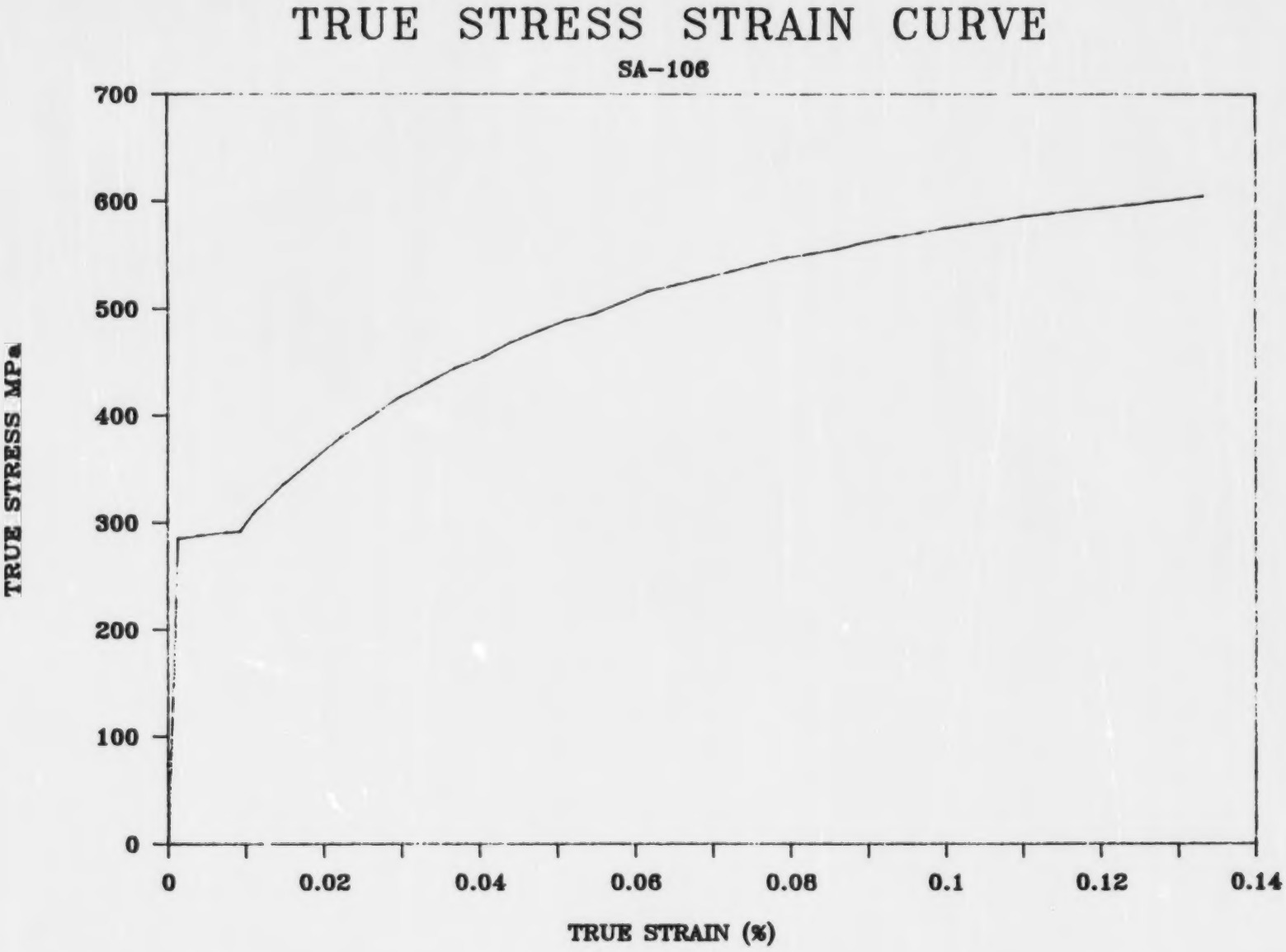

Figure 3.17: Stress-strain curve for SA106 grade B Pipe Steel.

D. COMPARISON OF J-RESISTANCE CURVES

1. General

Figures 4-1 through to 4-7 provide a summary of the results obtained in this study. Each of the figures is a composite of J-resistance curves which serve to assess i) the influence of specimen orientation and location of specimen within the parent material, ii) the effect of specimen thickness and iii) the differences, in the case of the plate steel, of the results obtained from compact tension and three point bend tests.

All J-resistance curves shown have been plotted to represent that level of crack extension data obtained during each test; no theoretical extension of the J-resistance beyond this this level is shown on any of the illustrations in this section.

2. Plate Steel Results

Figures 4-1 and 4-2 provide a comparison of the J-resistance curves obtained from three point bend and compact tension specimen respectively for three different specimen thicknesses. These results, while limited, indicate the following:

i) a specimen size dependence, which is more clearly illustrated for the compact tension specimens

ii) lower J-resistance curves have been obtained for compact tension tests with increasing specimen thickness.

3. Pipe Steel Results

The influence of specimen orientation for 0.5 inch, 1.0 inch and 1.25 inch thick specimens in the 'A' and 'B' orientations is consistent for each of these thicknesses as shown in Figures 4-3 to 4-5 respectively. It will also be noted that the results for the 0.5 thick specimens in the 'A' orientation for specimens cut from the outer, center and inner locations of the through wall thickness yield very similar results. From this result, it can be concluded that the location of the specimen in the through wall thickness has a minimal influence on the developed J-resistance curves.

Figure 4-4 provides a complete set of orientation data for 1 inch thick specimens with orientations A, B, C and D. It will be noted, with reference to Figure 2-7, that the B and D orientations align the crack plane with the Z plane of the parent pipe, whereas the A and C orientations align the crack plane of the specimen with the θ direction. It is of interest to note the location of the B and D curves as compared with the A and C curves; the results for the 1.0 inch specimens do indicate a clear difference in the J-resistance curves coinciding with the crack plane coincident with the Z and θ planes. This observation is supported by the equivalent results obtained for the 0.5 inch (Figure 4-3) and the 1.25 inch (Figure 4-5) specimens. This correlation is more clearly illustrated in Figures 4-6 and 4-7 in which the effect of specimen thickness in both the 'A' and 'B' direction is presented.

It will be noted for each of these orientations that the effect of specimen thickness is negligible. Given these results it is recommended that the inch thick specimen could be considered as a reasonable laboratory standard; it is the smallest size specimen for which some crack extension (1–1.5 mm) can be obtained under load control conditions.

The J-resistance curves presented illustrate a significant dependence on the orientation of the test specimen as cut from the parent material. This behaviour is best illustrated by Figure 4-4 in which the J-resistance curves of the four orientations tested are compared. It should be emphasized that the sequence of tests carried out for each of these orientations was random which indicates that orientation differences in the J-resistance curves do exist. To further assess this result a pole figure of the SA106 pipe steel was obtained [Ref. 7]. The pole figure is presented in Figure 4-8 and illustrates no preferential orientation for the (110) plane so that the material is essentially isotropic. This metallurgical observation is not supported by the J-resistance curves obtained.

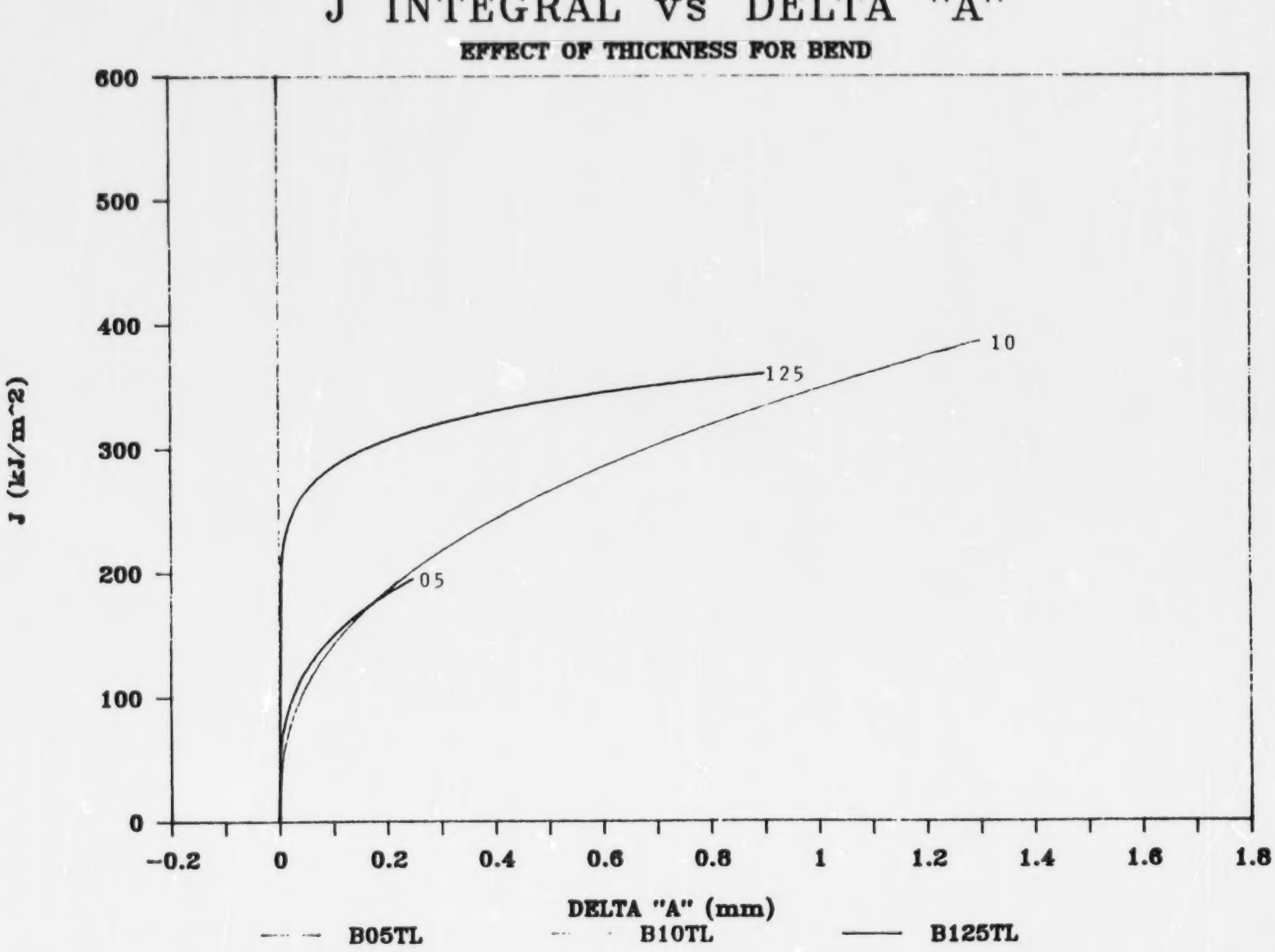

Figure 4-1: Comparison of J-Resistance Curves for Plate Steel Obtained from Three Point Bend Tests with Specimens of Different Thicknesses.

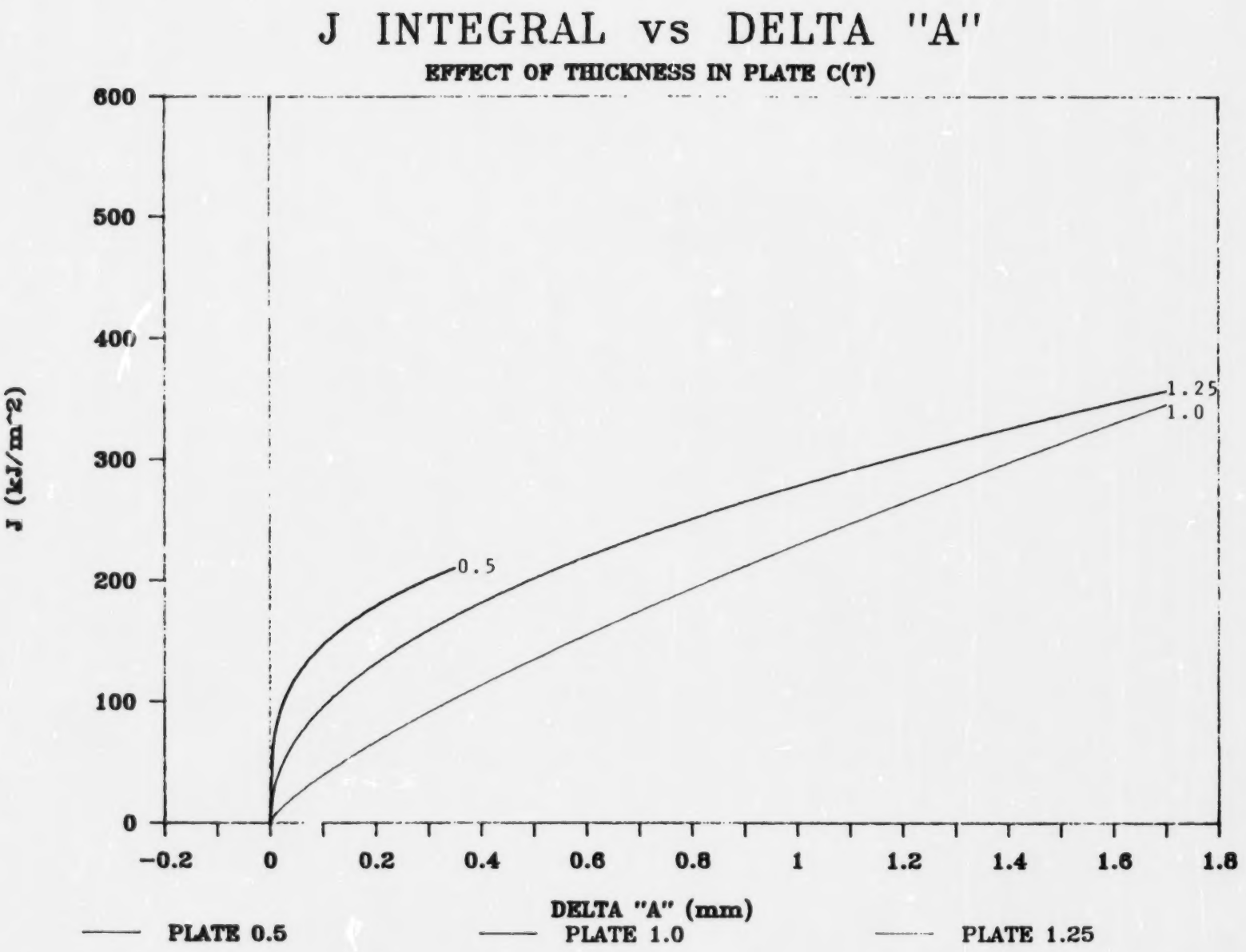

Figure 4-2: Comparison of J-Resistance Curves for Plate Steel Obtained from Compact Tension Tests with Specimens of Different Thicknesses.

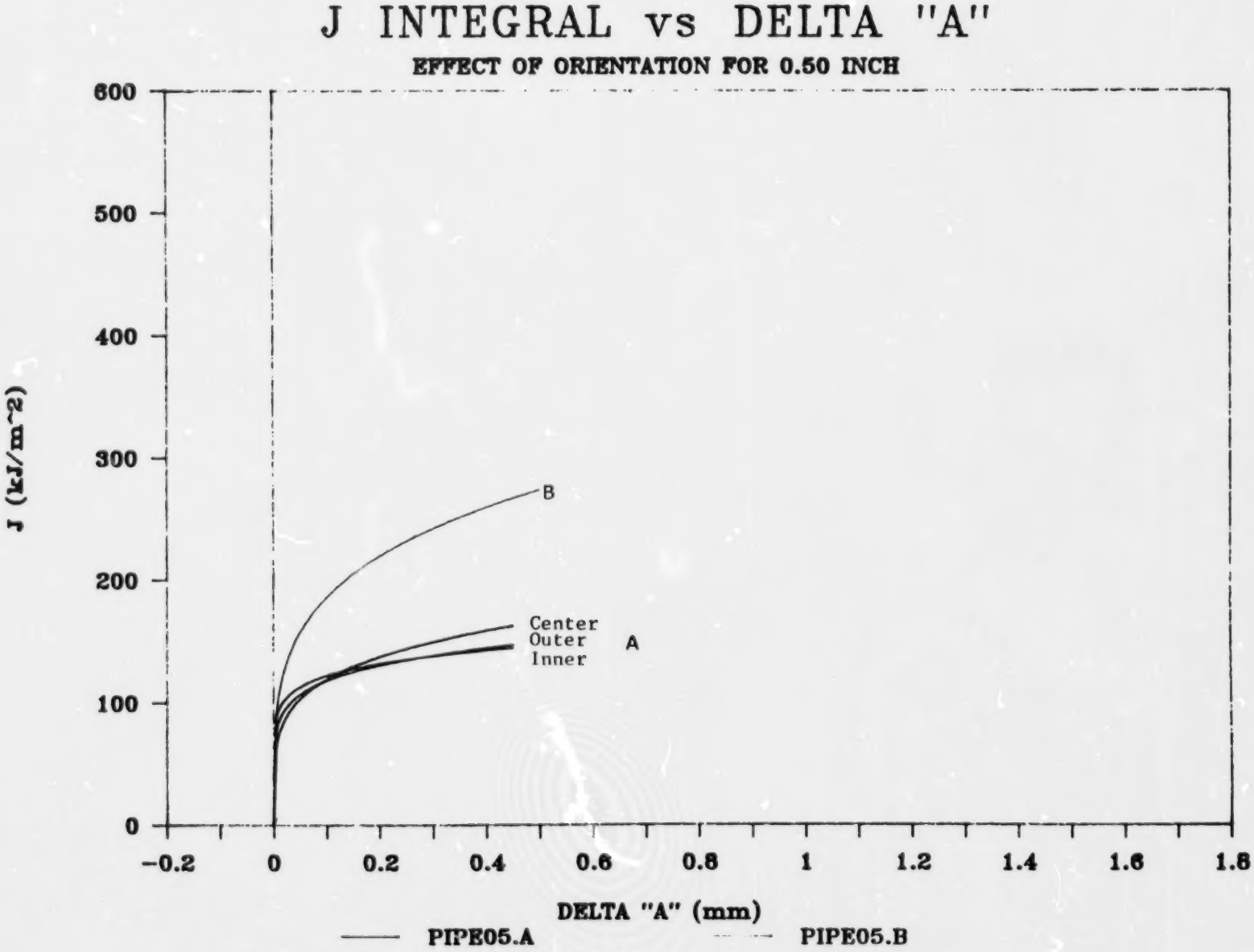

Figure 4-3: Comparison of J-Resistance Curves for Pipe Steel Obtained from 0.5 inch Compact Tension Specimens Selected from Orientation A and B.

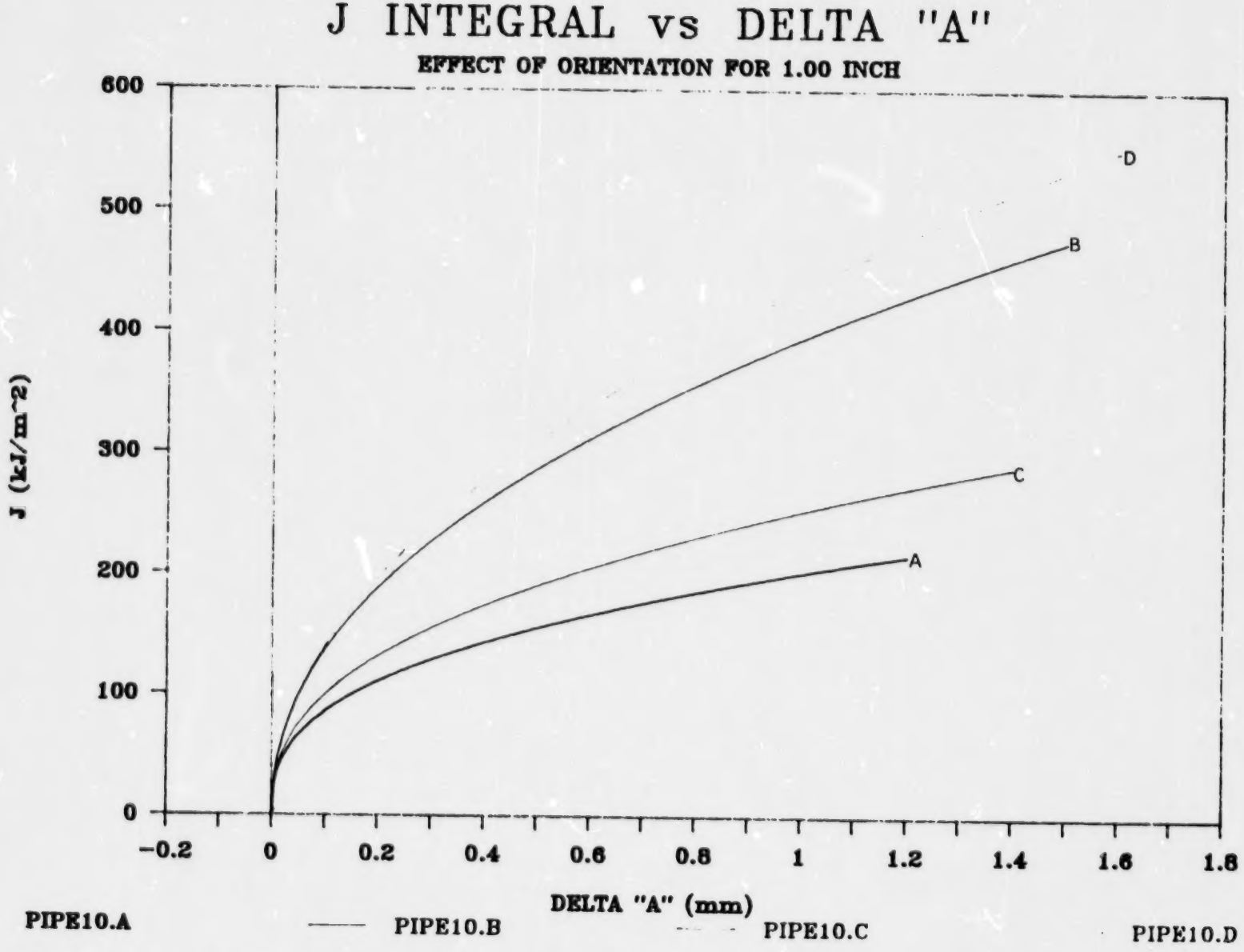

Figure 4-4: Comparison of J-Resistance Curves for Pipe Steel Obtained from 1.0 inch Compact Tension Specimens Selected from Orientations A, B, C and D.

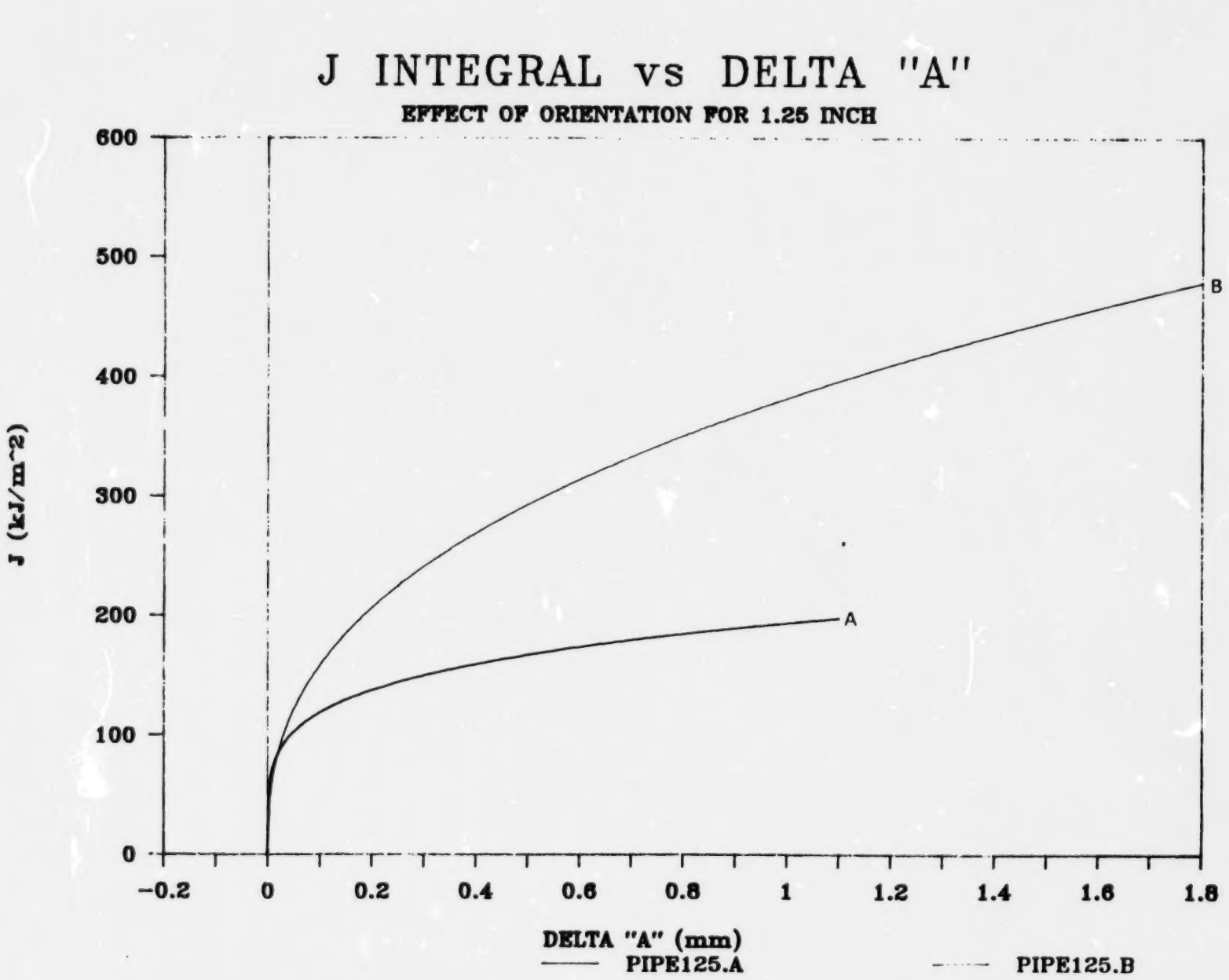

Figure 4-5: Comparison of J-Resistance Curves for Pipe Steel Obtained from 1.25 inch Compact Tension Specimens Selected from Orientation A and B.

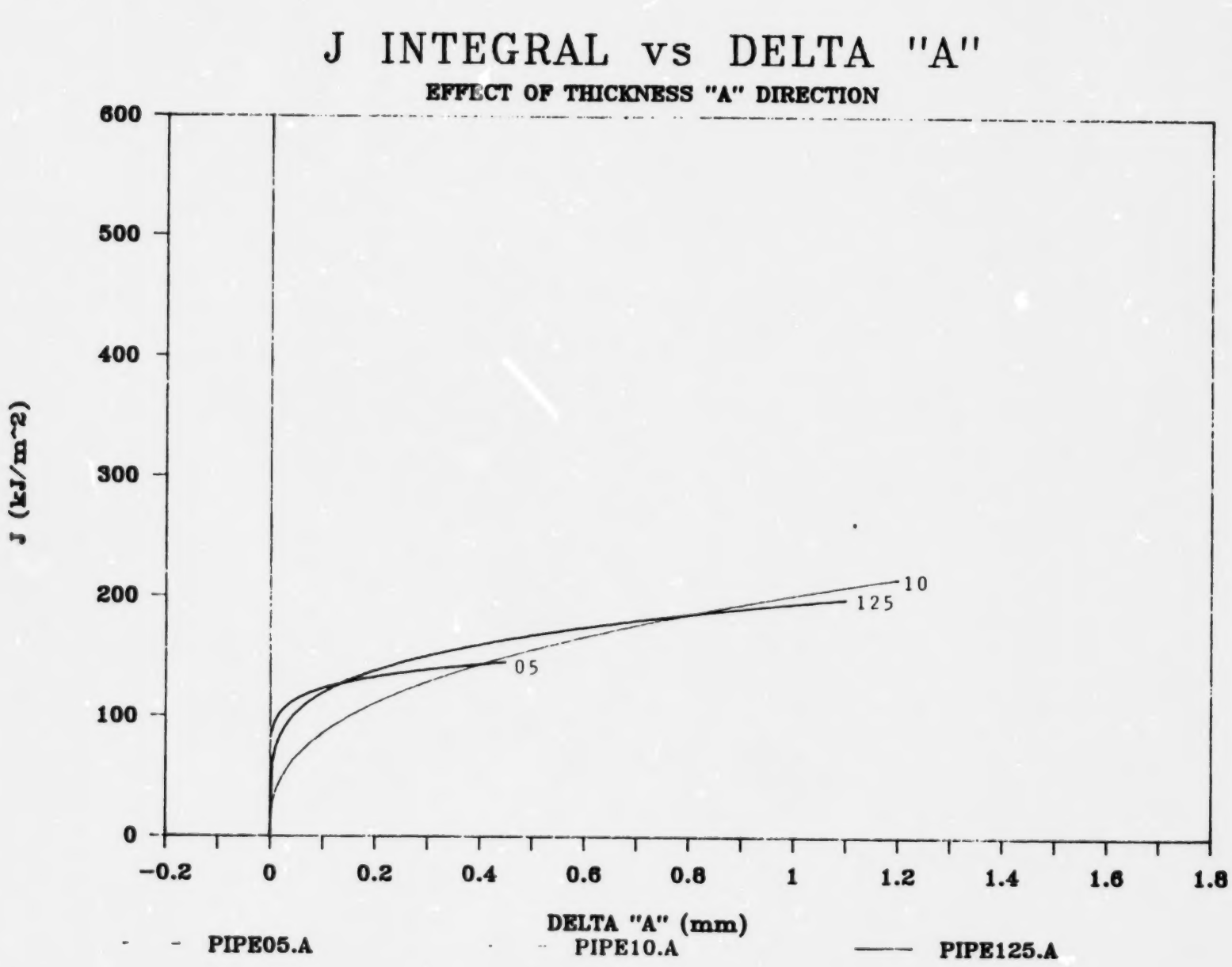

Figure 4-6: Comparison of J-Resistance Curves for Pipe Steel Obtained from Compact Tension Specimens of Different Thicknesses in the 'A' Direction.

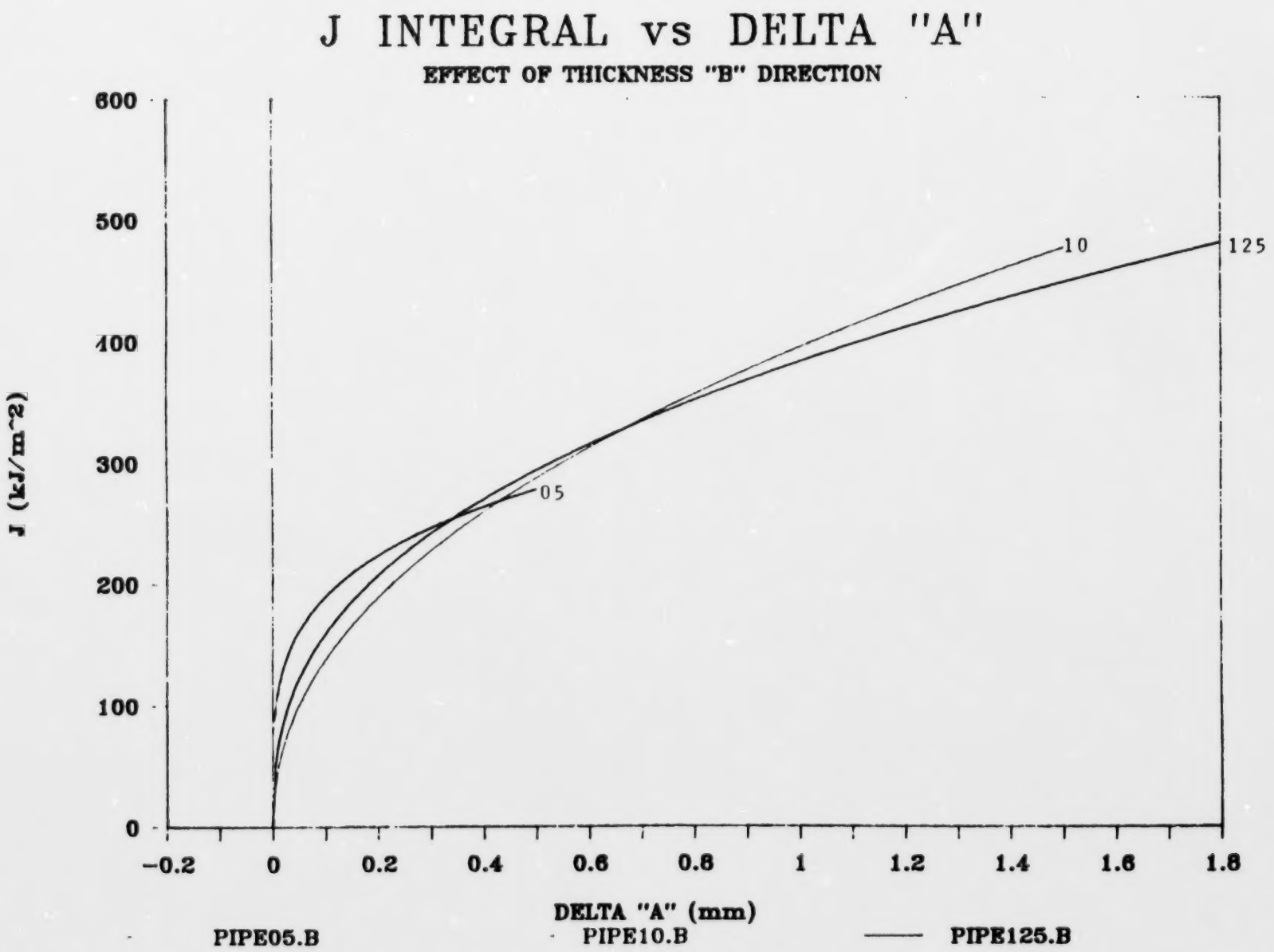

Figure 4-7: Comparison of J-Resistance Curves for Pipe Steel Obtained from Compact Tension Specimens of Different Thicknesses in the 'B' Direction.

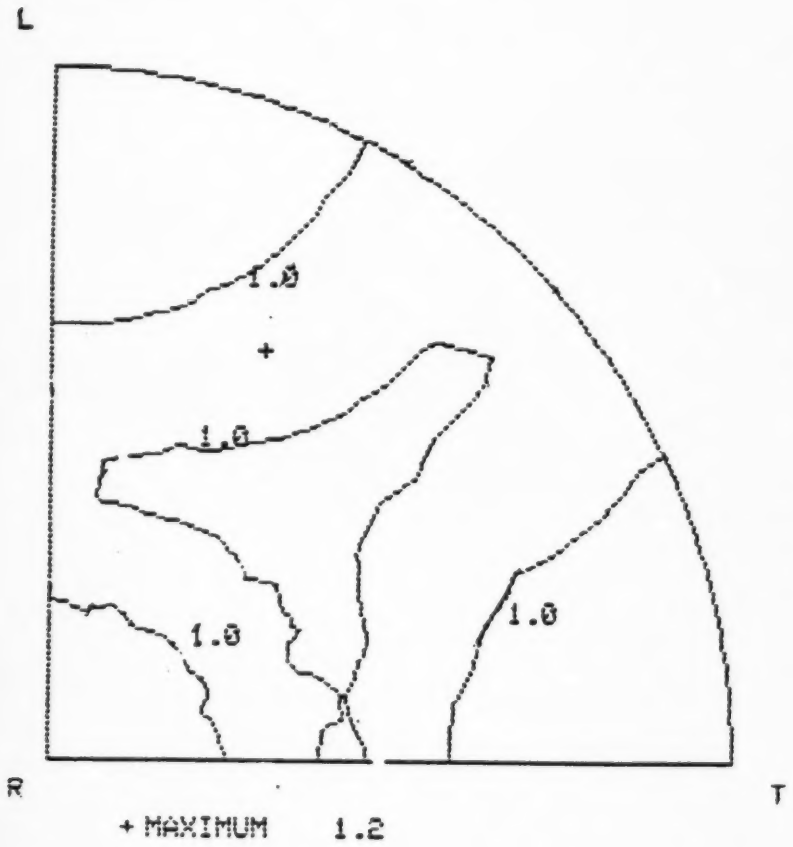

Figure 4-8: Pole Figure for SA106 Pipe Steel.

E. ASSESSMENT OF RESULTS

While the need exists to interpret laboratory data in its application to design considerations pertaining to crack propagation in tough ductile steels, it must be emphasized that insufficient data derived from laboratory scaled tests, full scale tests and correlations or projections of this data exists. It is therefore not possible to formulate clear-cut design procedures.

It is possible however to use the limited data available to assess the different procedures and it is in this context that the following discussion is presented.

Consider the preliminary case in which a flawed pipe is replaced by two limiting situations, namely, a through-the-wall crack and a part through crack around the entire circumference. These two limiting cases will, with all the inherent assumptions, permit the through-the-wall crack to be considered as a center-cracked panel and the circumferential (part through) crack to be treated as a single edge cracked panel. The models of each are presented in Figure 5-1.

It has been shown in the literature [Ref. 2] that the loads required to propagate the through-the-wall crack along the circumference are considerably lower than the loads required to propagate the circumferential crack in the radial direction if, of course, the material J-resistance curve is independent of the orientation. From the above, it is clear that the critical situation is the through-the-wall crack which propagates around the circumference on the Z plane. This orientation coincides with the 'B' direction for the pipe steel tests undertaken in this study. It will be noted from the material J-resistance curves corresponding to the 'B' and 'D' directions as given in Figure 4-4 that the resistance offered by the material for the 'B' direction is considerably less than that for the 'D' direction. Coupling the weaker material resistance in the 'B' direction with the geometric and loading considerations referred to above leads to the conclusion that the through-the-wall crack is certainly the more critical of the two idealized cases considered.

However, two further idealized models require investigation. These are identical to those described previously, but are now orientated in the axial direction as opposed to the circumferential direction. The models are illustrated in Figure 5-2. For the reasons already identified, the more critical model is the center cracked panel leading to the propagation of the crack in the axial direction on a θ plane. This orientation coincides with the 'A' direction for the tests undertaken in this study. It therefore remains to assess which of the center cracked panel models represents the more critical situation between those identified in Figure 5-1(b) and 5-2(a). To do this requires some knowledge of the loads imposed; for the present, it will be assumed that the loading is due to internal pressure only which implies, because of the circular geometry, that the model shown in Figure 5-2(a) is subjected to a higher stress than the model in Figure 5-1(b) for the same internal pressure. The model of Figure 5-2(a) clearly represents the more critical situation for flaws of similar size. However, if consideration is also given to the J-resistance offered by the material in the direction of crack growth as shown in Figure 4-4 for directions 'A' and 'B', it must be concluded that the material resistance in the 'A' direction is inferior which in turn further downgrades the critical model shown in Figure 5-2(a).

While the models identified in Figures 5-1 and 5-2 are recognized as an oversimplification, they do provide some insight into the preferred directions of crack propagation. A further refinement, developed from the above considerations, is presented in Figure 5-3 for a small semi-circular flaw located on the inner wall surface of the pipe corresponding to i) an orientation of the crack in the Z-plane as shown in Figure 5-3(a) and ii) an orientation of the crack in the θ plane. The Z and θ planes correspond to those of a polar coordinate system. For Figure 5-3(a), the flaw, while positioned in the Z-plane can grow in either a radial or a circumferential direction. These directions are shown and designated as directions D and B which correspond to the orientation of the test data referred to in Section D. Similarly from Figure 5-3(b), the flaw, while positioned in the θ plane, can grow in the radial direction C or the axial direction A.

The possible growth of these surface flaws in both cases is illustrated in Figure 5-3; from the J-resistance curves for the pipe steel, shown in Figure 4-4, it is likely, but not proven, that the contour of the crack will preferentially extend in the A and B directions as a result of the lesser resistance offered by the material each of these directions as compared to the J-resistance curves obtained for the C and D directions respectively. It can of course be argued that any initial elliptical flaw will preferentially grow to a circular flaw. This is accepted provided the J-resistance properties of the material are independent of orientation.

From the above arguments it would appear that a surface flaw would be less likely to grow through the wall thickness of the pipe in the radial direction and result in 'leak-before-break'. In preference, the flaw would grow in the axial or circumferential direction. These arguments simply follow from the test data obtained for specimens of different orientation. It is important to note, however, that the J-resistance curves of the material obtained for the A and C directions is considerably less that those obtained for the B and D directions which indicates that the case shown in Figure 5-3(b) is more critical than that represented in Figure 5-3(a) for the conditions presented. (The reverse could be true if the pipe section was subjected to bending and the location of the flaw coincided with the location of the maximum stress.)

This difference is clearly illustrated in Figure 5-4 where the tear modulus and J_{IC} for the direction A and B have been plotted. Also, since the difference in the J-resistance curves for directions A and C is small, it is possible for the case shown in Figure 5-3(b) that this situation could lead to a 'leak-before-break' condition.

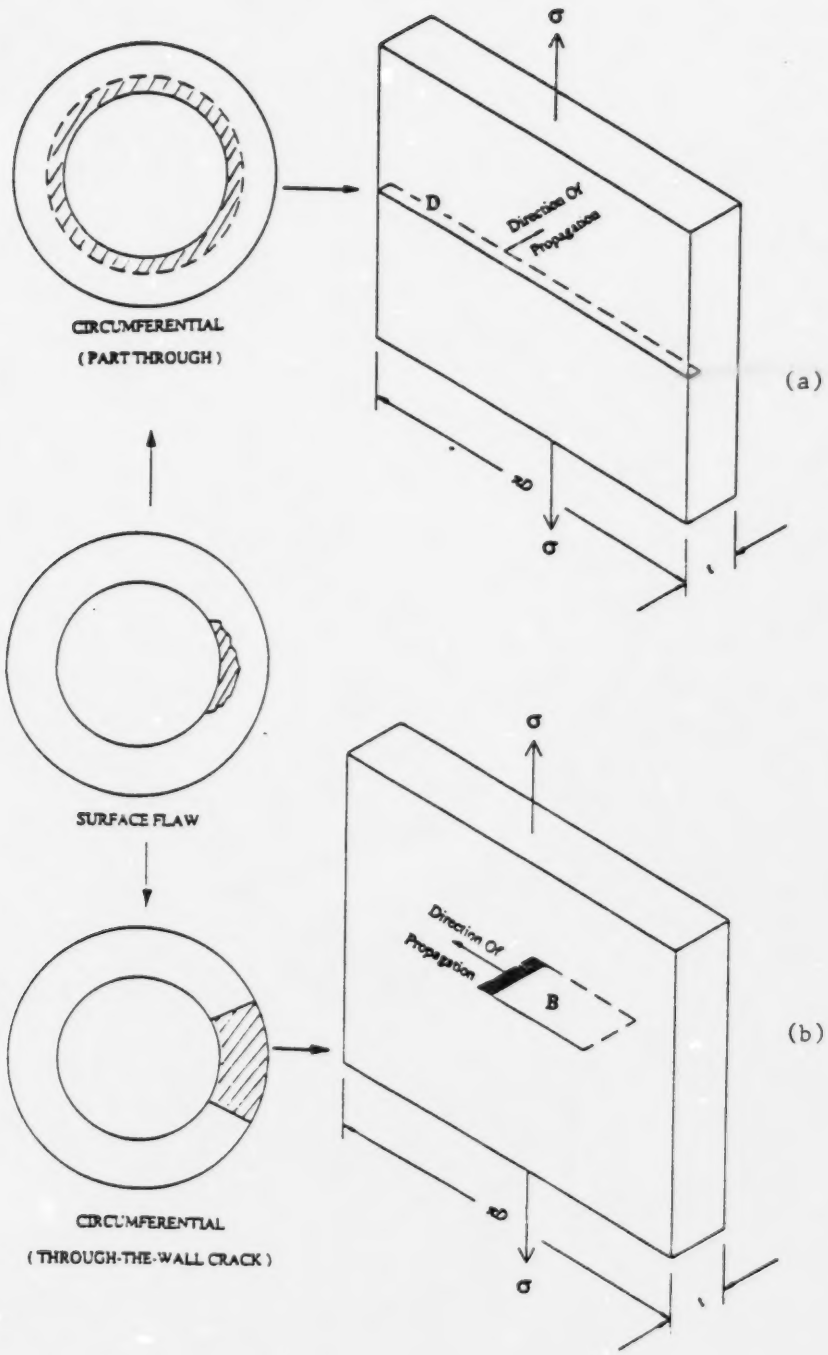

Figure 5-1: Models Representing the Direction of Crack Propagation.

(a) Edge Crack Propagating Radially Across the Circumference.

(b) Centre Cracked Panel with Crack Propagating in the Circumferential Direction.

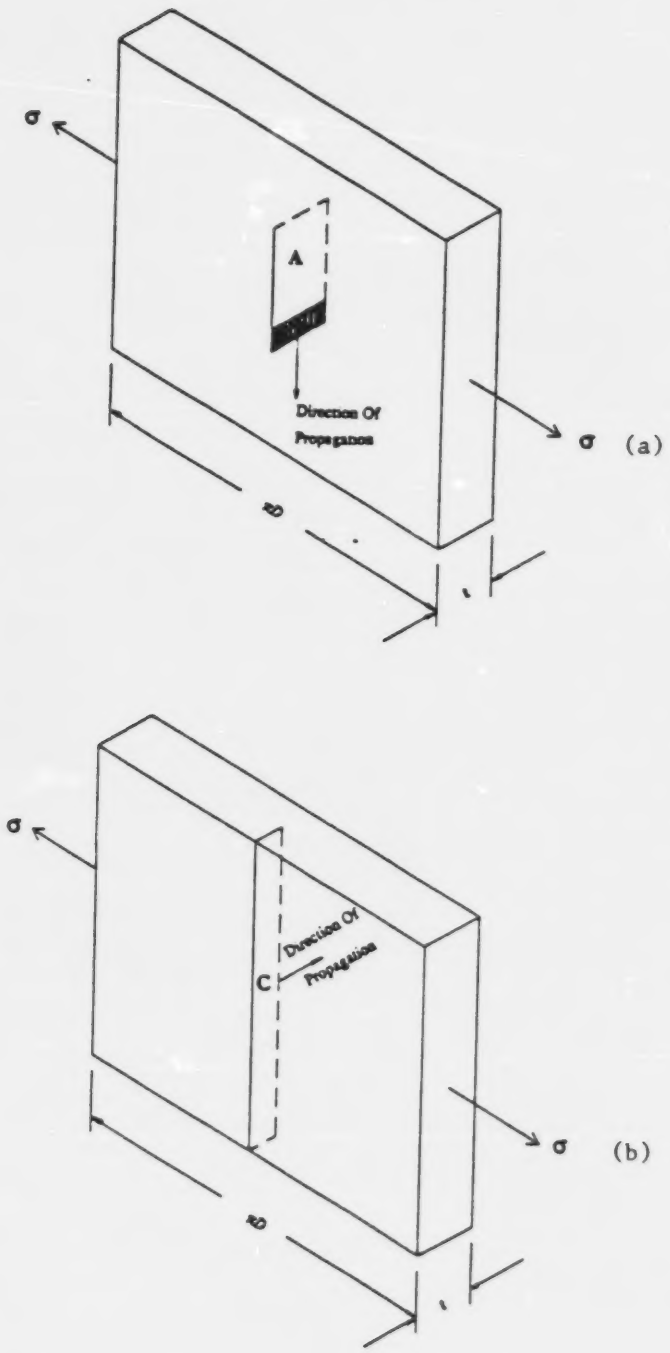

Figure 5-2: Models Representing the Direction of Crack Propagation.
(a) Centre Cracked Panel with Crack Propagating in the Axial Direction.
(b) Edge Crack along the Axis of the Pipe Propagating Radially.

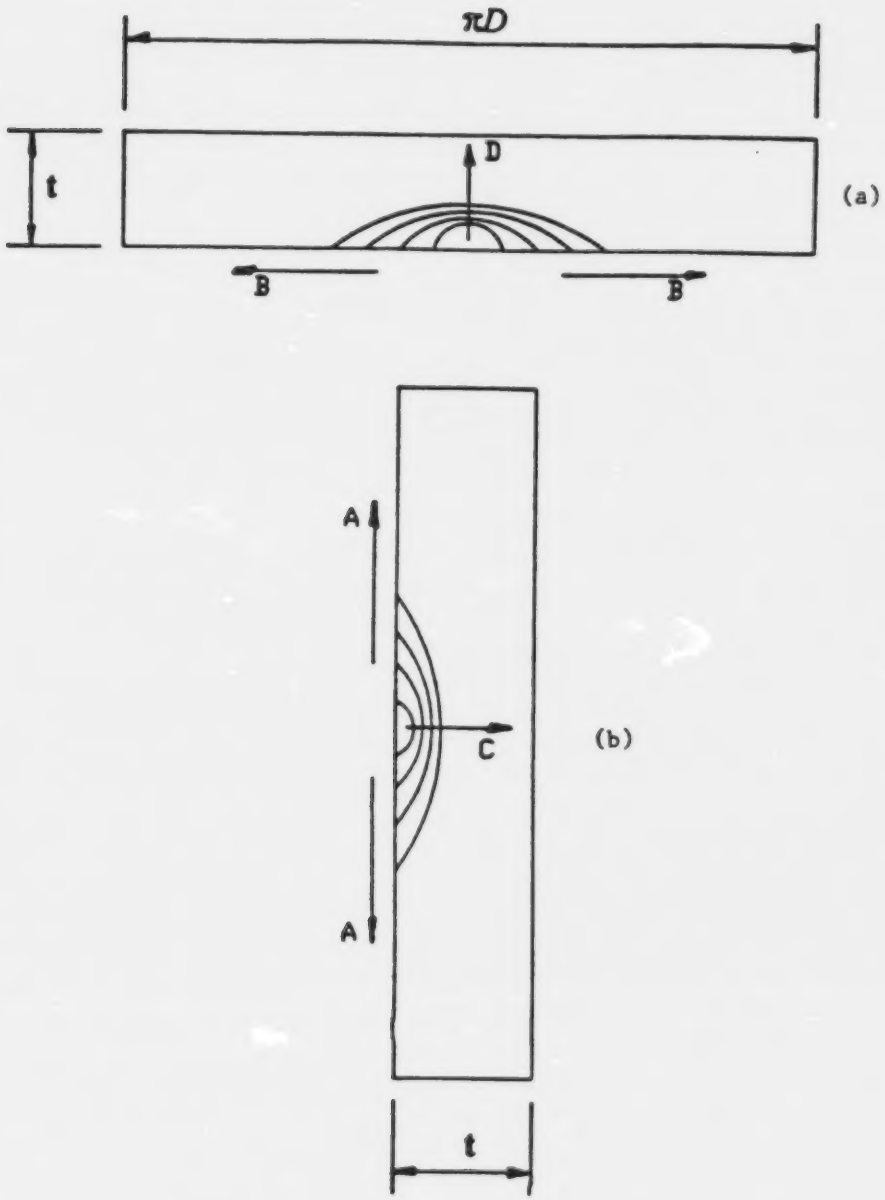

Figure 5-3: Proposed Crack Growth of a Surface Flaw.

(a) Surface Flaw on the Z-plane (propagating in the radial (D) and circumferential (B) directions).

(b) Surface Flaw on the θ Plane (propagating in the radial (C) and axial (A) directions).

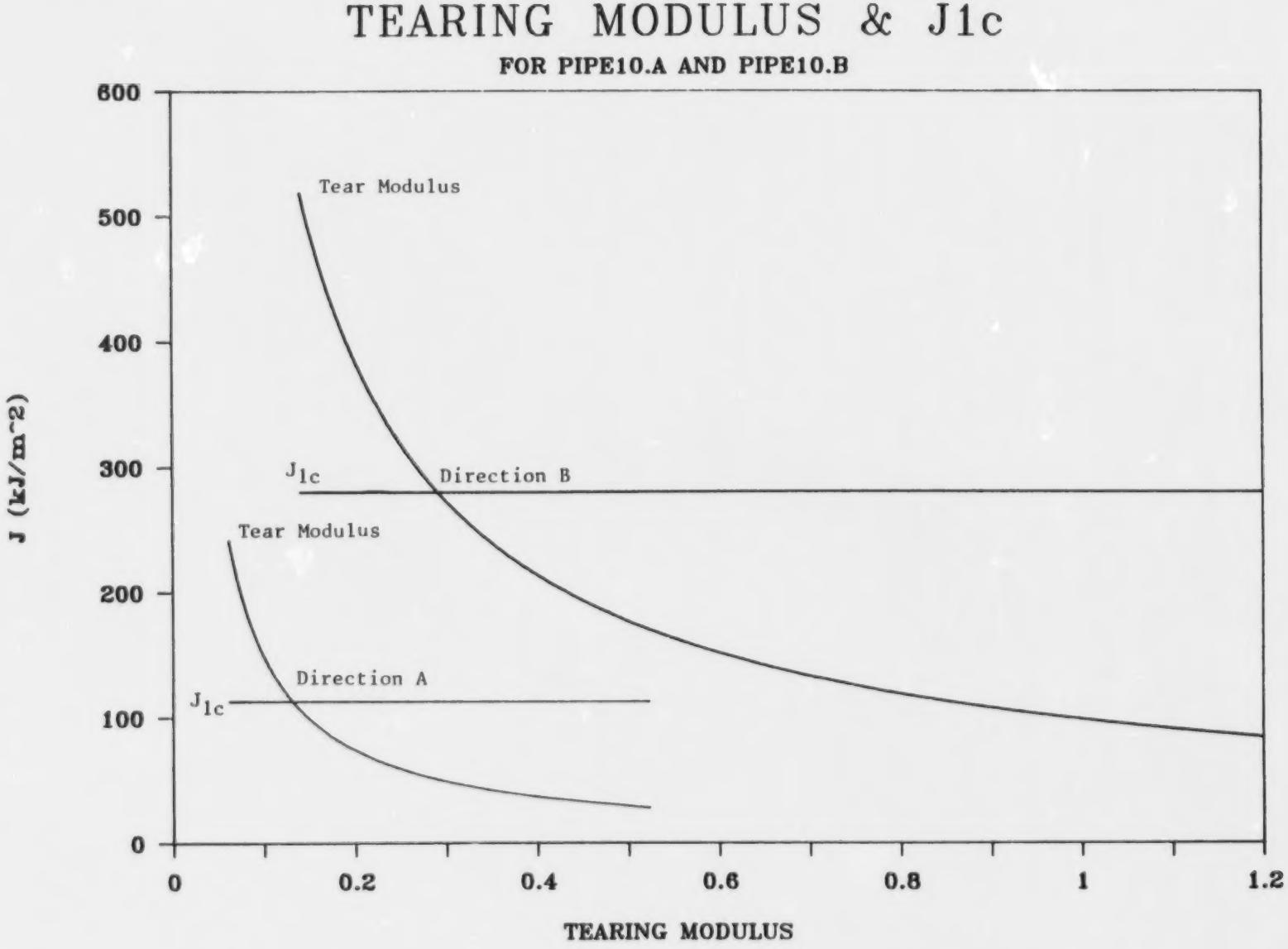

Figure 5-4: Tearing Modulus and J_{1c} obtained from J-resistance Curves in the A and B Directions.

F. CONCLUSIONS

The conclusions which can be made from the test results presented in this report are summarized below.

1. Given the importance to replicate test results, it would appear that the test procedure and experimental set-up for compact tension specimens leads to more consistent results as compared to three point bend test data.
2. For the plate steel, it would appear that the lowest bound J-resistance curve is obtained with increased specimen thickness when using compact tension specimens. For the pipe steel, the lowest bound J-resistance curve was obtained for both the A and B orientations (see Figures 4-6 and 4-7) when using a one inch thick specimen at small crack extensions. As the crack extension in increased, the lowest bound is given by specimens of increased thickness, i.e. 1.25 inches. It is, however, important to note that the J-resistance curves for both the A and B orientations, while different for each orientation, appear to indicate an independence of specimen thickness.
3. The J-resistance curves obtained for all one inch specimens at each of the four orientations provide consistent results within each orientation and indicate a clear material resistance difference for crack extension in the circumferential (B) and axial (A) directions.
4. The J-resistance curves developed have been obtained using load control as distinct from displacement control. This method allowed for a maximum crack extension of 1.8 mm when using 1.00 and 1.25 inch thick specimens. The magnitude of crack extension obtained when using 0.5 inch thick specimens is small and is not recommended for load control when the objective is to establish a J-resistance curve for the material.
5. On the use of load control, it is important to note that while displacement control could produce an increased crack extension, the ASTM test method indicates that R curves be restricted to a small crack extension given by a_{max} being equal to 0.1 of the remaining specimen ligament to maintain a J controlled growth at the crack tip region. Furthermore, J controlled growth is defined for $\omega > 1$ where $\omega = b/J(dJ/da)$. Also for plane strain $J_{max} \leq (b.\sigma_f)/20$ where 'b' is the remaining ligament. For the tests carried out, these conditions are 'generally' satisfied.
6. It would appear from the pipe steel results that the J-resistance curves, obtained from the compact tension tests, approach consistent values when the specimen thickness approaches a plane strain condition, i.e. 1-1.25 inches. This is not inconsistant with the different J-resistance curves obtained for the various specimen orientations, since the material is not necessarily isotropic.
7. The development of J-resistance curves requires a knowledge of the yield and ultimate strengths of the material investigated. It is important in the selection of materials that specification limits of the yield and ultimate strengths be closely monitored. The magnitude of the difference between the yield and ultimate stress levels provides a measure of the elastoplastic behaviour of the material and requires careful correlation with J-resistance curve experimentation.

G. RECOMMENDATIONS

The following recommendations are presented for consideration. It is anticipated that the recommendations, if adequately developed, will enhance our capability to give direction to the design process.

1. Undertake further experimentation using 1 inch thick SA106 grade B compact tension specimens with both load and displacement control. Assess the J-resistance curves obtained by these methods in relation to the yield and ultimate strength of the materials tested. It may be necessary to tighten the specifications of the yield and ultimate strength of the pipe steels to understand or improve the scatter associated with J-resistance measurements. This could require the development of suitable techniques to evaluate the yield and ultimate strengths of the materials in the various pipe orientations.
2. Endeavour to compile all test data derived from appropriate J-resistance curve experimentation of ferritic steels such as SA106 grade B for load and displacement control conditions. Assess this data in relation to the J controlled growth definition. Develop an understanding of the J-resistance behaviour of a specific ferritic steel, i.e. SA106 grade B as distinct from attempting to develop a general approach (as it relates to design considerations) for all elasto-plastic materials.
3. Investigate the variables associated with the use of experimental J-resistance curves and J-driving curves for selected pipe geometries and flaws under defined loading conditions. Such a study can be undertaken utilizing empirical relationships derived from finite element results which is referred to as an engineering elasto-plastic approach of solution. This study could then be extended to the direct application of finite element packages as indicated below.
4. Undertake an extensive assessment of different finite element software packages which are capable of simulating crack initiation and stable crack growth. Categorize these packages according a (a) J-integral, (b) CTOD, (c) CTOA calculation ability, etc. To do this successfully and economically will require the identification of user sites, i.e. sites where the various packages are well known to users who can understand the finer differences of the algorithms to manipulate stable crack initiation/growth problems. In this context, it may be preferential to also set up a small test problem; one representative of a compact tension specimen and the second representative of an axial crack extension situation in a pressurized pipe section. This could be a costly undertaking, but is necessary to assess the interrelation between material J-resistance curves and the J-driving curves of a particular problem.

REFERENCES

1. "Standard Test Method for Determining J-R Curves", ASTM, 12th draft, July 25th, 1985, E24.08 Subcommittee.

2. Shih, C.F., Andrews, W.R., German, M.D., Van Stone, R.H. and Wilkinson, J.P.D. "Methodology for Plastic Fracture", EPRI contract RP 601-2, combined 7th and 8th Quarterly Report prepared by General Electric Company, July 31, 1978.

3. Venter, R.D. and Hoeppner, D.W. "Crack and Fracture Behaviour in Tough Ductile Materials", Atomic Energy Control Board Report, Ref. AECB INFO-0169, October, 1985.

4. Scarth, D.A., Kim, Y.J. and Vanderglas, M.L. "A Critical Review on the Application of Elastic-Plastic Fracture Mechanics to Nuclear Pressure Vessel and Piping Systems, Ontario Hydro Research Division, report no. 85-257-K, October 28, 1985.

5. "Round-Robin Problem for Ductile Growth of Part-Through Crack in Carbon Steel Plate", Central Research Institute of Electric Power Industry, Japan, September 1986.

6. Papaspyropoulos, V., Marschall, C. and Landow, M. "Predictions of J-R Curves With Large Crack Growth from Small Specimen Data", September 1986.

7. Metals Handbook 1985, edited by Boyer, H.E. and Gall, T.C., American Society of Metals, Metals Park, Ohio 44073.

8. Vanderglas, M.L. "A Three Dimensional Numerical Study of the Effects of Free Surfaces on the J-Integral", Ontario Hydro Research Division, report no. 85-296-K.

9. Wilkowski, G.M., Ahmad, J., Barnes, C.R., Broek, D., Durst, F., Guerrieri, D., Kramer, G., Landow, M., Marschall, C.W., Maxey, W., Nakagaki, M., Scott, P., Papaspyropoulos, V., Pasupathi, V. and Popelar, C. "Degraded Piping Program – Phase II Progress", Bartelle's Columbus Division.

10. "The 'State-of-the-Art' in Crack Tip Opening Displacement (CTOD) Testing and Analysis: Part 1 Background and Testing Methods", reviewed by Harrison, J.D., Metal Construction, September 1980.

APPENDIX A

TEST METHOD FOR DETERMINING J-R CURVES

All experimental data given in this report was obtained using the ASTM Standard Method for Determining J-R Curves, E24.08, 12th Draft, 25 July 1985. Although this version of the specification has since been superseded, changes have been of a minor nature such that the data reported here are still valid.

TEST EQUIPMENT

All tests were automatically controlled by an IBM AT personal computer. Loadline displacement was monitored via a Cyborg ISAAC 91I system, with a two-channel 16-bit A/D card. The specimen loading pattern was output from the computer using a 12-bit D/A board connected to the 442 controller of the MTS 810 Test System.

Test automation was employed for two reasons. First, the tests were generally of long duration, and therefore manual control of the loading pattern was not practical. Second, computer control assures repeatability of the loading pattern among all tests. An example of a typical loading pattern is shown in Figure A-1. In general, the incremental step in load between cycles of the loading pattern was not kept constant for the entire duration of a test. Instead, the step size was decreased as the crack grew, in an effort to promote some degree of stable crack growth.

TEST PROCEDURE

In following the procedure described by ASTM specification E24.08, several points of interest were noted; in presenting these notes, reference is made to the test data obtained for each test and presented in Appendix B.

1. Load Control Versus Displacement Control

Load control was used to obtain all J-R data given in this report. The selection of load control as opposed to displacement control was based on the finite resolution of the A/D converter. Under displacement control, each incremental step in displacement, before the initiation of crack growth, would result in a very large incremental change in load. Preliminary tests indicated that this would result in a very uneven, stepped loading pattern which might affect the material response of the specimen. For this reason, load control was adopted for all tests.

The primary disadvantage of load control becomes apparent after crack growth has initiated; it becomes increasingly difficult to avoid unstable crack propagation. For this reason, the amount of crack growth observed in some tests, particularly for 0.5 inch specimens, is less than ideal, e.g., Figures B-14 and B-15. It should be remembered, however, that the proper use of J-integral techniques is limited to the initiation of crack growth; i.e., J should not be used as a parameter to characterize crack propagation. This is because the J-integral concept is based on deformation plasticity theory, which becomes invalid in the presence of significant unloading of a specimen. In the presence of crack growth beyond 1 or 2 mm, significant unloading does take place behind the crack front.

2. Specimen Side Grooves

The ASTM Specification E24.08 calls for side grooving of specimens after pre-cracking. By performing the pre-cracking first, the net result is a straighter crack front than could be achieved if the order of operations were reversed. This is because the crack advance is somewhat retarded on the outer surface of the specimen where a state of plane stress is known to exist. Side grooving of the pre-cracked specimen removes the retarded section of the crack front, leaving a relatively straight leading edge.

The possible disadvantage in delaying the side grooving until after pre-cracking is that the side grooves may not line up exactly with the crack. This problem was not observed to any significant extent in these tests.

3. Crack Length Measurement

Destructive examination of the specimens at the conclusion of each test revealed that the crack front was not smooth, but rather displayed a somewhat tortuous path. This made a visual measurement of the final crack size prone to a small uncertainty. Under these conditions, it was not possible to confirm the accuracy of the compliance measurements of crack length to the accuracy desired.

4. Negative Crack Growth

Compliance measurements of many of the specimens indicated that there was a period of "negative crack growth" in the early stages of the loading program. Typical cases are illustrated by Figures B-7 to B-16. Such results are equivalent to stating that the compliance of the specimen actually decreased slightly during the early stages of the test program. Such results have been noted by a number of authors, although a proper explanation of the phenomenon has never been conclusively determined. Repeated tests have indicated that improper alignment of the specimen, clip gauge, or knife edges can produce distorted $J-\Delta a$ curves, e.g., specimen B125LT.1 of Figure B-3. However, a more subtle phenomenon is believed to be at work for most of the other specimens. Possible contributing causes include a strain-hardening effect, uneveness in the crack front, or a consistent source of error in the compliance measurement.

Determining the source of this anomalous crack growth data is desirable in order to assess the proper way to analyze the resulting $J-\Delta a$ curve. One solution is to ignore all data points that indicate negative crack growth. A second solution is to shift all data points to the right so that a curve joining the data points would naturally go through the origin. Provided considerable crack extension has been recorded, these two methods should result in very similar power-law curves to describe the data. For this report, the former of the two solutions was adopted. A least squares fit was then used to determine the optimum parameters to fit a power law to all data indicating positive crack growth.

5. Bend Versus Compact Tension Specimens

In general, bend specimens were found to be relatively difficult to properly align as compared to compact tension specimens. For the 1.25 inch bend specimens, proper alignment of the knife edges posed a particular problem. It was concluded that knife edges should be machined into the specimens rather than be glued in place. All SA-106 pipe specimens had machined-in knife edges as well as three plate specimens CT05.5, CT10.7 and CT10.8.

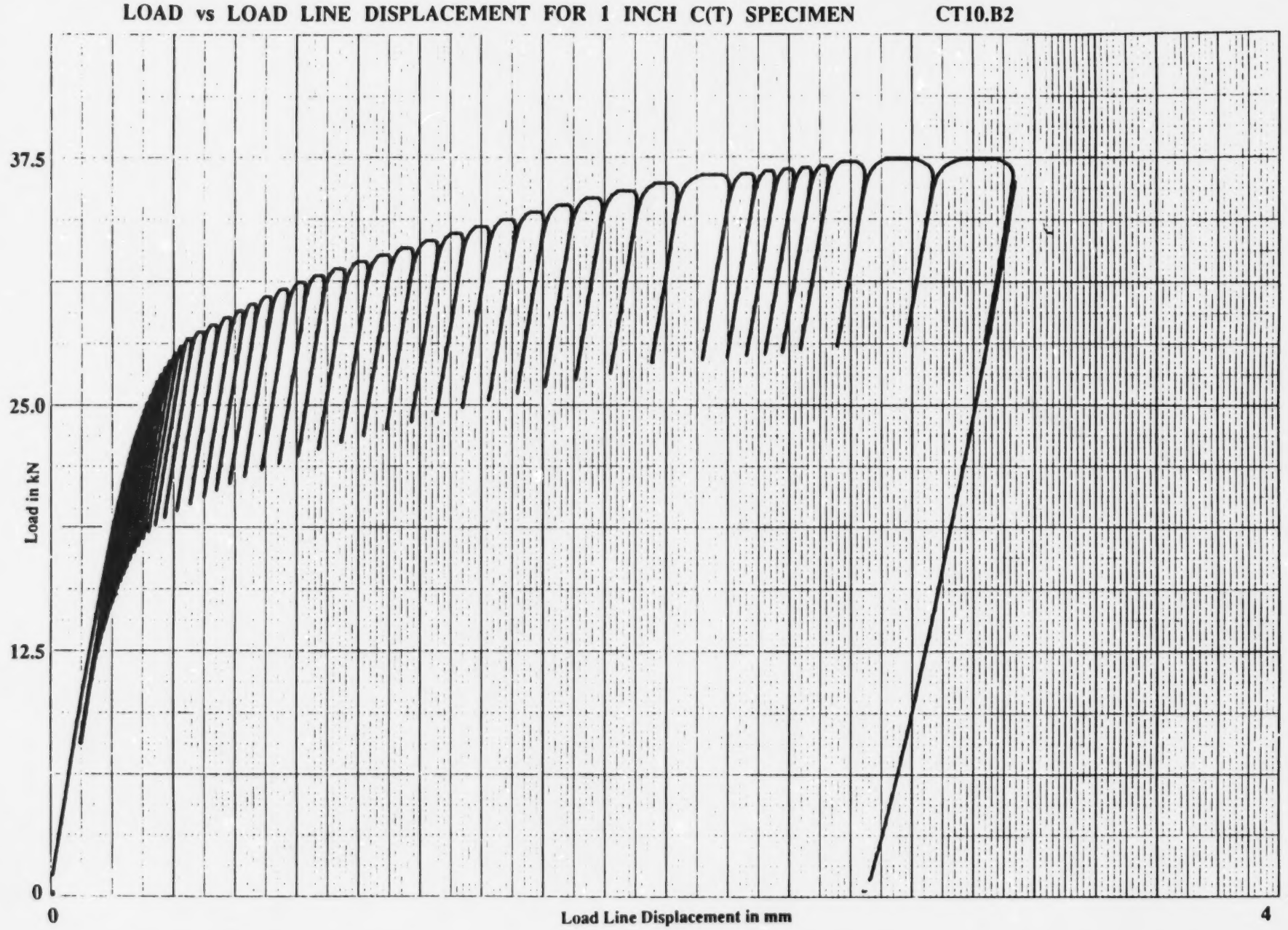

Figure A-1. Load vs Load Line Displacement for 1 inch C(T) Specimen CT10.B2

APPENDIX B

EXPERIMENTAL TEST DATA

The figures contained in this appendix represent the base experimental data obtained for all tests carried out on the ASTM516 grade 70 plate steel (Figures B-1 to B-6) and SA106 grade B pipe steel (Figures B-7 to B-16).

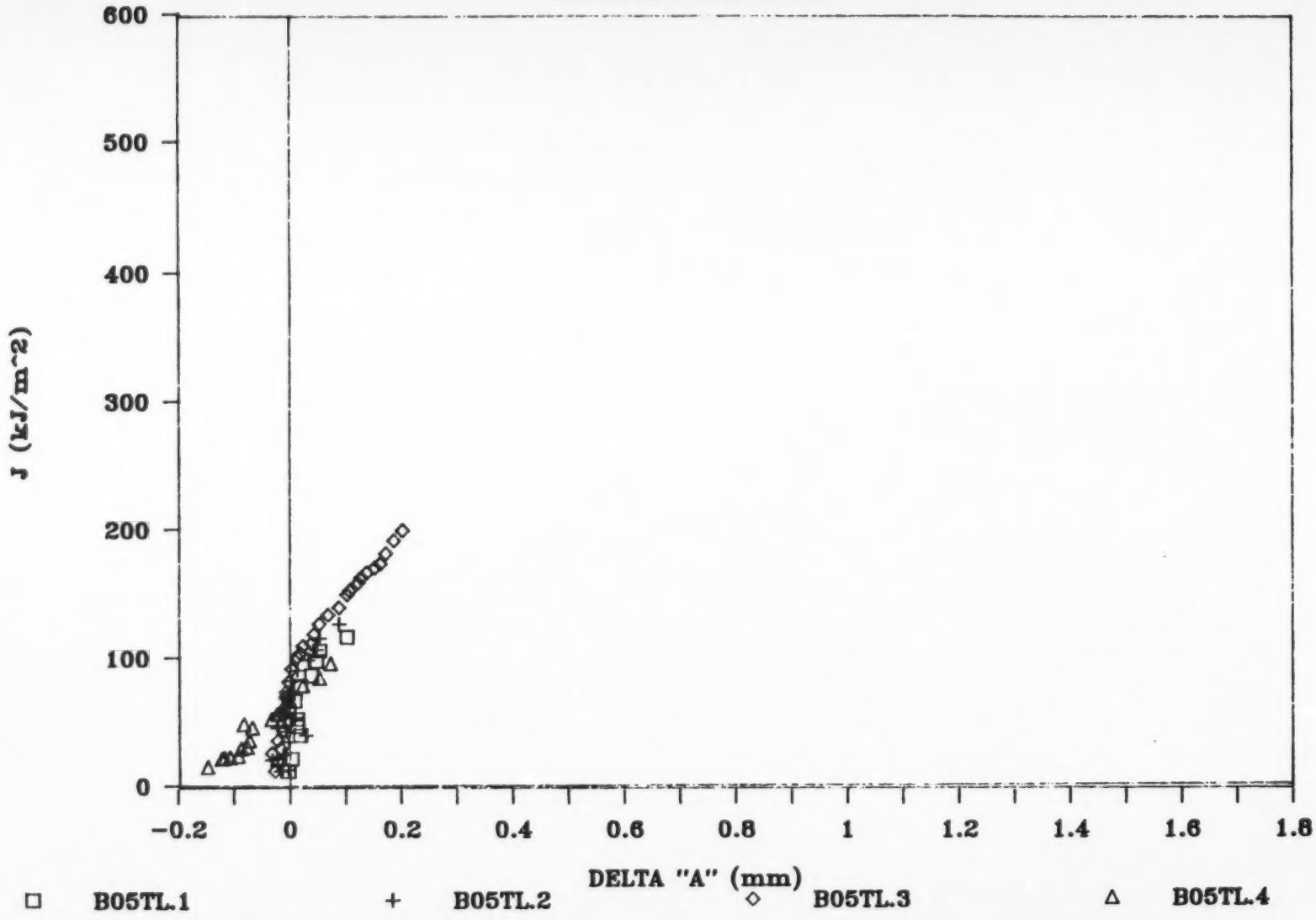

Figure B-1: Experimental Test Data of the J-Integral Versus Δa for Three Point Bend Tests on Plate Steel. Specimens 0.5 inch Thick Coded as B05TL.1-4.

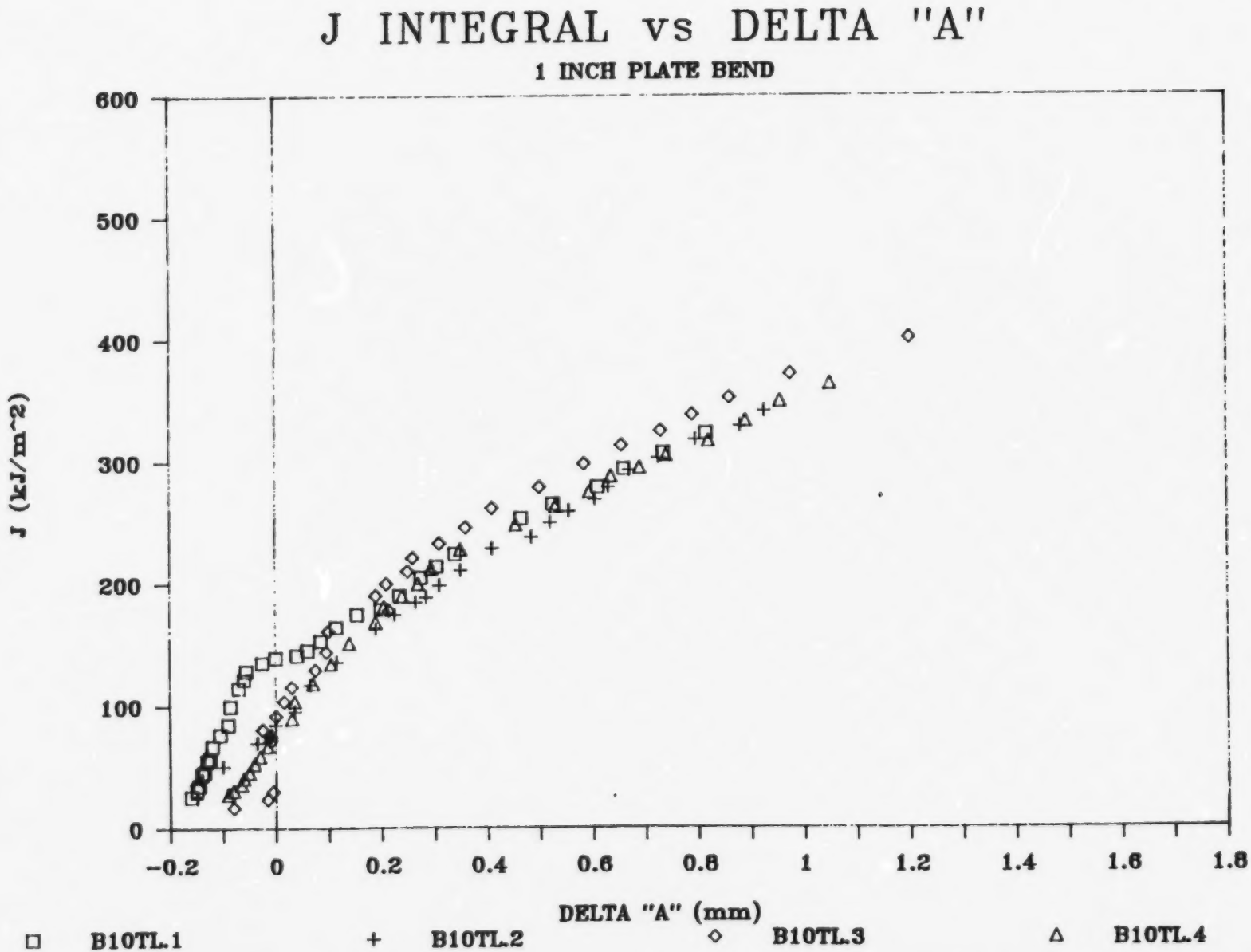

Figure B-2: Experimental Test Data of the J-Integral Versus Δa for Three Point Bend Tests on Plate Steel. Specimens 1.0 inch Thick Coded as B10TL.1-4.

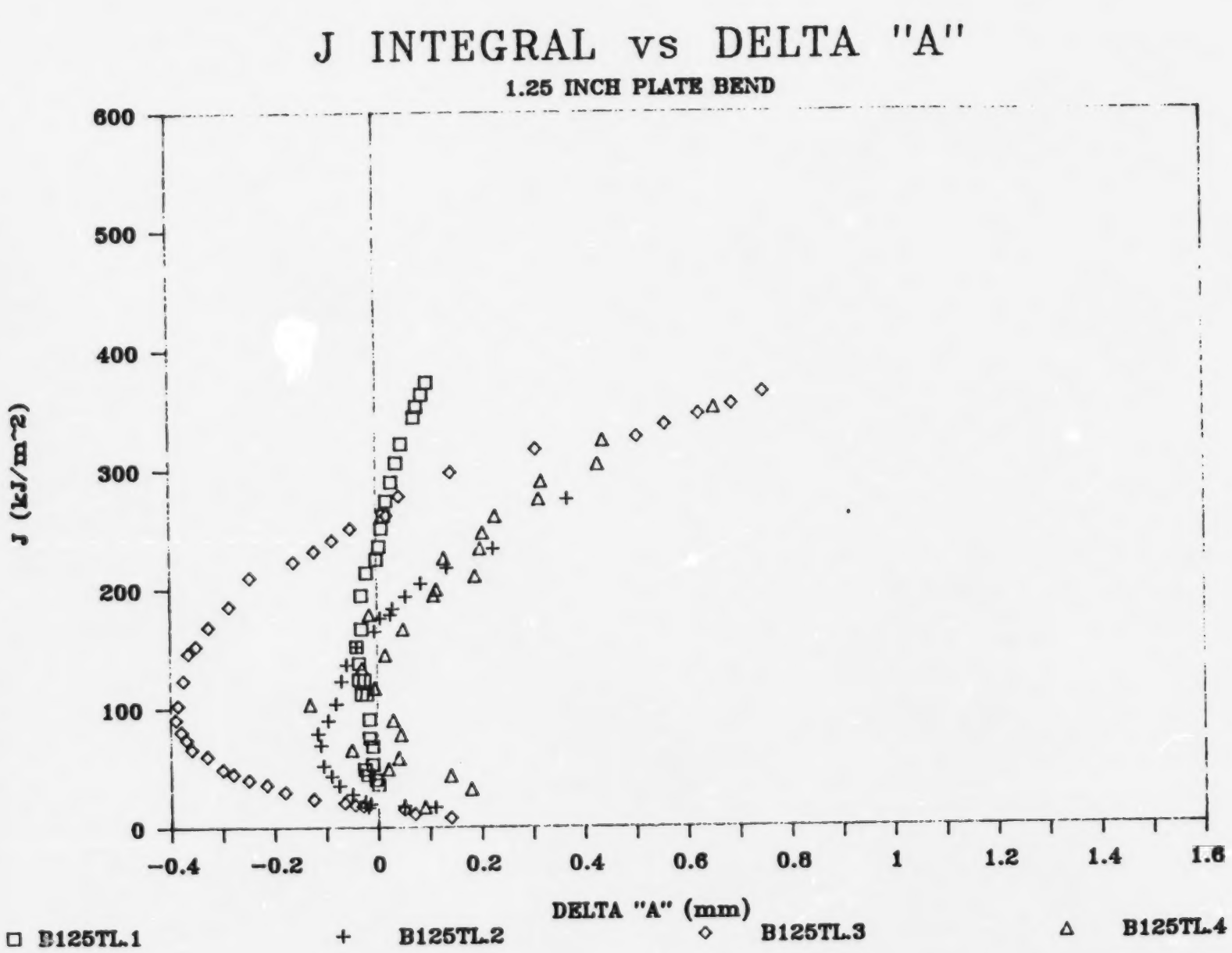

Figure B-3: Experimental Test Data of the J-Integral Versus Δa for Three Point Bend Tests on Plate Steel. Specimens 1.25 inch Thick Coded as B125TL.1-4.

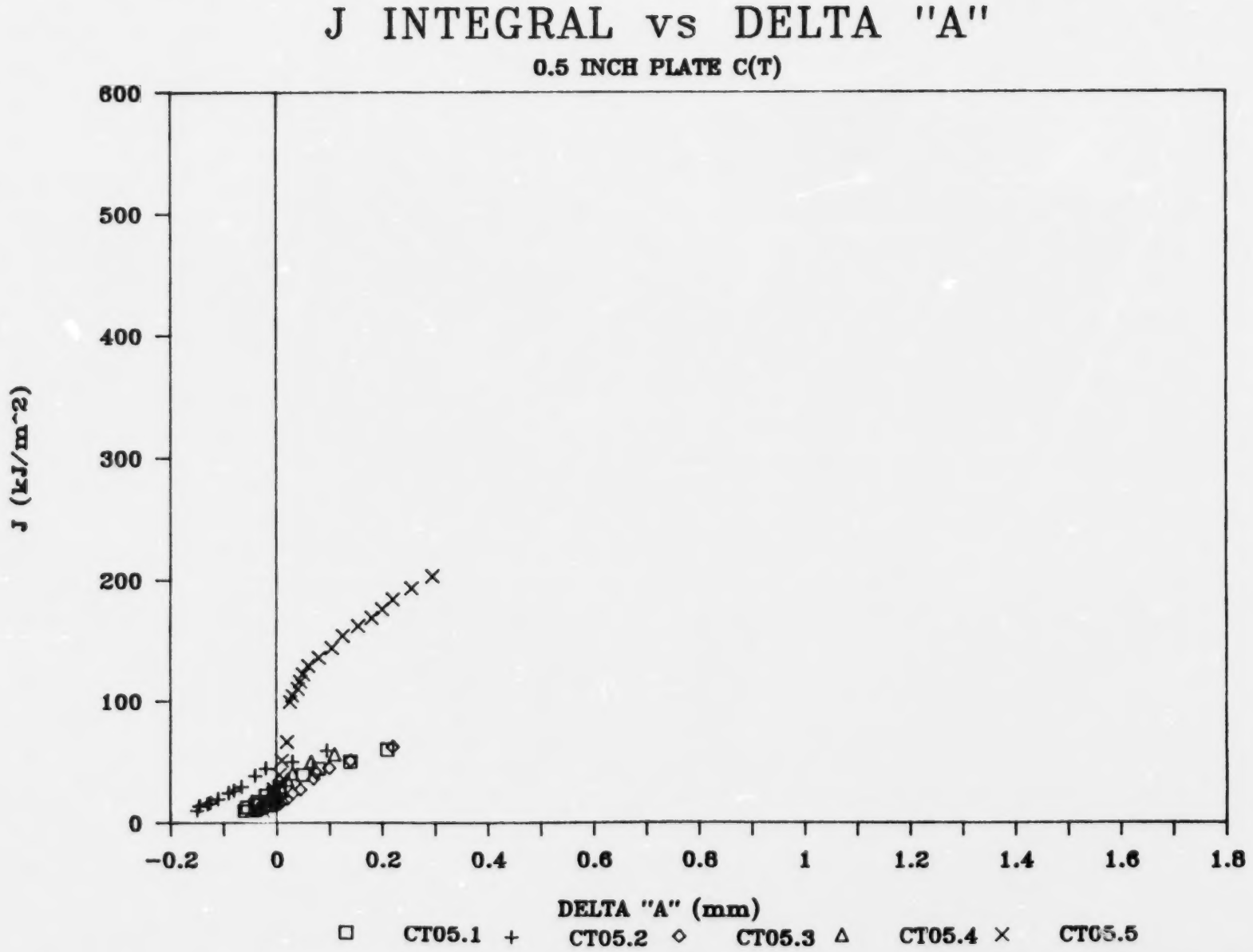

Figure B-4: Experimental Test Data of the J-Integral Versus Δa for Compact Tension Tests on Plate Steel. Specimens 0.5 inch Thick Coded as CT05.1-5.

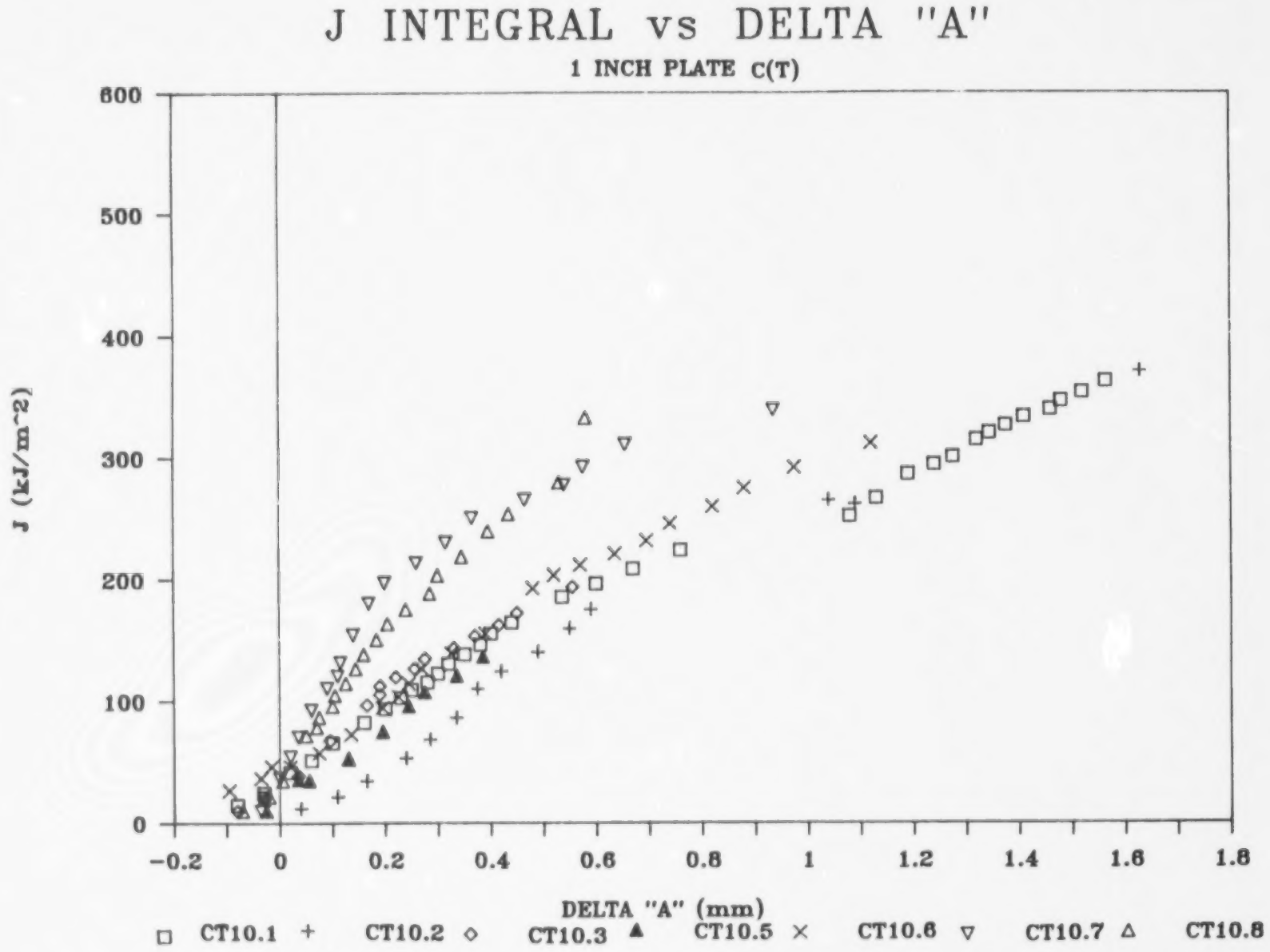

Figure B-5: Experimental Test Data of the J-Integral Versus Δa for Compact Tension Tests on Plate Steel. Specimens 1.0 inch Thick Coded as CT10.1-8.

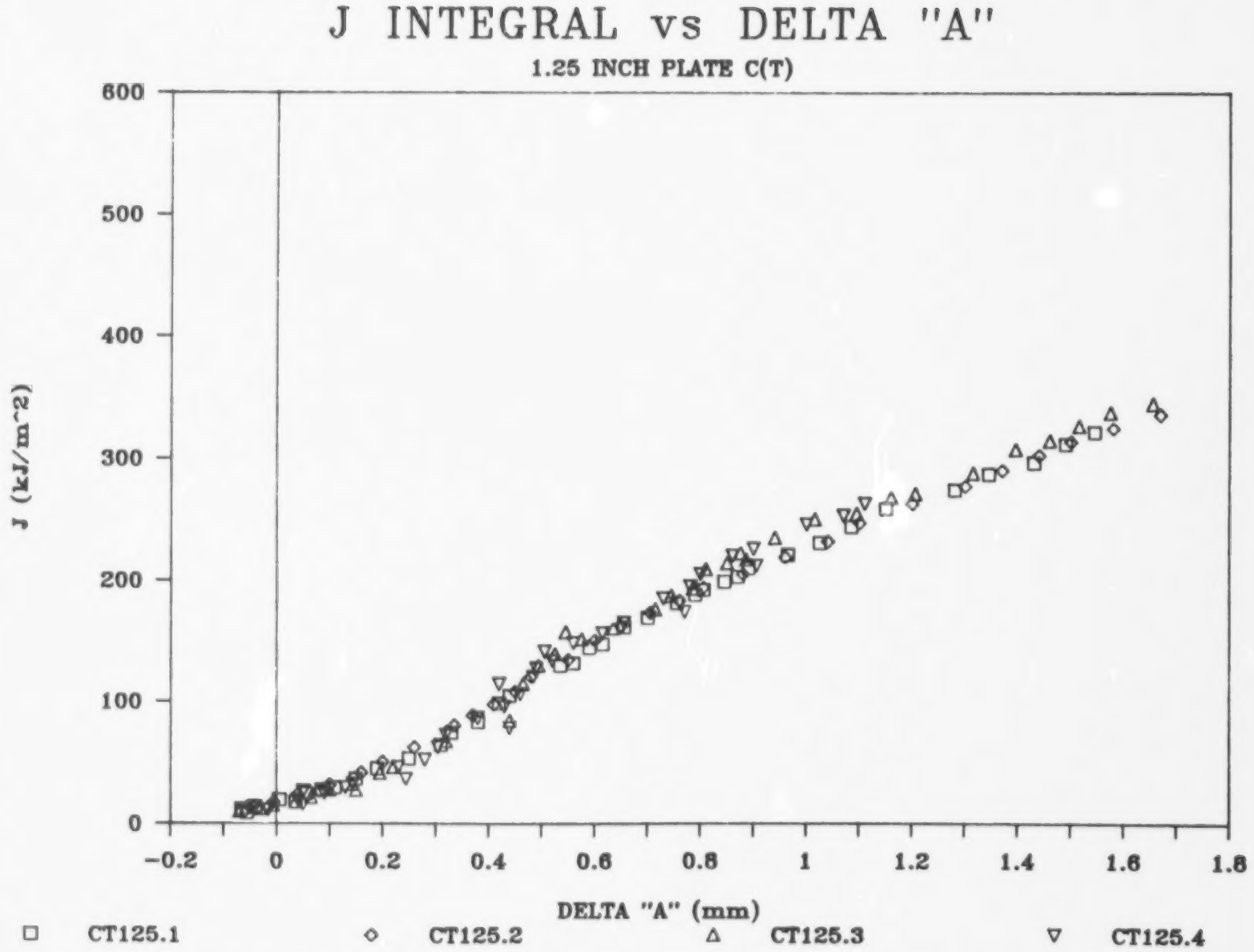

Figure B-6: Experimental Test Data of the J-Integral Versus Δa for Compact Tension Tests on Plate Steel. Specimens 1.25 inch Thick Coded as CT125.1-4.

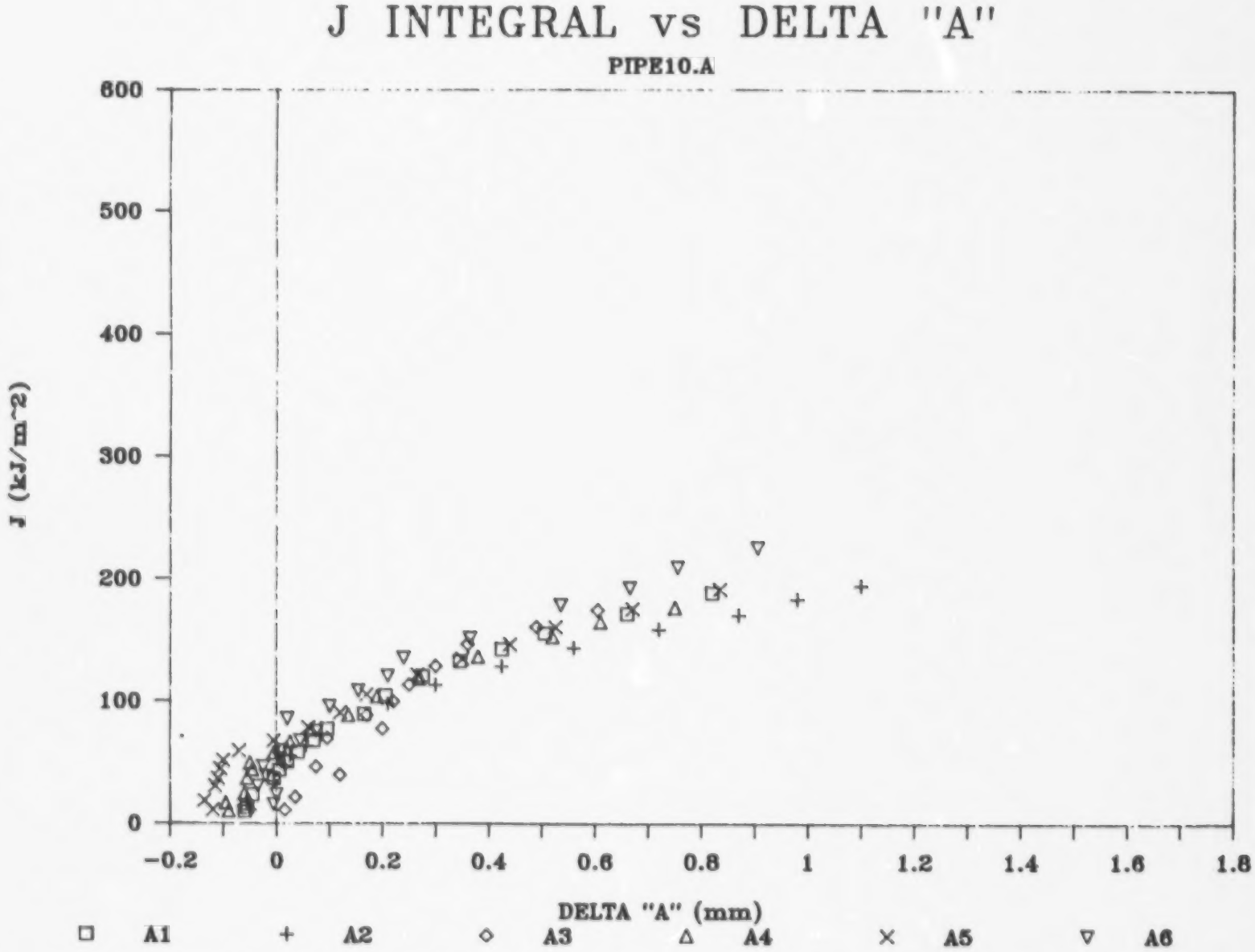

Figure B-7: Experimental Test Data of the J-Integral Versus Δa for Compact Tension Tests on Pipe Steel. Specimens 1.0 inch Thick Coded as PIPE 10.A1-6.

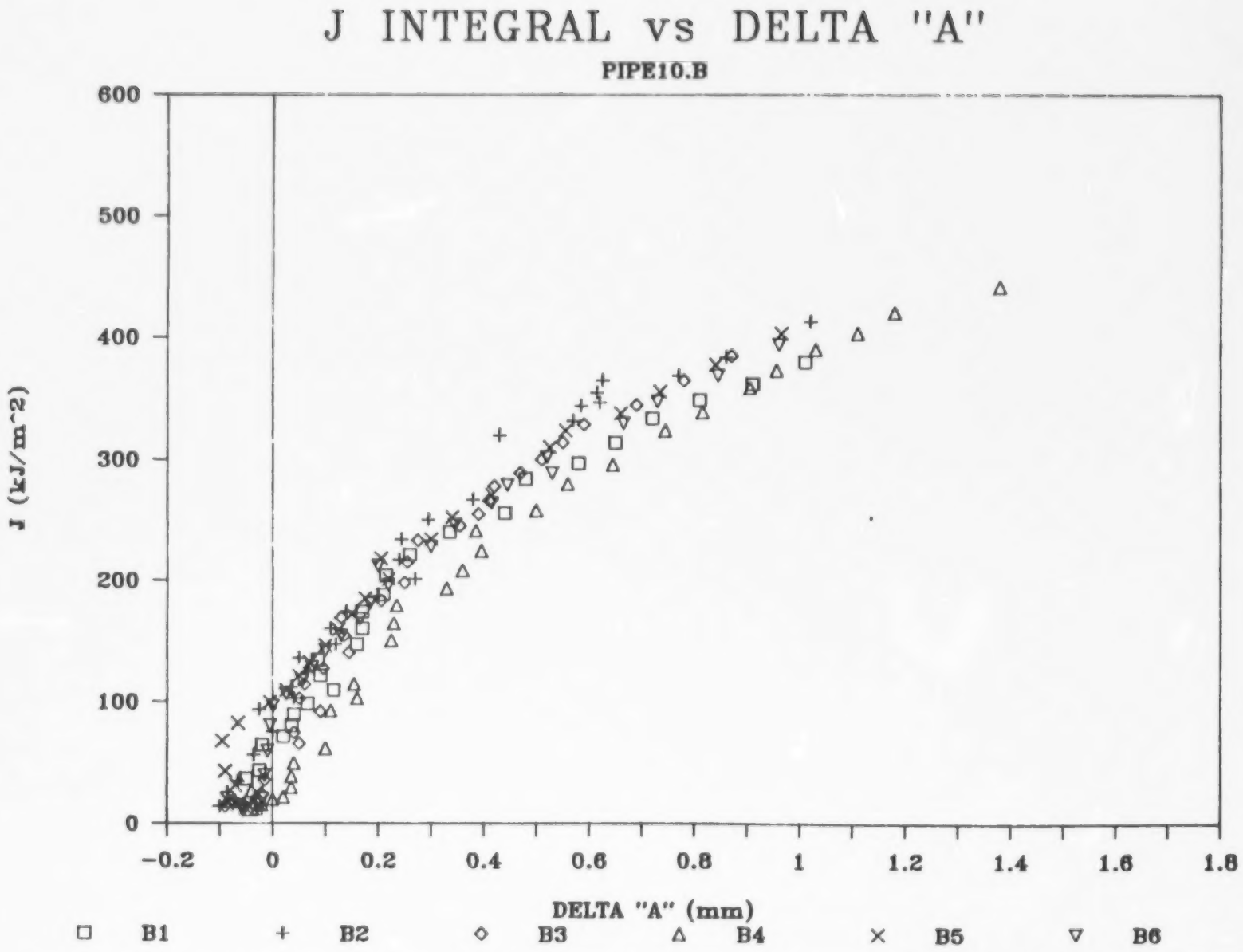

Figure B-8: Experimental Test Data of the J-Integral Versus Δa for Compact Tension Tests on Pipe Steel. Specimens 1.0 inch Thick Coded as PIPE 10.B1-6.

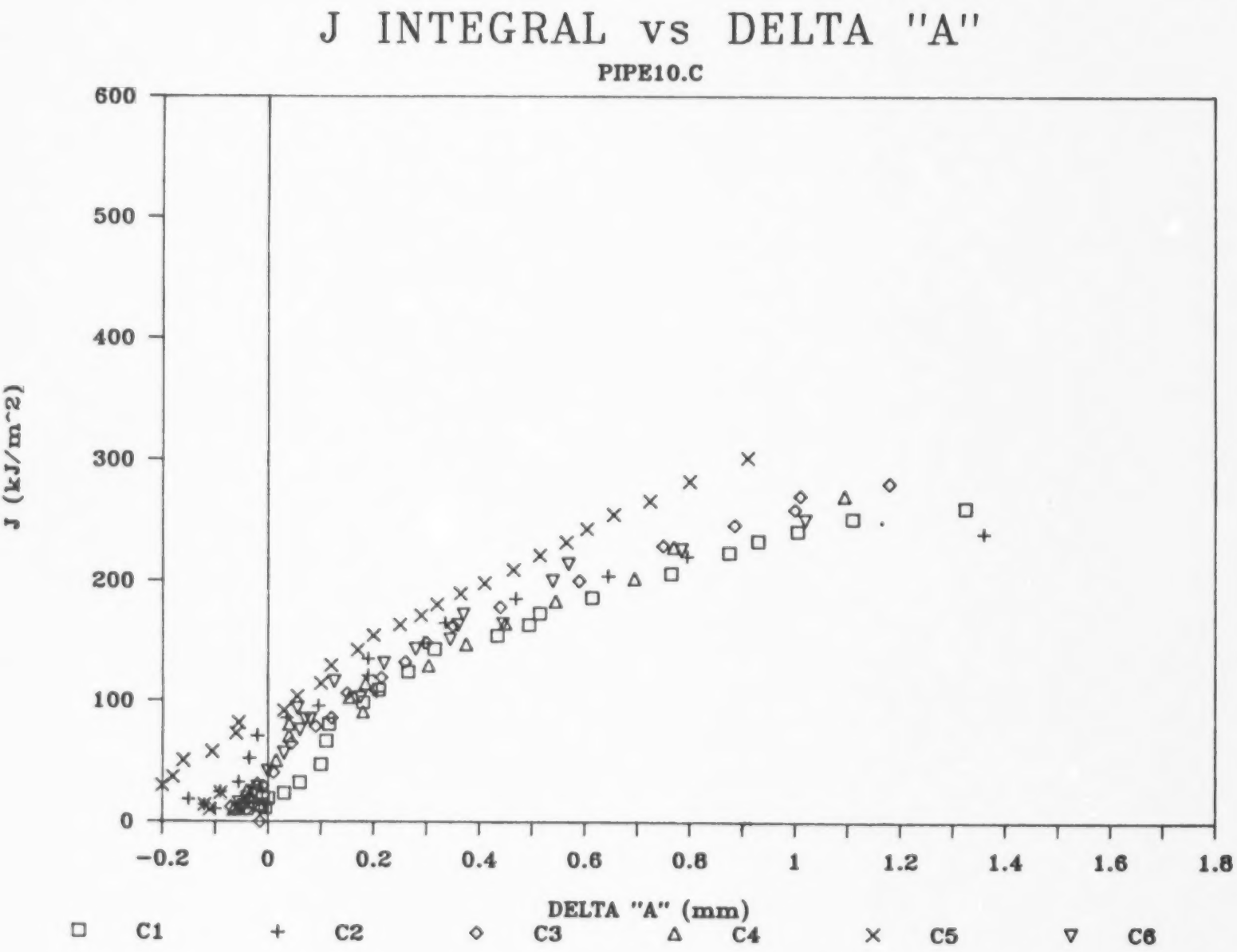

Figure B-9: Experimental Test Data of the J-Integral Versus Δa for Compact Tension Tests on Pipe Steel. Specimens 1.0 inch Thick Coded as PIPE 10.C1-6.

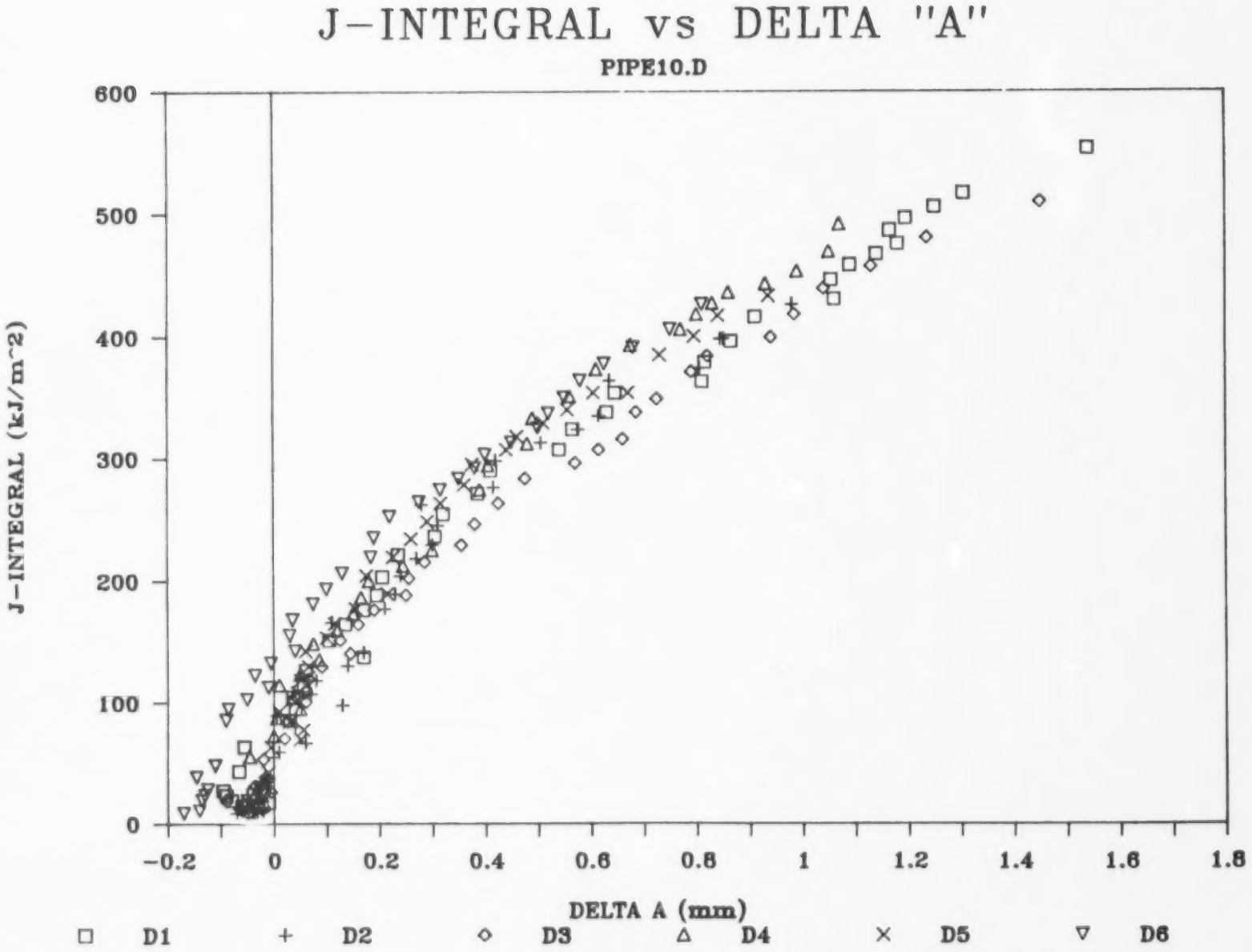

Figure B-10: Experimental Test Data of the J-Integral Versus Δa for Compact Tension Tests on Pipe Steel. Specimens 1.0 inch Thick Coded as PIPE 10.D1-6.

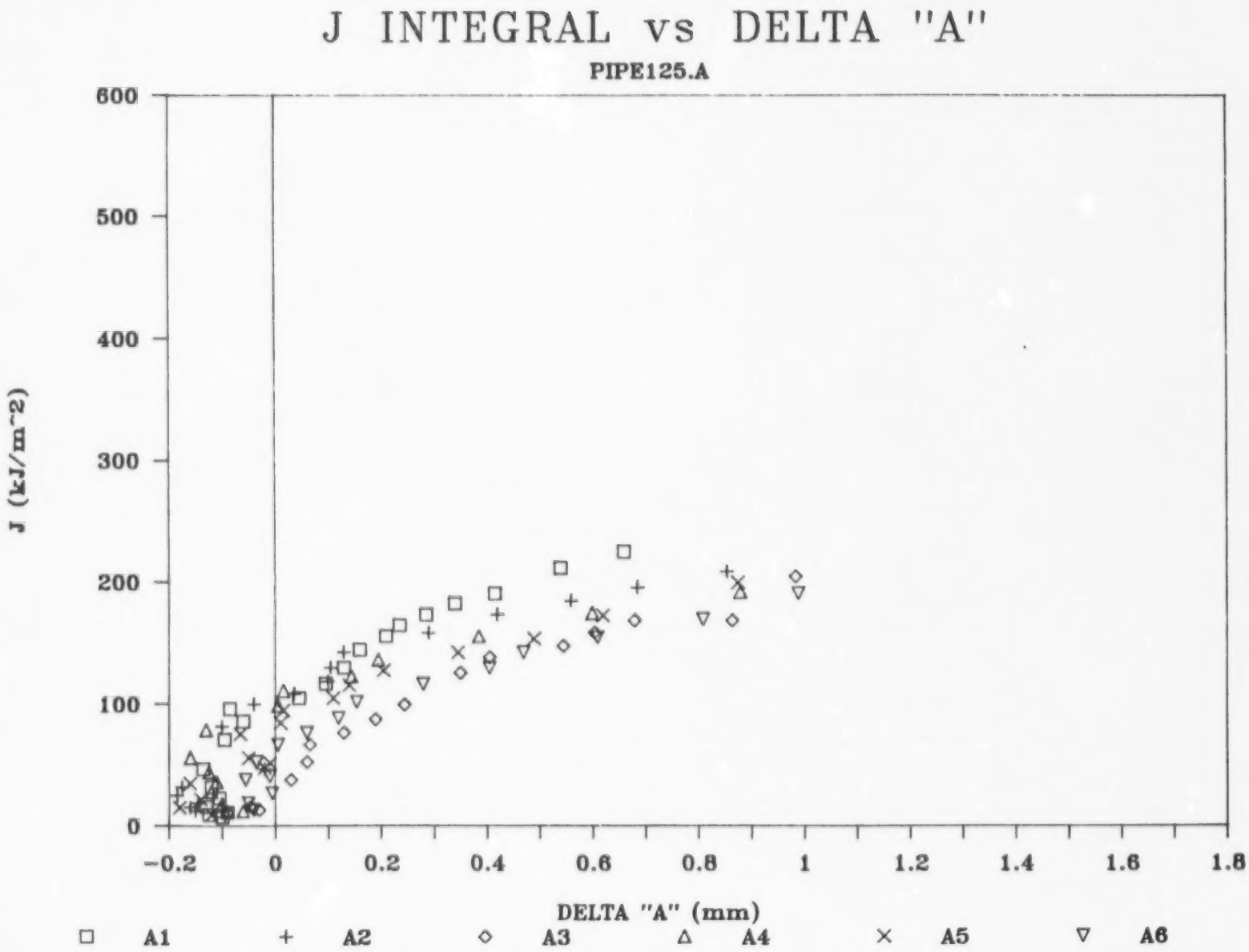

Figure B-11: Experimental Test Data of the J-Integral Versus Δa for Compact Tension Tests on Pipe Steel. Specimens 1.25 inch Thick Coded as PIPE 125.A1-6.

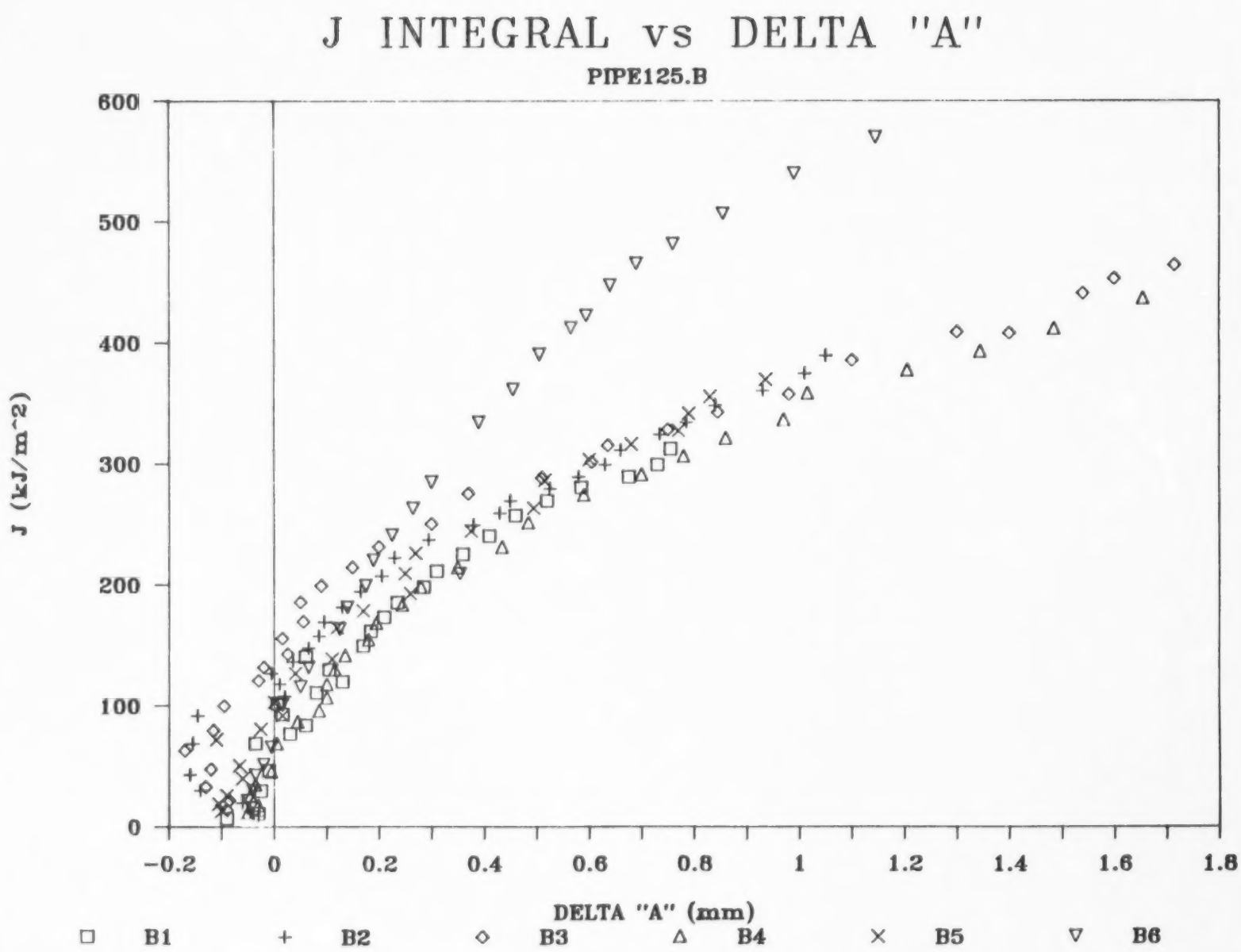

Figure B-12: Experimental Test Data of the J-Integral Versus Δa for Compact Tension Tests on Pipe Steel. Specimens 1.25 inch Thick Coded as PIPE 125.B1-6.

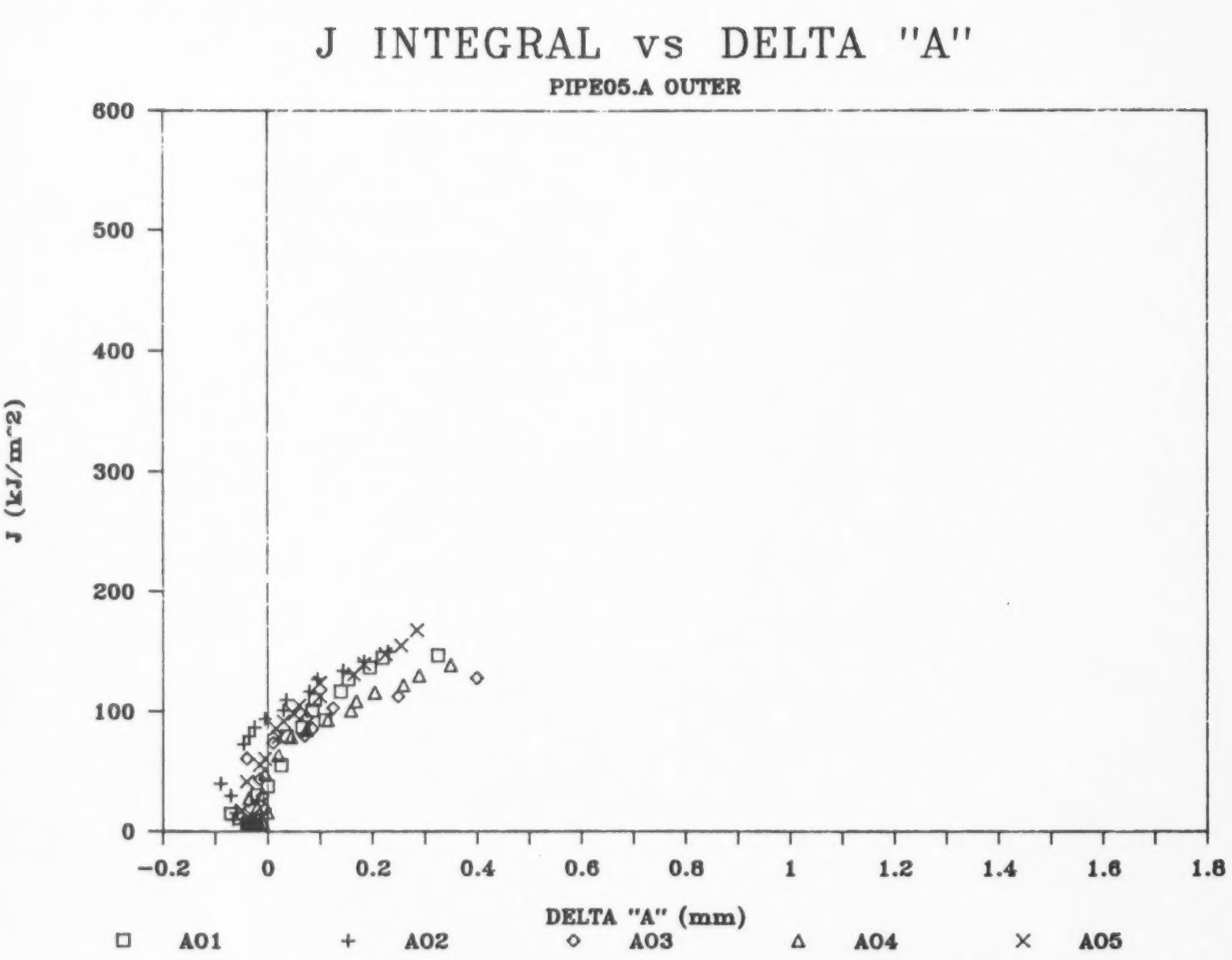

Figure B-13: Experimental Test Data of the J-Integral Versus Δa for Compact Tension Tests on Pipe Steel. Specimens 0.5 inch Thick Coded as PIPE 05.A01-5.

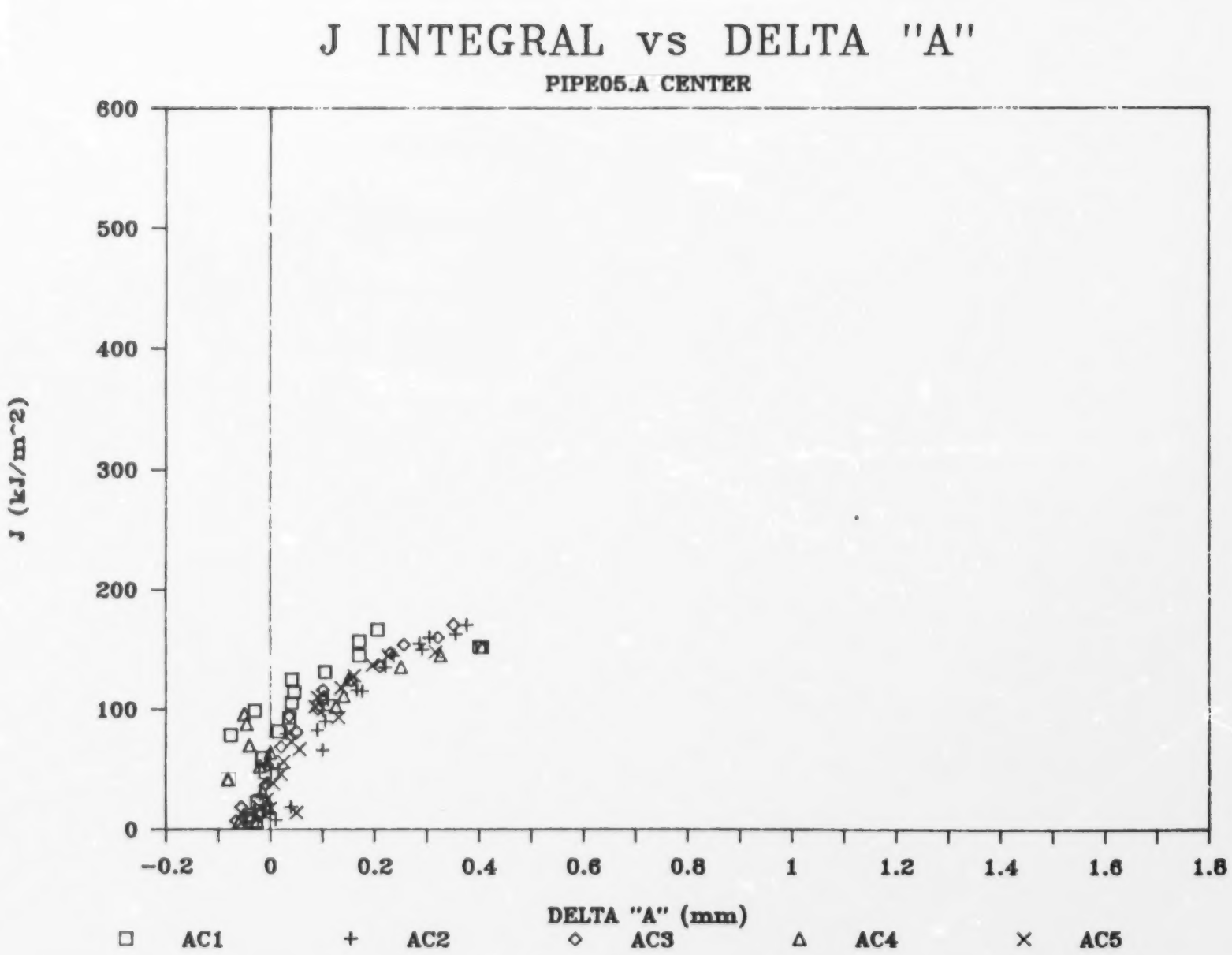

Figure B-14: Experimental Test Data of the J-Integral Versus Δa for Compact Tension Tests on Pipe Steel. Specimens 0.5 inch Thick Coded as PIPE 05.AC1-5.

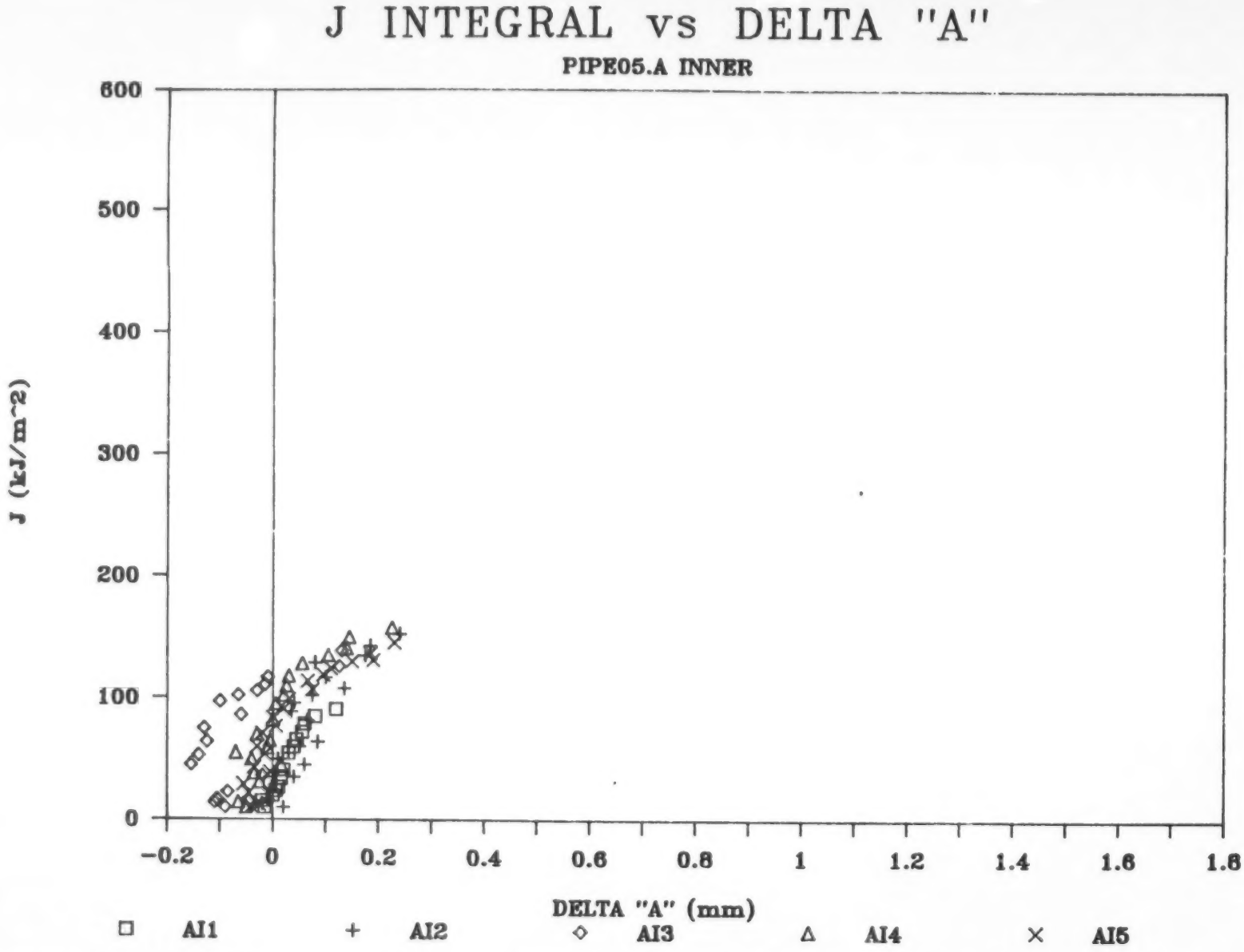

Figure B-15: Experimental Test Data of the J-Integral Versus Δa for Compact Tension Tests on Pipe Steel. Specimens 0.5 inch Thick Coded as PIPE 05.AI1-5.

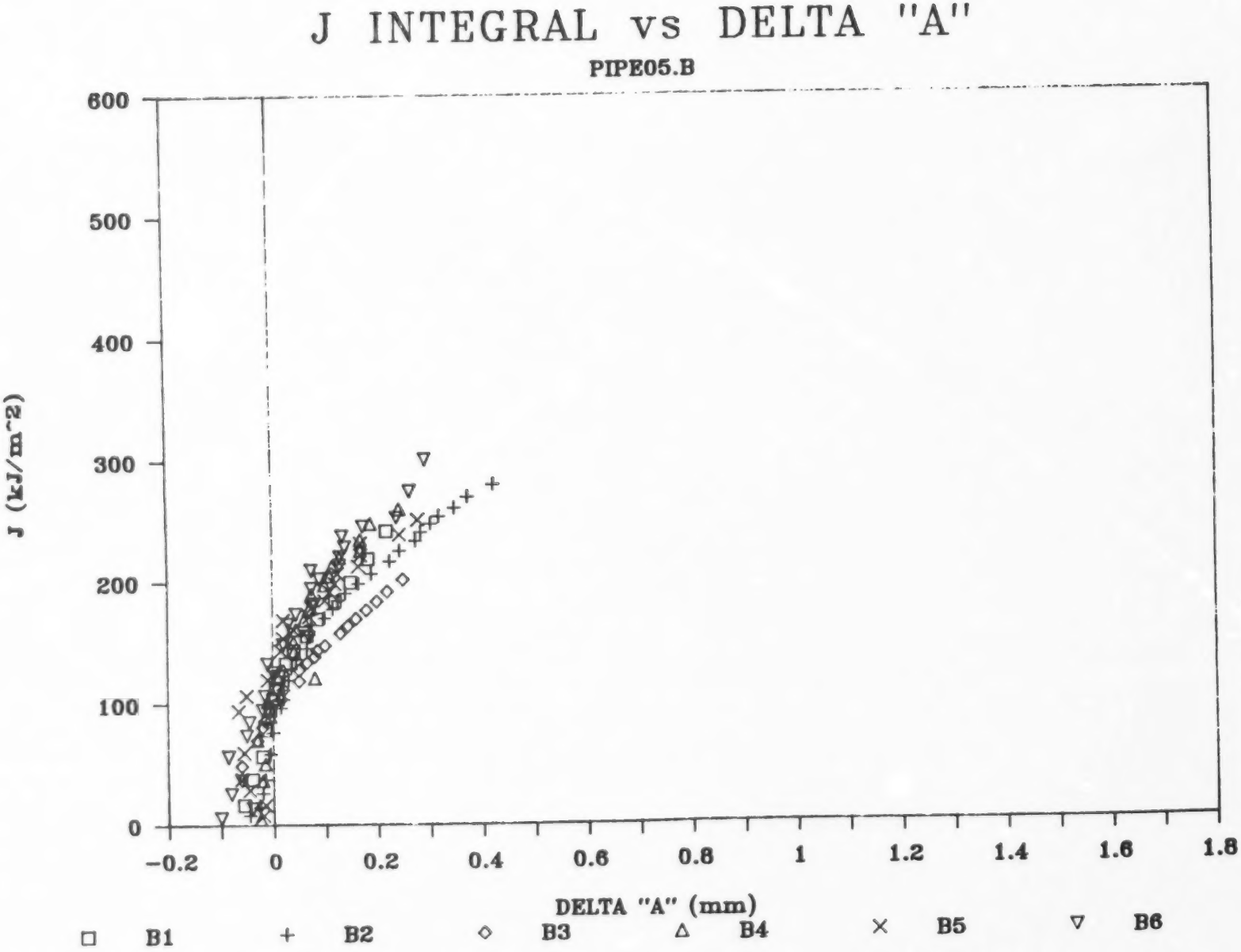

Figure B-16: Experimental Test Data of the J-Integral Versus Δa for Compact Tension Tests on Pipe Steel. Specimens 0.5 inch Thick Coded as PIPE 05.B1-6.